KONINKLIJK BELGISCH INSTITUUT VOOR NATUURWETENSCHAPPEN
OD NATUUR - BEHEERSEENHEID VAN HET MATEMATISCH MODEL

MOnitoring en MOdellering van het cohesieve sedimenttransport en evaluatie van de effecten op het mariene ecosysteem ten gevolge van bagger- en stortoperatie (MOMO)

Activiteitsrapport (1 januari 2014 -30 juni 2014)

Michael Fettweis, Matthias Baeye, Frederic Francken, Dries Van den Eynde

MOMO/7/MF/201408/NL/AR/1

museum
Operational Directorate Natural Environment
OD Nature I OD Natuur I DO Nature

KBIN-OD Natuur - BMM
Gulledelle 100
B–1200 Brussel
België

Inhoudstafel

1. Inleiding

1.1. Voorwerp van deze opdracht

Het MOMO-project (MOnitoring en MOdellering van het cohesieve sedimenttransport en de evaluatie van de effecten op het mariene ecosysteem ten gevolge van bagger- en stort-operatie) maakt deel uit van de algemene en permanente verplichtingen van monitoring en evaluatie van de effecten van alle menselijke activiteiten op het mariene ecosysteem waaraan België gebonden is overeenkomstig het Verdrag inzake de bescherming van het mariene milieu van de noordoostelijke Atlantische Oceaan (1992, OSPAR-Verdrag). De OSPAR Commissie heeft de objectieven van haar huidig "Joint Assessment and Monitoring Programme" (JAMP) gedefinieerd tot 2010 met de publicatie van een holistisch Quality Status Report Noordzee en waarvoor de federale overheid en de gewesten technische en wetenschappelijke bijdragen moeten afleveren ten laste van hun eigen middelen.

De menselijke activiteit die hier in het bijzonder wordt beoogd, is het storten in zee van baggerspecie waarvoor OSPAR een uitzondering heeft gemaakt op de algemene regel "alle stortingen in zee zijn verboden" (zie OSPAR-Verdrag, Bijlage II over de voorkoming en uitschakeling van verontreiniging door storting of verbranding). Het algemene doel van de opdracht is het bestuderen van de cohesieve sedimenten op het Belgisch Continentaal Plat (BCP) en dit met behulp van zowel numerieke modellen als het uitvoeren van metingen. De combinatie van monitoring en modellering zal gegevens kunnen aanleveren over de transportprocessen van deze fijne fractie en is daarom fundamenteel bij het be-antwoorden van vragen over de samenstelling, de oorsprong en het verblijf ervan op het BCP, de veranderingen in de karakteristieken van dit sediment ten gevolge van de bagger- en stortoperaties, de effecten van de natuurlijke variabiliteit, de impact op het mariene ecosysteem in het bijzonder door de wijziging van habitats, de schatting van de netto input van gevaarlijke stoffen op het mariene milieu en de mogelijkheden om deze laatste twee te beperken.

Een samenvatting van de resultaten uit de voorbije vergunningsperioden kan gevonden worden in het "Syntheserapport over de effecten op het mariene milieu van baggerspeciestortingen" (Lauwaert et al. 2004; 2006; 2008; 2009a, 2009b, 2011a, 2011b, 2014) dat uitgevoerd werd conform art. 10 van het K.B. van 12 maart 2000 ter definiëring van de procedure voor machtiging van het storten in de Noordzee van bepaalde stoffen en materialen.

1.2. Algemene doelstellingen

Het onderzoek uitgevoerd in het MOMO project kadert in de algemene doelstellingen om de baggerwerken op het BCP en in de kusthavens te verminderen en om een gedetailleerd inzicht te verwerven van de fysische processen die plaatsvinden in het mariene kader waarbinnen deze baggerwerken worden uitgevoerd. Dit impliceert enerzijds beleids-ondersteunend onderzoek naar de vermindering van de sedimentatie op de bagger-plaatsen en het evalueren van alternatieve stortmethoden. Anderzijds is onderzoek naar knelpunten voor het plannen en schatten van de effecten van de baggerwerken vereist. Dit is specifiek gericht op het dynamische gedrag van silb in de waterkolom en op de bodem en zal uitgevoerd worden met behulp van modellen en in situ metingen. De specifieke acties die binnen dit onderzoek uitgevoerd worden om de algemene doel-stellingen in te vullen zijn:

1. Streven naar een efficiënter stortbeleid door:

- optimalisatie van de stortlocaties. Gebaseerd op onderzoek uitgevoerd in de voorbije jaren (zie vorige syntheserapporten) zal een terreinproef worden uitgevoerd om de efficiëntie van een stortlocatie ten westen van Zeebrugge te bepalen;
- gebruik te maken van een operationeel stortmodel. Dit model zal geïntegreerd worden in de binnen BMM beschikbare operationele modellen. Het model zal gebruikt worden om in functie van de voorspelde fysische (wind, stroming, golven, sedimenttransport, recirculatie), economische (afstand, grootte baggerschip) en ecologische aspecten op korte termijn een keuze te kunnen maken tussen de beschikbare stortlocaties. Hiervoor zal binnen de huidige periode het slibtransportmodel gevalideerd worden op de geografische variabiliteit van de turbiditeitszones en de flocculatie van het slib.

2. Continue monitoring van het fysisch-sedimentologische milieu waarbinnen de baggerwerken worden uitgevoerd en aanpassing van de monitoring aan de nog op te stellen targets voor het bereiken van de goede milieutoestand (GES), zoals gedefinieerd zal worden binnen MSFD;

3. Uitbouw en optimalisatie van het numerieke modelinstrumentarium, ter ondersteuning en verfijning van acties 1 en 2.

1.3. Onderzoek januari 2014 – december 2016

In het bijzonder is bij het opstellen van de hieronder vermelde taken rekening gehouden met de aanbevelingen voor de minister ter ondersteuning van de ontwikkeling van een versterkt milieubeleid zoals geformuleerd in het "Syntheserapport over de effecten op het mariene milieu van baggerspeciestortingen (2011)" dat uitgevoerd werd conform art. 10 van het K.B. van 12 maart 2000 ter definiëring van de procedure voor machtiging van het storten in de Noordzee van bepaalde stoffen en materialen

Taak 1: In situ metingen en data analyse

Monitoring moet gericht zijn op het begrijpen van processen, zodoende dat de waargenomen variabiliteit in een correcte kader geplaatst kan worden. In vele kustzones is er een gebrek aan langdurige en hoogfrequente data over sleutelparameters die de milieutoestand beschrijven, zoals turbiditeit en SPM concentratie. De tripodemetingen in het kader van het MOMO project te MOW1 vormen een uitzondering hierop gezien hun langdurig karakter. De eerste verankeringen werden in 2004 uitgevoerd, vanaf november 2009 worden er continue metingen gedaan. Deze data laten toe om om zowel de natuurlijke variabiliteit, de langdurige trends en de effecten van menselijke ingrepen op de turbiditeit te achterhalen. Een groot deel van de activiteiten is daarom gericht op zowel het uitvoeren van de metingen, het garanderen van kwalitatief hoogwaardige data en het archiveren, rapporteren en interpreteren ervan.

Taak 1.1 Langdurige metingen

Sinds eind 2009 worden er continue metingen uitgevoerd te MOW1 met behulp van een meetframe (tripode). Met dit frame worden stromingen, slibconcentratie, korrelgrootte-verdeling van het suspensiemateriaal, saliniteit, temperatuur, waterdiepte en zeebodem altimetrie gemeten. Om een continue tijdreeks te hebben, wordt gebruik gemaakt van 2 tripodes. Na ongeveer 1 maand wordt de verankerde tripode voor onderhoud aan wal gebracht en wordt de tweede op de meetlocatie verankerd.

In 2013 werd gestart met langdurige metingen met behulp van een OBS-5 sensor vastgemaakt aan de AW boei; deze metingen zullen verdergezet worden. De data geven informatie over de SPM concentratie aan het oppervlak en zijn aldus complementair aan

de bodemnabije metingen met de tripode. De data zijn ook van belang voor het calibreren en valideren van de oppervlakte SPM concentraties uit satellietbeelden.

Taak 1.2 Calibratie van sensoren tijdens in situ metingen

Tijdens 4 meetcampagnes per jaar met de R/V Belgica zullen een voldoende aantal 13-uursmetingen uitgevoerd worden met als hoofdoel het calibreren van optische of akoestische sensoren en het verzamelen van verticale profielen. De metingen zullen plaatsvinden in het kustgebied van het BCP. De optische metingen (transmissometer, Optical Backscatter Sensor) zullen gecalibreerd worden met de opgemeten hoeveelheid materie in suspensie (gravimetrische bepalingen na filtratie) om te komen tot massa concentraties. Naast de totale hoeveelheid aan suspensiemateriaal (SPM) wordt ook de concentratie aan POC/PON, chlorophyl (Chl-a, Chl-b) en phaeofytine (a, b) bepaald. Stalen van suspensiemateriaal zullen genomen worden met de centrifuge om de samenstelling ervan te bepalen.

Taak 1.3: Data archivering en rapportage

De meetdata worden gearchiveerd en er wordt een kwaliteitsanalyse uitgevoerd, zodat de goede data onderscheiden kunnen worden van slechte of niet betrouwbare data. Slechte data kunnen bv optreden doordat het instrument slecht heeft gewerkt en verkeerd werd ingesteld. Niet betrouwbare data zijn typisch geassicieerd met bv biofouling. De data en metadata worden gearchiveerd.

Taak 1.4: Verwerking en interpretatie van metingen

De metingen vergaard tijdens de 13-uursmetingen aan boord van de Belgica en met de tripode worden verwerkt en geïnterpreteerd. Hiervoor werden in het verleden reeds heel wat procedures (software) toegepast of ontwikkeld, zoals de berekening van de bodem-schuifspanning uit turbulentiemetingen, entropieanalyse op partikelgrootteverdelingen, de opsplitising van multimodale partikelgrootteverdeling in een som van lognormale verdelingen, het groeperen van de data volgens getij, meteorologie, klimatologie en seizoenen. Deze methodes (zullen opgenomen worden) zijn opgenomen in de standaardverwerking van de data. De alsus verwerkte data dienen als basis voor het verder gebruik binnenin wetenschappelijke vragen (zie taak 2.2, 2.3 en 4.2, 4.4).

Taak 2: Onderzoek en monitoring alternatieve stortstrategie onderhouds-baggerwerk voorhaven Zeebrugge

De BMM is auteur van de voorbereidende studies voor de terreinproef en zal de terreinproef mee opvolgen. BMM-OD Natuur zal verantwoordelijk zijn voor het uitvoeren van de langdurige frame metingen (lopen tot eind april 2014) en de statistische verwerking van de resultaten (Taak 2.1). De resultaten van de metingen zullen gebruikt worden bij de analyse van de efficiëntie van de baggerproef (Taak 2.3). Door de BMM-OD Natuur zullen ook met behulp van het Automatic Underway Monitoring System (AUMS) op het onderzoeksschip Belgica opnames gemaakt worden van de sedimentconcentratie binnen de haven (Taak 2.2). Deze gegevens zullen ter beschikking gesteld worden voor verdere verwerking. BMM-OD Natuur zal deel uitmaken van de stuurgroep.

Taak 2.1: Uitvoeren van lange termijn metingen in de omgeving van de haven van Zeebrugge voor het opvolgen van de terreinproef, en het bestuderen van de interne sedimentdynamiek in de haven

Voor dit deel van de opdracht is de BMM-OD Natuur verantwoordelijk voor het uitvoeren van de metingen en het aanleveren van de gevalideerde data voor verdere verwerking in de factual data rapportering en omzetting naar het standaardformaat. Het betreft twee meetframes, een ter hoogte van de meetpaal MOW 1 (als achtergrondwaarde, zie Taak

1.1) en een ander ter hoogte van de ingang van de haven van Zeebrugge (WZ-boei). Deze meetframes dienen afdoend de saliniteit, stromingen, sedimentconcentratie en korrelgrootteverdeling te meten.

Taak 2.2: Beschrijving van de omgevingscondities

Gedurende de meetperiode van de langdurige metingen dienen ook de verschillende externe factoren die een invloed kunnen hebben op de interne slibdynamiek in de haven nauwkeurig bijgehouden worden en dit gedurende dezelfde periode als de metingen in taak 2.1. De BMM-OD Natuur is verantwoordelijk voor het opleveren van informatie over de sedimentconcentraties uit het AUMS aan boord van de Belgica.

Taak 2.3: Analyse efficiëntie baggerproef

Na afloop van de baggerproef dient de efficiëntie van de uitgevoerde proef geschat te worden. Hiervoor dient als eerste een T0 toestand gedefinieerd te worden, waarbij op basis van de binnen Taak 2.1 en Taak 2.2 verzamelde data een inschatting kan gemaakt worden van de mogelijke events die tijdens de proef hebben plaatsgevonden, en hun invloed op de resultaten van de baggerproef. De BMM-OD Natuur zal een statistische benadering van de efficiëntie van de baggerproef uitvoeren, waarbij nagegaan wordt in hoeverre de tijdens de baggerproef gemeten waardes op de twee frames afwijken van de waardes die gemeten werden buiten de stortproef. Deze analyse werd reeds toegepast bij de evalueren van de baggerproef in het Albert II dok.

Taak 3: Uitbouw en optimalisatie van het modelinstrumentarium

Taak 3.1: Validatie van het slibtransportmodel

Het tijdens de voorbije jaren verbeterde en aangepaste slibtransportmodel zal worden gevalideerd met behulp van de langdurige meetreeksen en de satellietbeelden. Hierbij zal dezelfde methode als in Baeye et al. (2011) en zoals in taak 1.4 worden gebruikt om de modelresultaten te groeperen en te klasseren volgens windrichting, weertype en getij. Het voordeel van deze werkwijze is dat niet zozeer gekeken wordt of de correlatie tussen meting en modelresultaat in één of meerder punt goed is, maar dat globaal nagegaan wordt of het model de SPM dynamica op het BCP goed kan reproduceren. Deze taak zal in nauwe samenwerking met het WLH gebeuren die eenzelfde benadering zullen toe passen op hun model (contacten zijn gelegd met B De Maerschalk).

Taak 3.2: Operationeel stortmodel

Dit model zal geïntegreerd worden in de binnen BMM-OD Natuur beschikbare operationele modellen. Het model zal gebruikt worden om in functie van de voorspelde fysische (wind, stroming, golven, sedimenttransport, recirculatie), economische (afstand, grootte baggerschip) en ecologische aspecten op korte termijn een keuze te kunnen maken tussen de beschikbare stortlocaties. Hiervoor zal binnen de huidige periode het slibtransportmodel gevalideerd worden op de geografische variabiliteit van de turbiditeitszones en de flocculatie van het slib.

Taak 4: Oplossingen voor knelpunten

Taak 4.1: Kwaliteitscontrole van de data en de integratie ervan in de monitoing voor de KRMS

Taak 4.1.1: KRMS monitoring

De data verzameld in Taak 1, zullen worden opgenomen in de nog op te zetten monitoringsverplichtingen van de Belgische Staat (07/2014) in het kader van de Kaderrichtlijn Mariene Strategie (MFSD). De KRMS monitoring zal in 2015 starten en zal dienen om de toestand van het mariene milieu te evalueren aan de goede milieutoestand

(GES), zoals opgetseld door de Belgische Staat in 2012 (Belgische Staat 2012a, 2012b).

Er zal verder geëvalueerd worden of het MOMO meetprogramma aan de monitoringsverplichtingen die voor de KRMS (MFSD) moeten worden opgesteld zal voldoen en/of er aanpassingen nodig zijn. De wetenschappelijke vragen die hier bekeken worden hebben vooral betrekking op de geografische spreiding van de data. Is het voldoende om – zoals nu gebeurt – te berusten op satellietbeelden voor de geografische en in situ meetreeksen voor de temporele spreiding of dienen we te opteren voor één vast meetpunt (MOW1) en bijkomend een aantal andere punten (Nieuwpoort, Kwintebank, Gootebank) waar random in de tijd gemeten wordt met een tripode gedurende telkens een periode van ongeveer 1 maand. Hiervoor zou bv de tripode die nu ingezet wordt voor de terreinproef gebruikt kunnen worden.

Taak 4.1.2:Kwaliteitscontrole

Een belangrijk aandachtspunt bij deze langdurige datareeksen is het garanderen van een gelijke kwaliteit in de tijd van de verzamelde data. De vraag die zich bij onze SPM concentratiemetingen stelt is niet zozeer het opmeten van hogere of lagere waarden, mogelijks veroozaakt door het toepassen van een andere stortstrategie, maar het garanderen dat deze waarden inderdaad veroorzaakt worden door menselijke activiteiten (bv storten) en niet het effect zijn van natuurlijke fluctuaties. De natuurlijke variabiliteit van SPM concentratie is groot en wordt veroorzaakt door de getijwerking, doodtij-springtijcyclus en meteorologische en klimatologische phenomenen. De tijdschalen gaan van seconden tot seizoenen, met mogelijks langere fluctuaties voor (nodale cylus, klimaatsverandering, zeespiegelstijging,...). Langdurige variaties kunnen bv geïdentifceerd worden als een trend of een cosinusfunctie met lage frequentie. Om kwaliteitsvolle data te kunnen leveren over een lange periode, die gebruikt kunnen worden om langdurige trends te identificeren, is het nodig om een rigoureuze kwaliteitscontrole uit te voeren. OBS alsook akoestische sensoren zijn gevoelig aan de samenstelling en korrelgrootte van het gesuspendeerde materiaal. Dit kan varieren in functie van de boven vermelde frequenties, maar hieromtrent is er nog geen afdoende duidelijkheid wat de metingen te MOW1 betreft.

- Hoe veranderen de calibratieconstanten i.f.v. externe parameters (doodtij-springtij, zomer-winter)? Hoe dikwijls moeten de sensoren in situ gecalibreerd worden om de rekening te kunnen houden met de mogelijke fluctuaties in samenstelling van het suspensiemateriaal?
- Wat is de fout op de metingen? Het uitvoeren van directe (waterstaal) en indirecte metingen (OBS, akoestische backscatter) van SPM concentratie gaat inherent gepaard met onzekerheden (meetfouten). In situ metingen zijn steeeds onderhevig aan onzekerheden tengevolge van random meetfouten (gebrek aan precisie), systematische fouten (onnauwkeurigheid), menselijke fouten, en de statistische variabiliteit van de parameter. De fouten hebben hun oorsprong in de onnauwkeurigheid en het gebrek aan precisie van het meetinstrument of de procedures (bv. waterstaalname en filtratie). Doel is om de fout op de verschillende onderdelen van de metingen (filtratie, calibratie, langdurige trends...) te schatten.

Taak 4.1.3: Aanvulling van ontbrekende data met behulp van statistische methodes

Het gebeurt regelmatig in de metingen te MOW1 dat de OBS sensoren verzadigen (vooral deze op 0.2 m) of uitvallen en er aldus gedurende een korte of langere perioden geen (betrouwbare) data beschikbaar zijn. In de statistiek bestaan technieken de ontbrekende data te reconstrueren. Er zal nagegaan worden wat de meets geschikte methode is om de tijdseries te vervolledigen.

Taak 4.2: Biologische effecten en de seizoenale variaties in SPM concentratie

De correlatie tussen biomassa (zoals o.a. POC en chlorophyl) en vlokgrootte en vorm wordt dikwijls aangehaald in de literatuur, maar dit bleek sterk plaatsgebonden te zijn en dikwijls gebaseerd op korte meetperioden. De lange tijdsreeks te MOW1 werd geanalyseerd in combinatie met satelliet data, de omgekeerde correlatie tussen de chlorophyll en de SPM concentratie is opvallend. Er werd de hypothese opgesteld, dat door de algenbloei in de lente de concentratie aan kleverige organische moleculen (TEPs) wordt verhoogd, waardoor meer macrovlokken gevormd worden, het SPM sneller bezinkt en moeilijker kan eroderen en aldus de SPM concentratie gaat afnemen. erder onderzoek richt zich naar:

1) Analyse van TEP concentraties. Tot nu toe worden geen TEP analyses uitgevoerd, nochthans is dit noodzakelijk om deze hypothese te toetsen. Er zal nagegaan worden hoe de TEPs geanalyseerd kunnen worden in waterstalen, wat en hoe dit meetprogramma uitgevoerd kan worden. Er wordt geopteerd om tegen 2015 met de eerste metingen te kunnen beginnen.
2) De invloed van lichthoeveelheid op de start van de algenbloei in de lente en de afname van de SPM concentratie;
3) Wat gebeurt er met het SPM dat uit de waterkolom verdwijnt door snellere sedimentatie in de zomer? Heeft dit een effect op de frequentie van hooggeconcentreerde slibsuspensies en mogelijks aanslibbing van vaargeulen en havens?
4) Verdere ontwikkeling van het flocculatiemodel zodat seizoenale effecten in rekening gebracht kunnen worden. Simulatie in 2D/3D met dit flocculatiemodel teneinde het model te valideren.

Taak 4.3: Alternatieve Stortstrategies Nieuwpoort

Er zal ondersteuning gegeven worden aan MDK in verband met het opzetten van een wetenschappelijke terreinproef om de impact van het verpompen van baggerspecie uit de haven van Nieuwpoort op een stortzone te evalueren. Details hiervan zullen op een vergadering van de technische werkgroep besproken worden.

Taak 4.4: Golfsystemen en hun impact op de zeebodem en de SPM concentratiel

Er bestaan verschillende sorten golven en golfsystemen (korte golven, deining) die een impact hebben op de zeebodem. Tot nu toe werd dit aspect nog niet in rekening gebracht in de analyse van de data. Wat is de impact van deinig of korte golven op de resuspensie van sedimenten? Wat zijn de belangrijkste parameters en wat is hun belang voor waterbouwkundige werken (baggeren)?

1.4. Publicaties (januari 2014 – december 2016)

Hieronder is een lijst met rapporten, publicaties, thesissen en presentatie op workshops en conferenties waar resultaten en data uit het MOMO project werden voorgesteld:

Activiteits-, Meet- en Syntheserapporten

Fettweis M, Baeye M, Francken F, Van den Eynde D. 2014. MOMO activiteitsrapport (1 januari - 30 juni 2014). BMM-rapport MOMO/7/MF/201408/NL/AR/1, 43pp + app.

Lauwaert B, Fettweis M, De Witte B, Devriese L, Van Hoeu G, Timmermans S, Martens C. 2014. Vooruitgangsrapport (juni 2014) over de effecten op het mariene milieu van baggerspeciestortingen (vergunningsperiode 01/01/2012 – 31/12/2016). Rapport uitgevoerd door KBIN-BMM, ILVO, CD, aMT. BL/2014/01, 20pp + app.

Conferenties/Workshops

Fettweis M, Lee B, Toorman E. 2014. Multimodal particle size distribution of fine-grained cohesive sediments: Observation and simulation. Reactive Transport Workshop, 20 May, Louvain-la-Neuve (Belgium).

Baeye M, Francken F, Fettweis M, Van den Eynde D. 2014. The first buoy for continuous measuring of surface Suspended Particulate Matter concentration on the Belgian inner shelf. VLIZ Young Marine Scientists' Day, March 7, Brugge (Belgium) (poster).

Fettweis M, Baeye M, Van der Zande, Van den Eynde D, Lee BJ. 2014. Seasonality of near-shore marine snow in the southern North Sea. VLIZ Young Marine Scientists' Day, March 7, Brugge (Belgium).

Thant S, Baeye M, Fettweis M, Monbaliu J, Van Rooij D. 2014. Extreme values of Suspended Particulate Matter concentration and their relation to wave systems along the Belgian inner shelf. VLIZ Young Marine Scientists' Day, March 7, Brugge (Belgium).

Publicaties (tijdschriften, hoofdstuk in boeken)

Van den Eynde D, Fettweis M**.** 2014. Towards the application of an operational sediment transport model fort the optimisation of dredging works in the Belgian coastal zone (southern North Sea). In: Dahlin H., Flemming N.C., Petersson S.E. (Eds.). Sustainable Operational Oceanography, 250-257.

Fettweis M, Baeye M, Van der Zande D, Van den Eynde D, Lee BJ. 2014. Seasonality of floc strength in the southern North Sea. Journal of Geophysical Research 118, doi: 10.1002/2013JC009750.

Lee BJ, Toorman E, Fettweis M. 2014. Multimodal particle size distribution of fine-grained sediments: Mathematical modeling and field investigations. Ocean Dynamics 64, 429-441. doi: 10.1007/s10236-014-0692-y

Thesis

Thant S. 2014. Study on wave systems and their impact on the seabed and water column turbidity in the Belgian coastal zone. Master thesis in Marine and Lacustrine Science and Management. UA, UGent and VUB. 43pp+app.

2. Langdurige metingen te MOW1: 2005-2013

Dit hoofdstuk geeft een overzicht van de beschikbare meetgegevens te MOW1 en sluit aan bij het vorige rapport (Fettweis et al. 2014a). In dit hoofdstuk ligt de nadruk op de OBS metingen; in het vorige rapport werden de ADP en LISST metingen voorgesteld.

2.1. Meetapparatuur

Stroming, saliniteit, temperatuur, SPM concentratie en partikelgrootteverdeling (PGV) werden gemeten met een tripode, zie figuur 2.1. De gemonteerde instrumentatie bestaat, onder andere uit drie D&A optical backscatter point sensoren (OBSen), een Sea-bird SBE37 CT, een SonTek® ADP current profiler en een Sequoia Scientific LISST (laser in situ scattering and transmissometry) 100 X type C. Alle data (uitgezonderd van de LISST) worden opgeslaan in twee SonTek Hydra data logging systemen. De LISST werd gemonteerd op ongeveer 2 meter boven de bodem (verder afgekort als mbb) en de OBSen op 0.2, 1 en 2 mbb. Het OBS signaal werd gebruikt om de backscatter van de ADP om te zetten naar SPM concentratie. De OBS voltage werd omgezet naar SPM concentratie met behulp van gefiltreerde waterstalen genomen tijdens verschillende meetcampagnes. De OBS werden afgeijkt om concentraties te meten tot ongeveer 3 g/l. Tijdens periodes met hoge turbulentie was de SPM concentratie regelmatig hoger dan 3 g/l, de OBS is dan gesatureerd en onderschat aldus de reële SPM concentratie.

De tripode werd verankerd te MOW1 gedurende 3-6 weken, waarna ze terug opgehaald en vervangen werd met een gelijkaardig tripodesysteem. Door deze langdurige verankering beschikken we over een representatief overzicht dat de natuurlijke variaties, zoals springtij-doodtij en meteorologische gebeurtenissen, weergeeft. De golfdata zijn afkomstig van de A2-boei (Meetnet Vlaamse Banken).

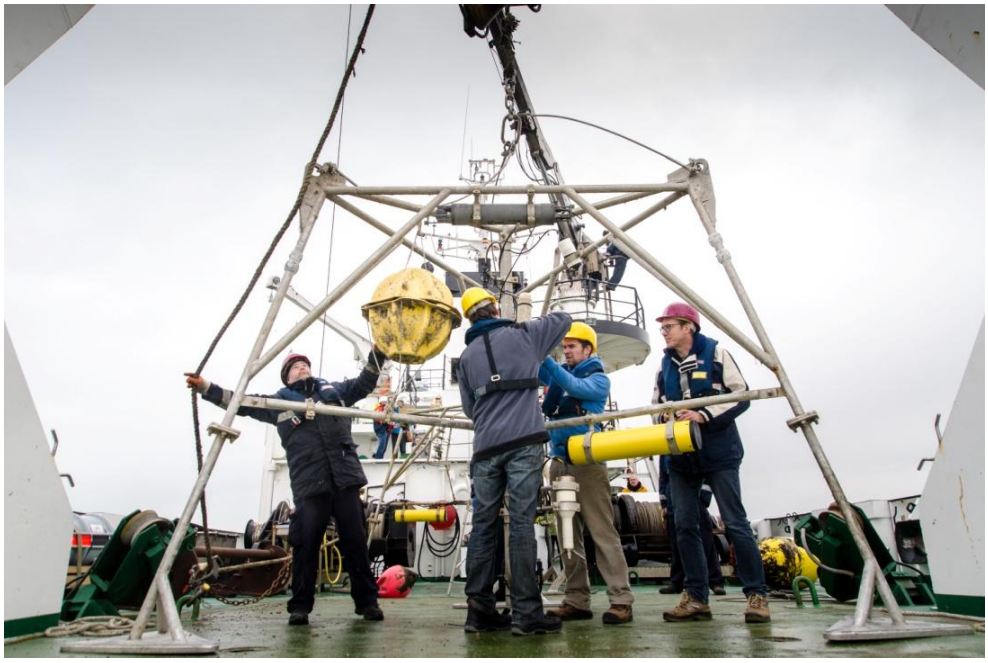

Figuur 2.1: Tripode meetsysteem klaar voor verankering te MOW1 op 28/11/2013. (foto genomen door Jorn Urbain, Belgische Marine).

2.2. Overzicht verankeringen: OBS

Er werden verschillende OBS instellingen gebruikt tijdens de verankeringen. Het meetinterval is afhankelijk of de OBS aan de ADP of de ADV bevestigd was. Voor de ADV, die hoog frequente metingen doet gedurende korte tijd, is het inteval tussen twee metingen groter (tussen 10 en 30 minuten). Bij de ADP werd er frequenter gemeten (1 tot 2 minuten). Verder werd gevoeligheid van de OBS regelmatig aangepast, zodat het meetbereik variierde tussen ongeveer 0-780 mg/l, 0-1550 mg/l of 0-3200 mg/l. In totaal werden 1153 (OBS 2 mab) en 1114 dagen (OBS 0.2 mab) aan data verzameld gedurende de 43 verankeringen te MOW1. Een overzicht van de OBS data kan gevonden worden in Figuur 2.2 en Tabellen 2.1-2.3.

De tijdseries van SPM concentraties per jaar worden ook getoond in Figuur 2.3. Hiervoor werden alle data geresampled (ADV) of geïnterpoleerd om de 15 minuten. Op de OBS data werd het getijsignaal eruitgefilterd met beulp van een low-pass filter (PL64) (Flagg et al., 1976).

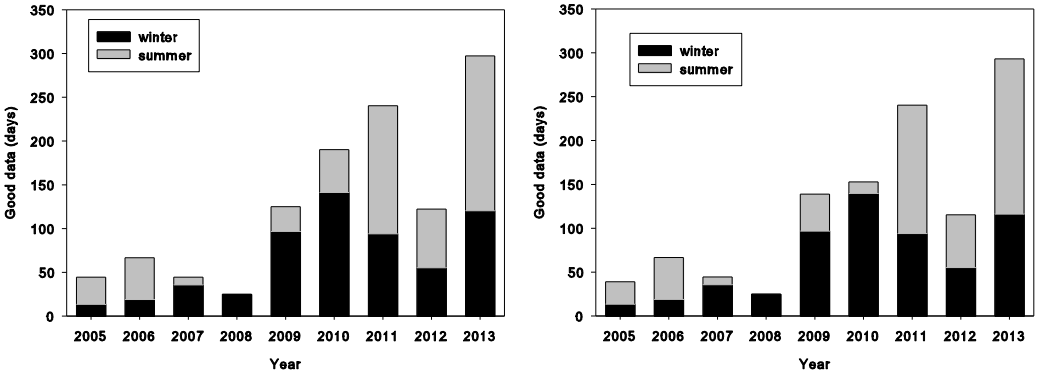

Figuur 2.2: Aantal goede OBS data (goede dagen) per jaar en seizoen (winter: januari-maart+oktober-december, zomer: april-september) en dit voor de periode 2005-2013, links OBS op 2 m en rechts op 0.2 m boven bodem.

Tabel 2.1: Aantal goede OBS data te MOW1 per jaar en seizoen (winter: januari-maart+oktober-december, zomer: april-september) en dit voor de periode 2005-2013.

	OBS 2 mab			OBS 0.2 mab		
	year	winter	summer	year	winter	summer
2005	43.78	13.80	29.98	38.80	13.80	25.00
2006	66.82	18.93	47.89	66.82	18.93	47.89
2007	44.69	35.88	8.81	44.69	35.88	8.81
2008	24.80	24.80	0	24.80	24.80	0
2009	124.74	97.41	27.33	138.66	97.41	41.25
2010	189.70	141.11	48.59	152.11	140.11	12.00
2011	239.57	94.89	144.68	239.57	94.89	144.68
2012	122.00	55.94	66.06	115.50	55.94	59.56
2013	296.73	120.93	175.80	292.65	116.85	17.85
2005-2013	1152.93	603.19	549.74	1113.60	598.61	514.99

Tabel 2.2: Overzicht van OBS (2 mab) metingen te MOW1.

Nr		measuring period	good data			OBS – SPM concentration			
			period (julian day)	days	data	max (mg/l)	saturation (mg/l)	% data saturated	inter-val (min)
5	ADV	07/02/2005-08/02/2005	38.51-39.30	0.78	454	645	-	0.00	2.5
6	ADV	04/04/2005-15/04/2005	94.46-105.31	10.84	77835	>765	765	6.03	0.2
7	ADV	22/06/2005-11/07/2005	173.34-192.48	19.14	137798	1456	-	0.00	0.2
8	ADV	22/11/2005-05/12/2005	326.35-339.37	13.02	622	1851	-	0.00	10
9	ADV	13/02/2006-27/02/2006	44.48-58.44	13.96	669	2147	-	0.00	30
10	ADV	27/03/2006-18/04/2006	86.46-108.37	21.92	1053	3103	-	0.00	30
11	ADV	15/05/2006-15/06/2006	135.49-166.42	30.94	1271	860	-	0.00	30
15	ADV	10/07/2007-19/07/2007	191.75-200.56	8.81	1270	589	-	0.00	10
16	ADV	23/10/2007-28/11/2007	296.53-332.41	35.88	5168	1965	-	0.00	10
21	ADV	17/11/2008-12/12/2008	322.58-347.38	24.80	3573	1662	-	0.00	10
22	ADV	09/02/2009-19/03/2009	40.49-78.32	37.83	5448	>3115	3115	0.01	10
23	ADV	26/03/2009-29/04/2009	85.34-119.33	33.99	4896	2252	-	0.00	10
27	-	10/09/2009-21/10/2009	-	0		-	-	-	-
30	ADP	06/11/2009-08/12/2009	310.36-342.63	32.27	45987	>1542	1542	0.02	1
31	ADP	11/12/2009-25/01/2010	345.35-25.25	44.90	65218	>1541	1541	0.41	1
32	ADV	25/01/2010-25/03/2010	25.65-84.43	58.78	8306	>783	783	0.57	10
33	ADP	25/03/2010-20/05/2010	84.46-140.60	56.13	80842	1329	-	0.00	1
37	ADP	06/09/2010-18/10/2010	-	-	-	-	-	-	2
38	ADV	18/10/2010-08/11/2010	291.55-312.99	21.43	2060	>759	759	0.49	15
39	ADP	17/11/2010-15/12/2010	321.50-349.61	28.11	20257	1578	-	0.00	2
40	ADV	15/12/2010-31/01/2011	349.68-12.00	16.31	2531	>686	686	12.76	15
41	-	31/01/2011-21/03/2011	-	0	-	-	-	-	-
42	ADV	21/03/2011-24/03/2011	80.73-83.25	2.52	243	430	-	0.00	15
43	ADV	24/03/2011-17/04/2011	83.32-107.70	24.38	2341	>757	757	0.38	15
44	ADP	29/04/2011-23/05/2011	119.43-143.68	24.25	17473	1375	-	0.00	15
45	ADV	23/05/2011-19/06/2011	143.64-170.59	26.94	2587	>3128	3128	0.35	15
46	ADP	11/07/2011-12/08/2011	192.68-224.73	32.05	23090	1540	-	0.00	2
47	ADV	18/08/2011-09/09/2011	230.65-252.39	21.74	3126	>780	780	0.13	10
48	ADP	09/09/2011-12/10/2011	252.35-285.64	33.29	23986	1466	-	0.00	2
49	ADV	12/10/2011-24/11/2011	285.77-322.55	36.78	3532	>780	780	0.23	15
50	ADP	24/11/2011-18/01/2012	328.38-18.96	55.58	39835	>778	778	3.63	2
51	ADV	24/02/2012-19/03/2012	-	0	-	-	-	-	15
52	ADP	19/03/2012-25/04/2012	79.65-116.52	36.86	26549	779	-	0.00	2
54	-	07/05/2012-28/06/2012	-	0		-	-	-	-
55	ADP	29/06-2012-23/08/2012	181.45-223.0	41.55	30203	>1575	1575	0.00	2
56	-	23/08/2012-15/10/2012	-	0	-	-	-	-	-
57	-	25/10/2012-05/12/2012	-	0	-	-	-	-	-
58	ADV	05/12/2012-24/01/2013	340.33-365.96	25.630	2462	>1529	1529	1.59	15
59	ADP	24/01/2013-07/03/2013	24.59-66.39	41.80	28727	>1539	1539	2.58	2
60	ADV	07/03/2013-28/03/2013	66.43-87.64	21.21	2037	>1529	1529	0.44	15
62	ADP	28/03/2013-22/04/2013	87.68-112.50	24.82	17889	>1575	1575	0.00	2
63	ADV	22/04/2013-17/05/2013	112.54-137.30	24.76	2378	1468	-	0.00	15
65	ADP	17/05/2013-27/06/2013	137.34-178.49	41.14	29636	1501	-	0.00	2
67	ADV	27/06/2013-24/07/2013	178.54-205.39	26.85	2579	891	-	0.00	15
69	ADP	24/07/2013-21/08/2013	205.43-233.61	28.19	20307	>1541	1541	0.01	2
71	ADV	21/08/2013-17/09/2013	233.65-260.49	26.84	2578	868	-	0.00	15
73	ADP	23/09/2013-16/10/2013	266.48-289.49	23.01	16579	>781	781	0.17	2
75	ADV	16/10/2013-12/11/2013	289.53-316.55	27.02	2595	1170	-	0.85	15
78	ADP	28/11/2013-09/12/2013	332.49-343.58	11.09	8003	>779	779	2.52	2
80	ADV	09/12/2013-27/03/2014	-	-	-	-	-	-	-

Tabel 2.3: Overzicht van OBS (0.2 mab) metingen te MOW1.

Nr		measuring period	good data			OBS – SPM concentration			
			period (julian day)	days	data	max (mg/l)	saturation (mg/l)	% data saturated	inter-val (min)
5	ADV	07/02/2005-08/02/2005	38.51-39.30	0.78	454	814	-	0.00	2.5
6	ADV	04/04/2005-15/04/2005	94.46-105.31	10.84	78065	>780	780	48.12	0.2
7	ADV	22/06/2005-11/07/2005	173.34-187.5	14.16	101925	>3165	3165	0.00	0.2
8	ADV	22/11/2005-05/12/2005	326.35-339.37	13.02	622	3126	-	0.00	10
9	ADV	13/02/2006-27/02/2006	44.48-58.44	13.96	668	>3216	3216	0.60	30
10	ADV	27/03/2006-18/04/2006	86.46-108.37	21.92	1052	3194	-	0.00	30
11	ADV	15/05/2006-15/06/2006	135.49-166.42	30.94	1285	3288	-	0.00	30
15	ADV	10/07/2007-19/07/2007	191.75-200.56	8.81	1269	2837	-	0.00	10
16	ADV	23/10/2007-28/11/2007	296.53-332.41	35.88	5168	>3220	3220	0.00	10
21	ADV	17/11/2008-12/12/2008	322.58-347.38	24.80	3541	>3114	3114	0.54	10
22	ADV	09/02/2009-19/03/2009	40.49-78.32	37.83	5355	>3219	3219	1.27	10
23	ADV	26/03/2009-29/04/2009	85.34-109.0	23.66	3403	>3219	3219	0.01	10
27	-	10/09/2009-21/10/2009	-	0		-	-	-	-
30	ADP	06/11/2009-08/12/2009	310.36-342.63	32.27	46488	>1577	1577	1.16	1
31	ADP	11/12/2009-25/01/2010	345.35-25.25	44.90	65218	>1578	1578	1.17	1
32	ADV	25/01/2010-25/03/2010	25.65-84.43	58.78	8465	3041	-	0.00	10
33	ADP	25/03/2010-20/05/2010	84.46-134.0	19.54	71339	>1577	1577	8.99	1
37	ADP	06/09/2010-18/10/2010	-	-		-	-	-	2
38	ADV	18/10/2010-08/11/2010	291.55-312.99	21.43	1281	>3124	3124	1.09	15
39	ADP	17/11/2010-15/12/2010	321.50-349.61	28.11	20257	>1539	1539	8.50	2
40	ADV	15/12/2010-31/01/2011	-	-	-	-	-	-	-
41	-	31/01/2011-21/03/2011	-	0	-	-	-	-	-
42	ADV	21/03/2011-24/03/2011	80.73-83.25	2.52	243	>3122	3122	2.88	15
43	ADV	24/03/2011-17/04/2011	83.32-107.70	24.38	2341	>3125	3125	1.11	15
44	ADP	29/04/2011-23/05/2011	119.43-143.68	24.25	17473	>1575	1575	3.47	15
45	ADV	23/05/2011-19/06/2011	143.64-170.59	26.94	2587	>3128	3128	4.17	15
46	ADP	11/07/2011-12/08/2011	192.68-224.73	32.05	18977	1530	-	5.32	2
47	ADV	18/08/2011-09/09/2011	230.65-252.39	21.74	3126	>3131	3131	10.27	10
48	ADP	09/09/2011-12/10/2011	252.35-285.64	33.29	23986	>1577	1577	7.18	2
49	ADV	12/10/2011-24/11/2011	285.77-322.55	36.78	3532	1669	-	0.00	15
50	ADP	24/11/2011-18/01/2012	328.38-18.96	55.58	39835	>1542	1542	1.05	2
51	ADV	24/02/2012-19/03/2012	-	0	-	-	-	-	15
52	ADP	19/03/2012-25/04/2012	79.65-116.52	36.86	26549	>1540	1540	1.21	2
54	-	07/05/2012-28/06/2012	-	0		-	-	-	-
55	ADP	29/06-2012-23/08/2012	181.45-216.5	35.05	25307	>1575	1575	0.57	2
56	-	23/08/2012-15/10/2012	-	0	-	-	-	-	-
57	-	25/10/2012-05/12/2012	-	0	-	-	-	-	-
58	ADV	05/12/2012-24/01/2013	340.33-365.96	25.63	2462	>3120	3120	2.56	15
59	ADP	24/01/2013-07/03/2013	24.59-66.39	41.80	28727	>1577	1577	5.45	2
60	ADV	07/03/2013-28/03/2013	66.43-87.64	21.21	2037	>3124	3124	0.44	15
62	ADP	28/03/2013-22/04/2013	87.68-112.50	24.82	17889	>1525	1525	6.33	2
63	ADV	22/04/2013-17/05/2013	112.54-137.30	24.76	2378	>3125	3125	0.29	15
65	ADP	17/05/2013-27/06/2013	137.34-178.49	41.14	29636	>1542	1542	3.17	2
67	ADV	27/06/2013-24/07/2013	178.54-205.39	26.85	2579	2777	-	0.00	15
69	ADP	24/07/2013-21/08/2013	205.43-233.61	28.19	20307	>1542	1580	1.31	2
71	ADV	21/08/2013-17/09/2013	233.65-260.49	26.84	2578	3124	-	0.00	15
73	ADP	23/09/2013-16/10/2013	266.48-289.49	23.01	16579	>1576	1576	2.12	2
75	ADV	16/10/2013-12/11/2013	289.53-316.55	27.02	2595	>3130	3130	0.85	15
78	ADP	28/11/2013-09/12/2013	332.49-339.50	7.01	5057	>1579	1579	1.70	2
80	ADV	09/12/2013-27/03/2014	-	-	-	-	-	-	-

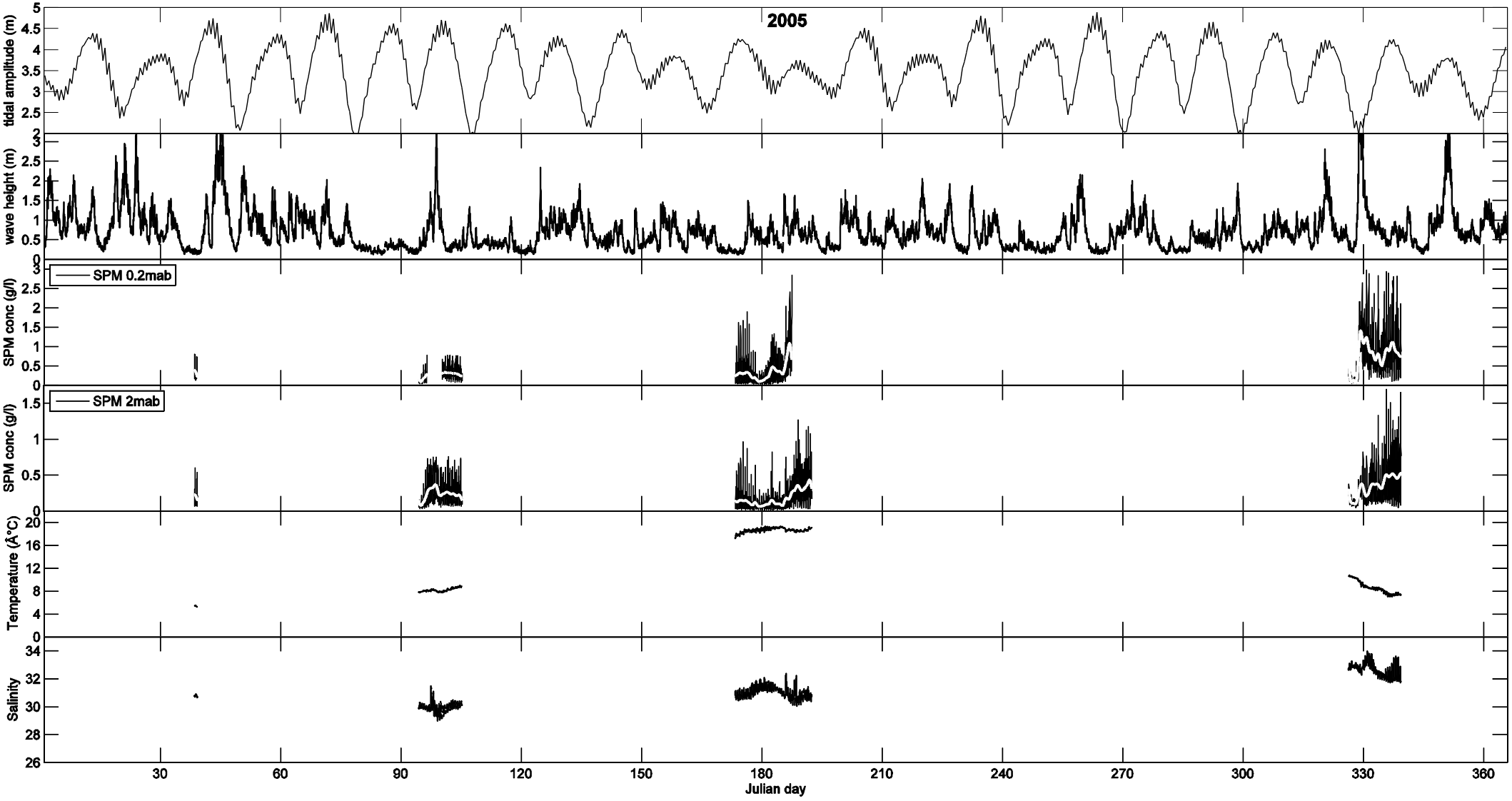

Figuur 2.3a: 2005, getijamplitude, significante golfhoogte, SPM concentratie, saliniteit en temperatuur te MOW1.

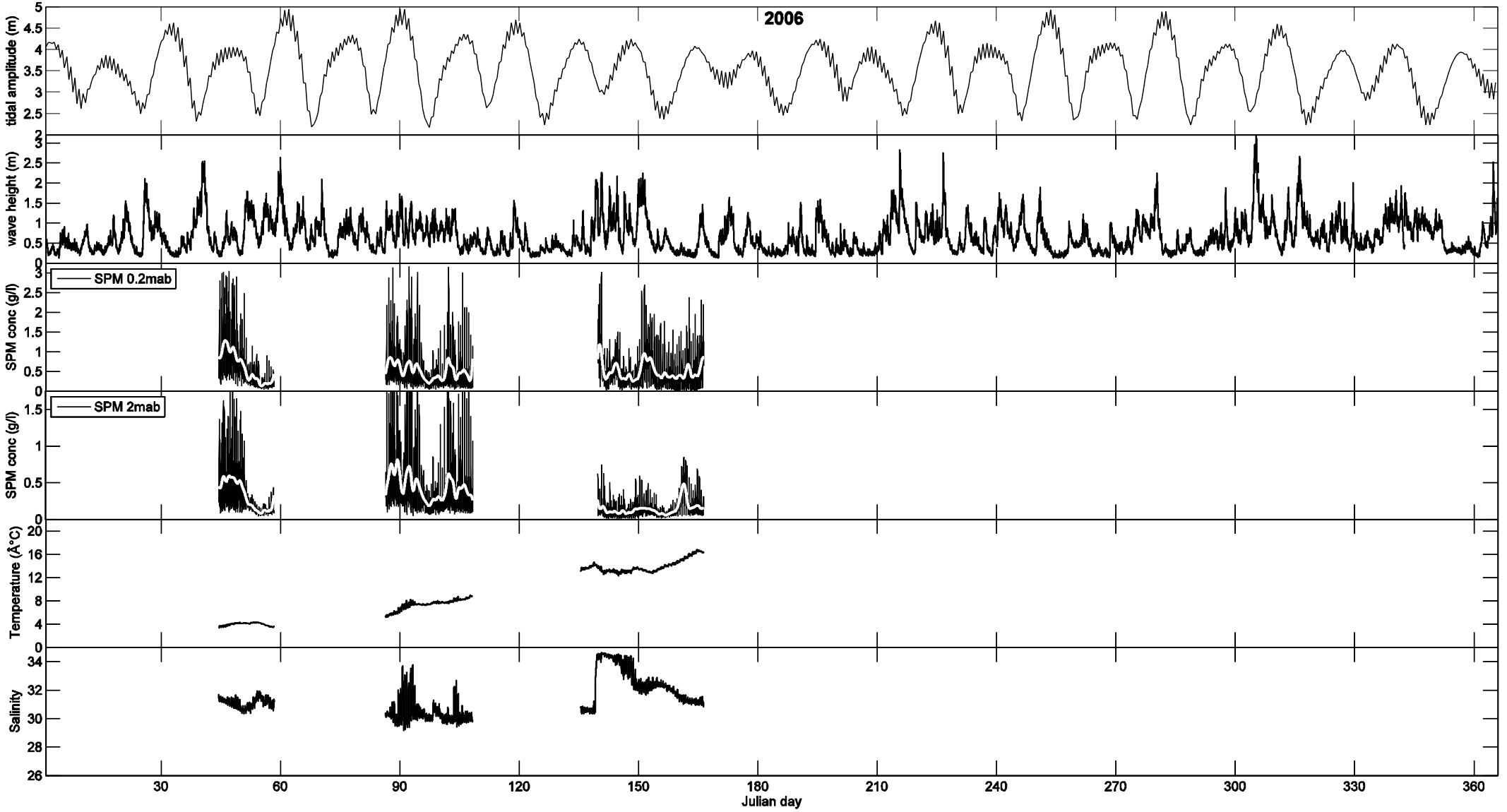

Figuur 2.3b: 2006, getijamplitude, significante golfhoogte, SPM concentratie, saliniteit en temperatuur te MOW1.

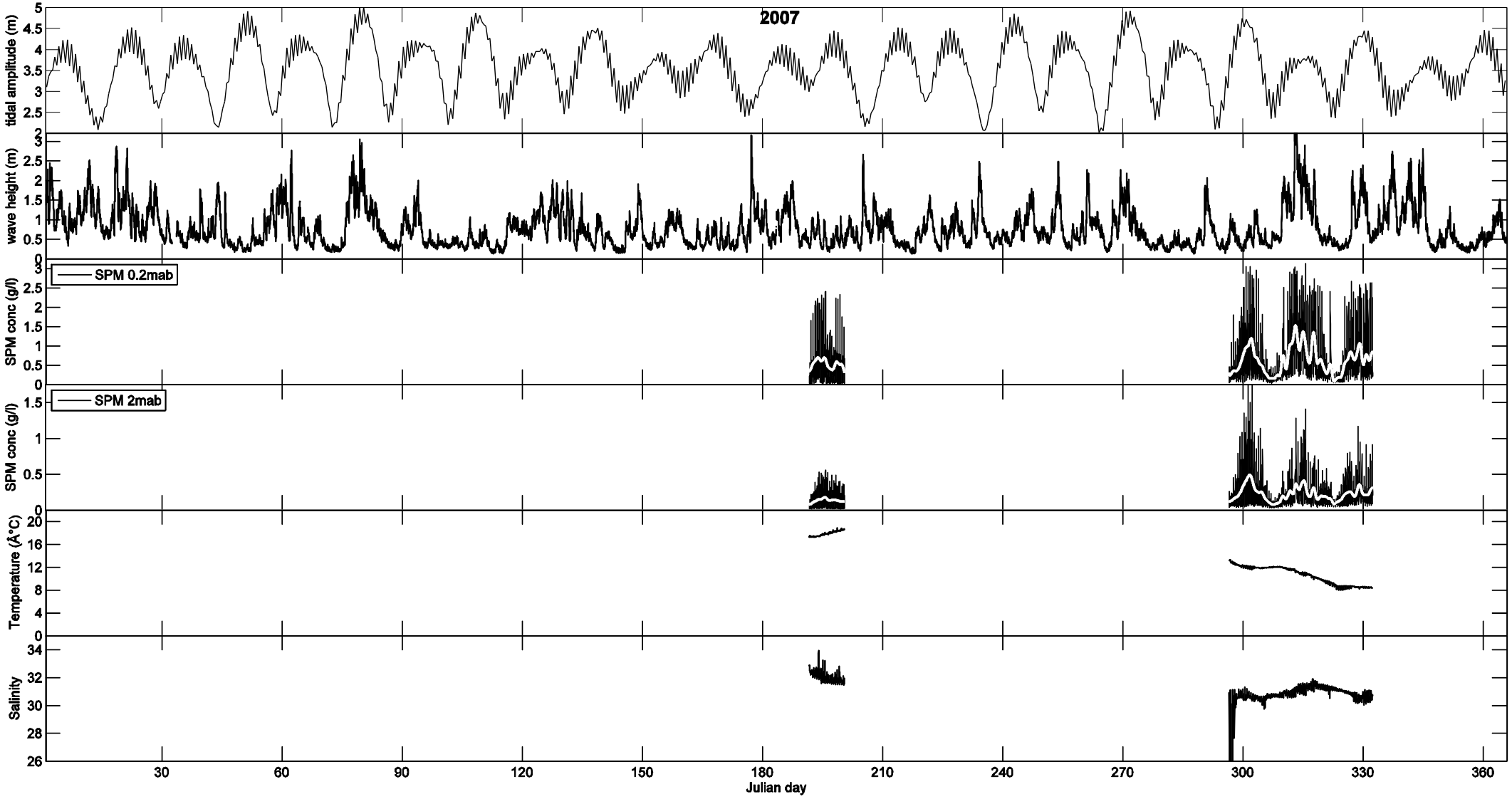

Figuur 2.3c: 2007, getijamplitude, significante golfhoogte, SPM concentratie, saliniteit en temperatuur te MOW1.

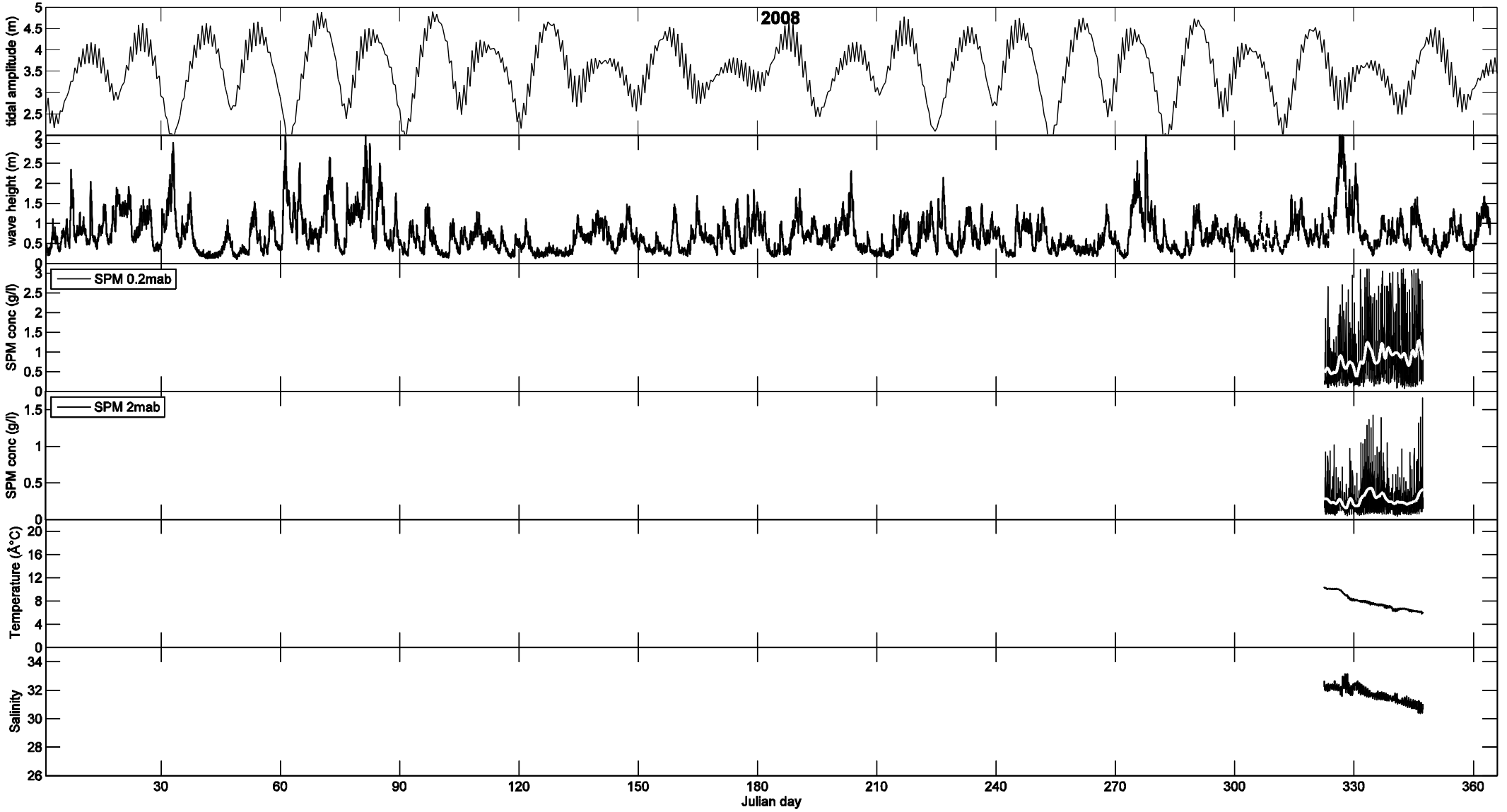

Figuur 2.3d: 2008, getijamplitude, significante golfhoogte, SPM concentratie, saliniteit en temperatuur te MOW1.

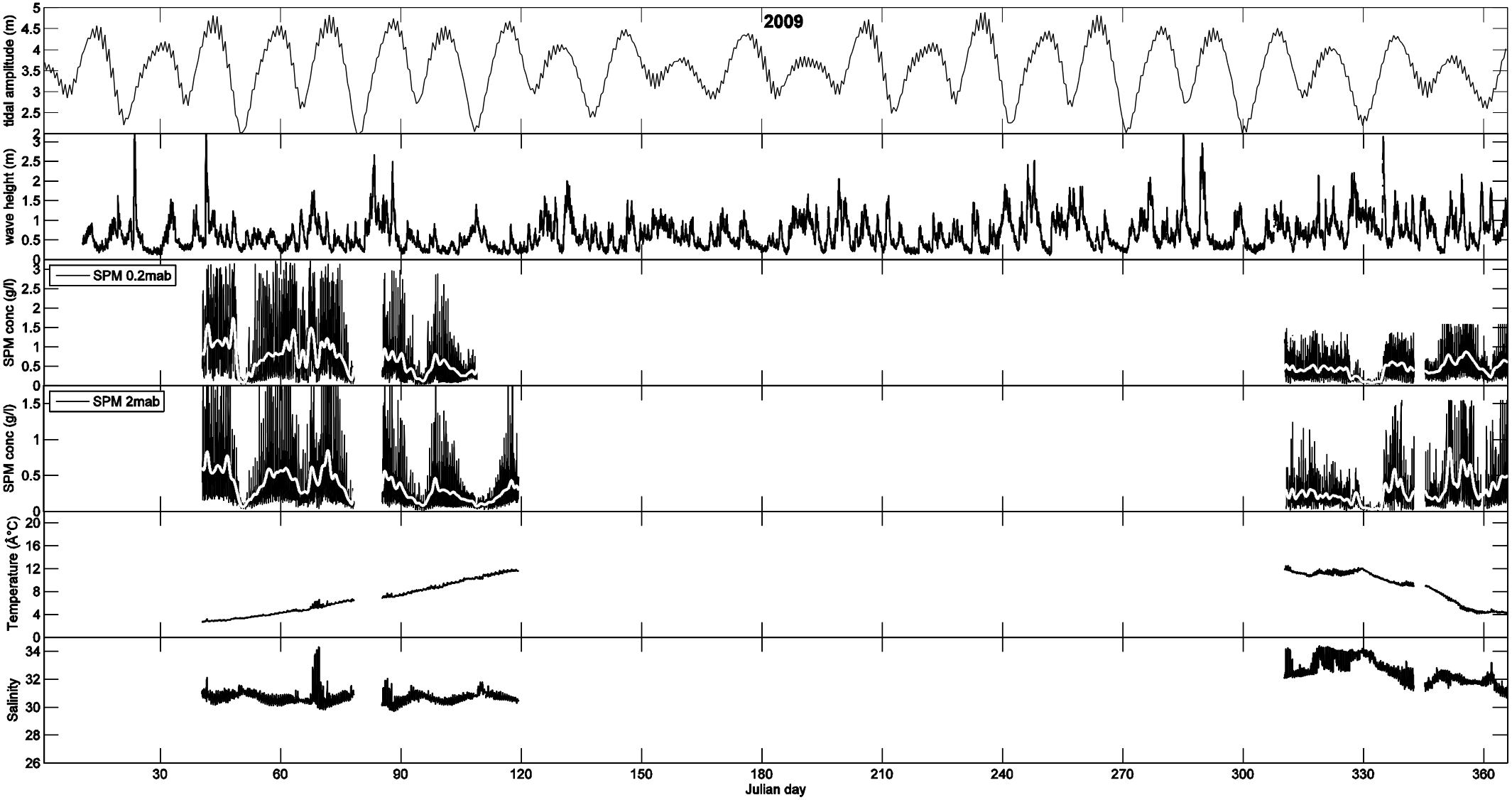

Figuur 2.3e: 2009, getijamplitude, significante golfhoogte, SPM concentratie, saliniteit en temperatuur te MOW1.

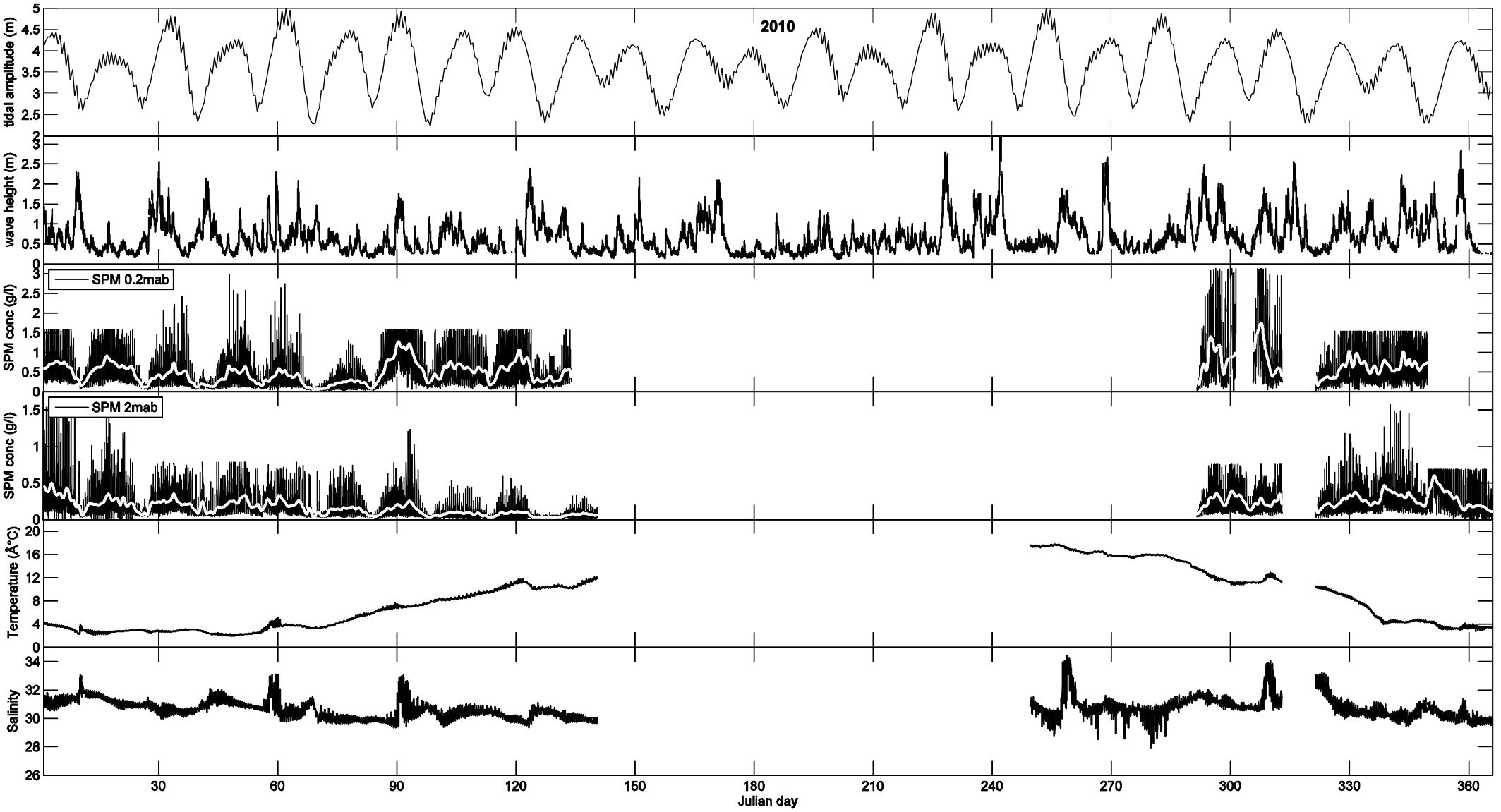

Figuur 2.3f: 2010, getijamplitude, significante golfhoogte, SPM concentratie, saliniteit en temperatuur te MOW1.

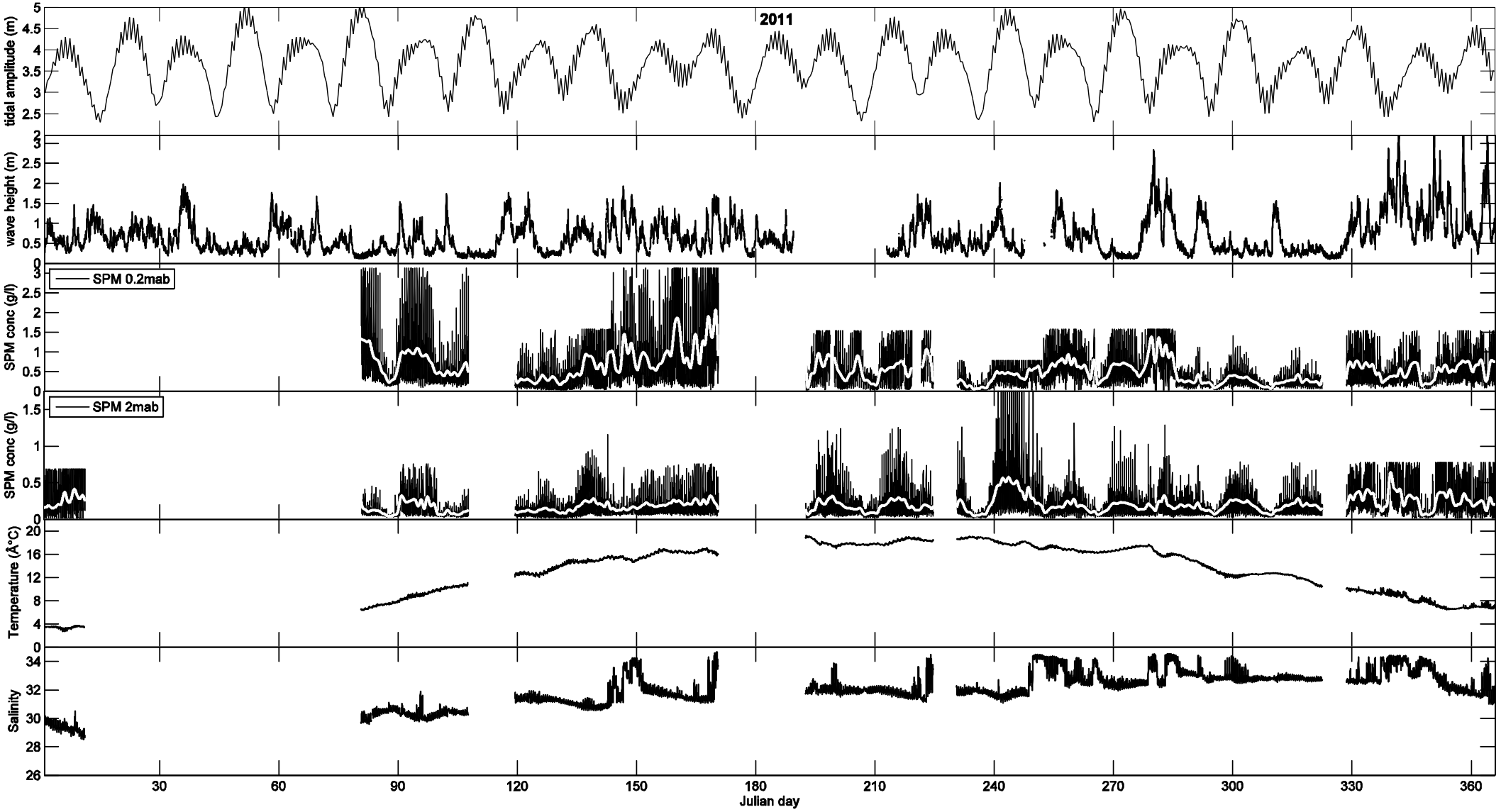

Figuur 2.3g: 2011, getijamplitude, significante golfhoogte, SPM concentratie, saliniteit en temperatuur te MOW1.

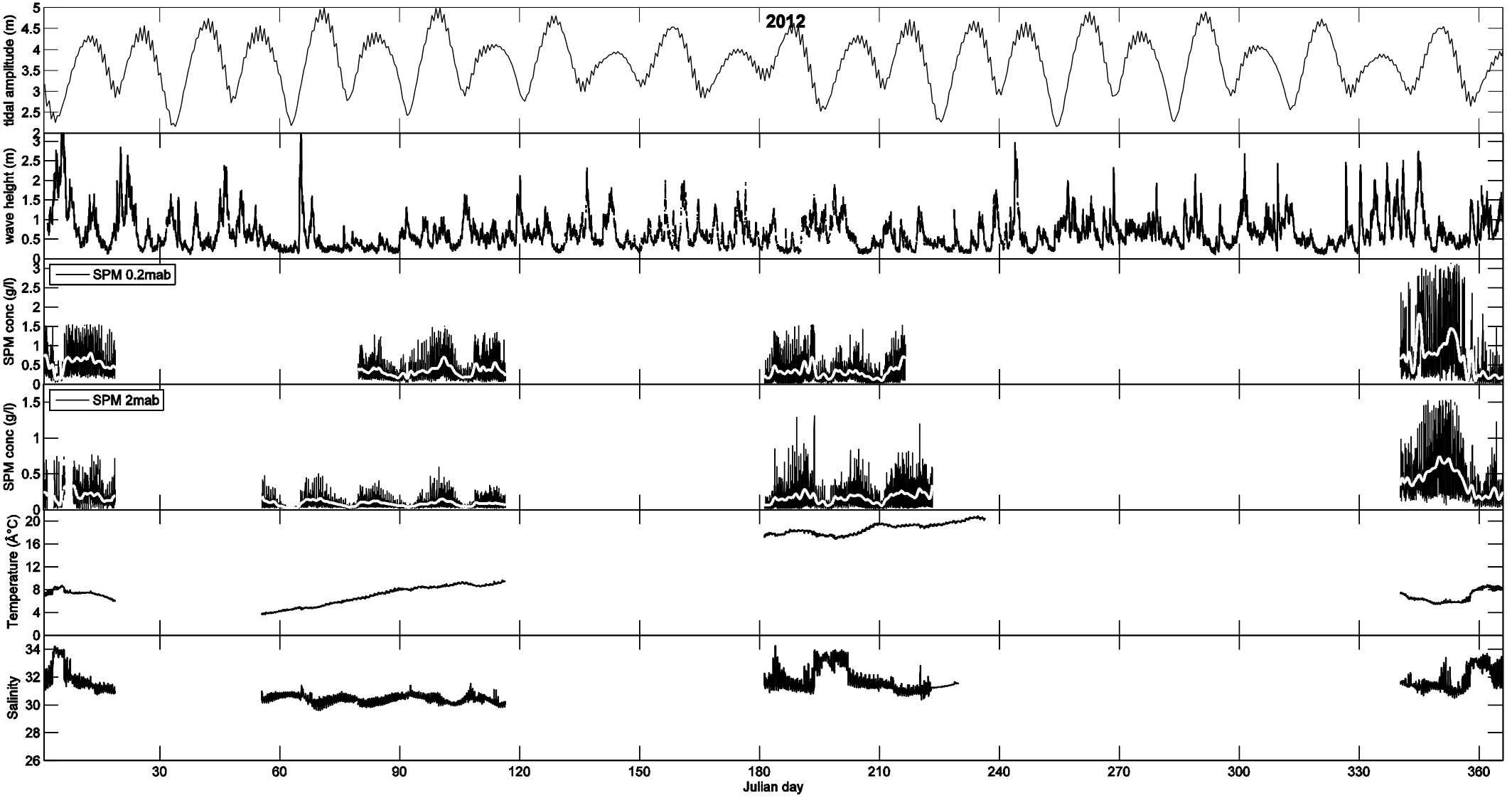

Figuur 2.3h: 2012, getijamplitude, significante golfhoogte, SPM concentratie, saliniteit en temperatuur te MOW1.

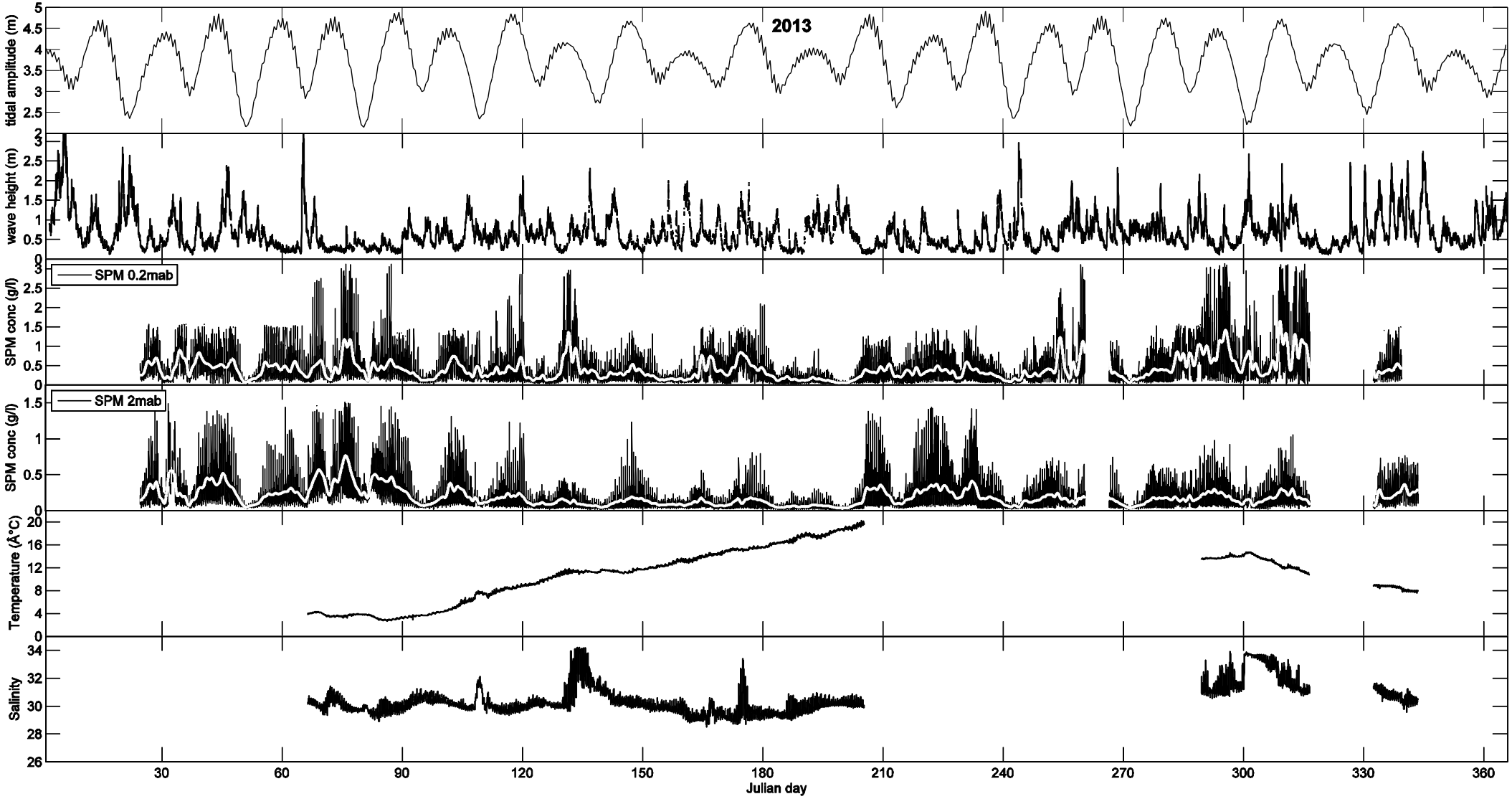

Figuur 2.3i: 2013, getijamplitude, significante golfhoogte, SPM concentratie, saliniteit en temperatuur te MOW1.

3. Classificatie van de data

Voor de classificatie van de data werd dezelfde methodologie gebruikt als beschreven in het vorige rapport (Fettweis et al. 2014a). De metingen omvatten 2096 (OBS 0.2 mab) en 2252 getijcycle (OBS 2 mab). Deze werden geklasseerd volgens getijamplitude en seizoenen. Hiervoor werd gebruik gemaakt van het harmonisch getijsignaal en dus niet van het gemeten getij. Er werd onderscheid gemaakt tussen superspringtij, springtij, gemiddeld tij, doodtij en superdoodtij. Deze indeling komt overeen met de P90 (4.41 m), P66 (3.95 m), P33 (3.31 m) en P10 (2.70 m) percentielen in getijamplitude, zie Tabel 3.1. Indeling in seizoenen werd beperkt tot de periode met lage en hoge oppervlakte SPM concentratie. De periode van april tot september (zomer) wordt gekarakteriseerd door lagere en deze van oktober tot maart door hogere SPM concentraties in de waterkolom (winter).

Voor de classifcatie volgens hydro-meteo condities werden de ADP stroomsnelheden opgesplitst in een alongshore en een cross-shore component. Op de alongshore component werd het getijsignaal eruit gefilter met behulp van een low-pass filter (PL64) (Flagg et al. 1976). In functie van de richting van deze residuele stroming werden de getijcycli gegroepeerd in 2 groepen: SW en NE. Negatieve waarden hebben een naar het SW gerichte residuele stroming, positieve een naar NE gerichte. De gesorteerde verdeling van getijcycli volgens residuele alongshore stroming wordt getoond in Tabel 3.2. De drempelwararde voor de groepering van de getijcycli is P85 (NE gerichte stroming) en P50 (SW gerichte stroming).

Tabel 3.1: Indeling van de data volgens getijamplitude.

Type getij	Amplitude	Frequentie
superspringtij	>4.41 m	10%
springtij	>3.95 m	33%
gemiddeld getij	3.31 – 3.95 m	33%
doodtij	<3.31 m	33%
superdoodtij	<2.70 m	10%

Tabel 3.2: Percentielen in residuele alongshore stroming.

Richting	Stroming (m/s)	Percentiel
NE	0.02	P90
-	0.00	P85
SW	-0.04	P66
SW	-0.06	P50
SW	-0.10	P33
SW0	-0.21	P10

In totaal beschikken we over 18 klassen of groepen. Voor elke klasse werd een gemiddeld verloop berekend door het geometrisch gemiddelde te berekenen. Een getijcyclus start met hoogwater (HW) en eindigt op het volgende HW. Elke getijcyclus werd geresampled om 50 datapunten (om de 15 minuten) per cyclus te bekomen. Voor elke gemiddelde getijcyclus worden fouten aangeduid die de standaardfout weergeven, dit is de geometrische standaardafwijking gedeeld door de vierkantswortel van het aantal getijden, *n* in de groep:

$$\text{standaardfout} = \frac{s}{\sqrt{n}} \tag{3.1}$$

4. Bodemnabije SPM dynamica te MOW1: OBS signaal

4.1. SPM concentratie: Alle data en seizoenen

De gemiddelde SPM concentratie tijdens een getij voor alle data en gegroepeerd volgens seizoen worden getoond in Figuren 4.1 en 4.2. De hoogste SPM concentraties treden op rond 1 uur voor LW (eb) en 2 uur na HW (vloed). De piek tijdens eb is hoger dan tijdens vloed, zie tabel 4.1. Tijdens vloed is er een dubbele piek aanwezig, waarbij de tweede groter is. Het maximum in SPM concentratie tijdens eb treedt iets vroeger op in de zomer dan in de winter. Minima in SPM concentratie zijn er rond 2 uur voor HW en 4 uur na HW.

In tegenstelling met de ADP-SPM concentraties, zijn de OBS SPM concentraties steeds groter in de winter dan de zomer. Maar ook hier merken we op dat het verschil tussen zomer en winter groter is op 2 m boven de bodem dan op 0.2 m. Zo is de maximale SPM concentratie op 0.2 m boven de bodem tijdens een vloed en eb respectievelijk 12% en 17% hoger dan in de zomer. Op 2 m boven de bodem is dit reeds 31% en 29%.

Tijdens kentering is het verschil tussen de seizoenen meer uitgesproken. In de zomer daalt de SPM concentratie relatief sterker dan in de winter. Tijdens de vloed-eb kentering is daarom de SPM concentratie op 0.2 m boven de bodem in de winter 52% hoger en tijdens de eb-vloed kentering zelfs 74%. Op 2 m boven de bodem is dit verschil meer uitgesproken en bedraag respectievelijk 119% en 116%. Deze bevindingen zijn in lijn met de LISST metingen en ondersteunen de bevindingen uit Fettweis et al. (2014a, 2014b) betreffende seizoenale variaties in SPM concentratie, waarin aangehaald wordt dat de biologische activiteit in de zomer voor een hoge concentratie aan kleverige organische molekulen (TEP) zorgt. Deze maken de macrovlokken sterker en verhogen hun frequentie in de zomer met als gevolg een snellere bezinking.

Het verloop van de SPM concentratie in Figuren 4.1 en 4.2 volgt maar deels de stroming. Ter verduideliking hernemen we hier een figuur (Figuur 4.3) uit Fettweis et al. (2014a), waarin we zien dat tijdens eb de piek in stroomsnelheid overeenkomt met de piek in SPM concentratie, maar dat tijdens vloed de piek in stroomsnelheid niet overeenkomt met de maximale waarde, maar met de secundaire piek in SPM concentratie die iets vroeger optreedt. Maximale SPM concentratie tijdens vloed is er pas na HW (zie Tabel 4.1).

Tabel 4.1: Invloed van seizoenen op SPM concentratie (mg/l) tijdens een getij: Maxima en minima.

	SPM 0.2 mab (mg/l)		SPM 2 mab (mg/l)	
	year			
max flood	1.7h after HW	415	1.2h after HW	171
slack	3.7h after HW	227	4.0h after HW	86
max ebb	0.7h before LW	537	0.5h before LW	241
slack	2.0h before HW	201	2.0 before HW	84
	winter			
max flood	2.0h after HW	448	1.7h after HW	206
slack	3.7h after HW	274	4.0h after HW	125
max ebb	0.7h before LW	578	0.5h before LW	272
slack	2.0h before HW	259	2.0 before HW	121
	summer			
max flood	1.5h after HW	400	0.5h after HW	157
slack	3.7h after HW	180	4.0h after HW	57
max ebb	0.7h before LW	492	0.5h before LW	211
slack	2.0h before HW	149	2.0h before HW	56

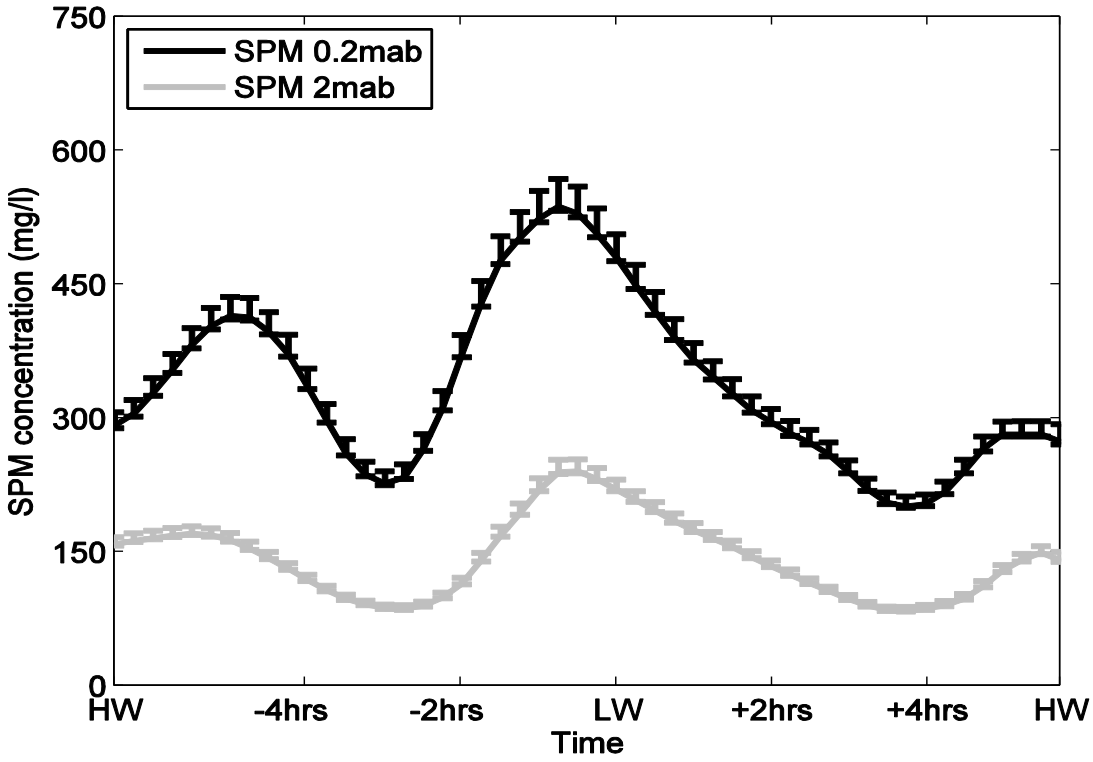

Figuur 4.1: Gemiddelde SPM concentratie(mg/l) tijdens een getij voor alle data op 0.2 en 2 meter boven de bodem.

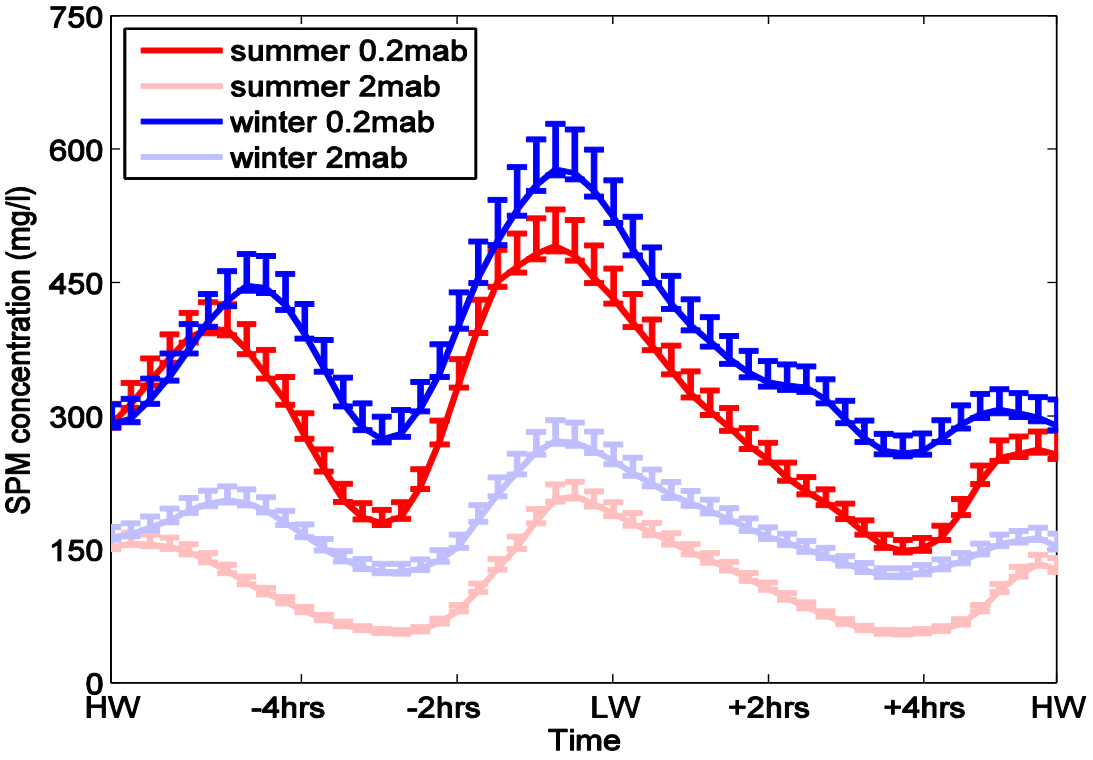

Figuur 4.2: Gemiddelde SPM concentratie(mg/l) tijdens een getij voor de winter (blauw) en de zomer (rood) op 0.2 en 2 meter boven de bodem.

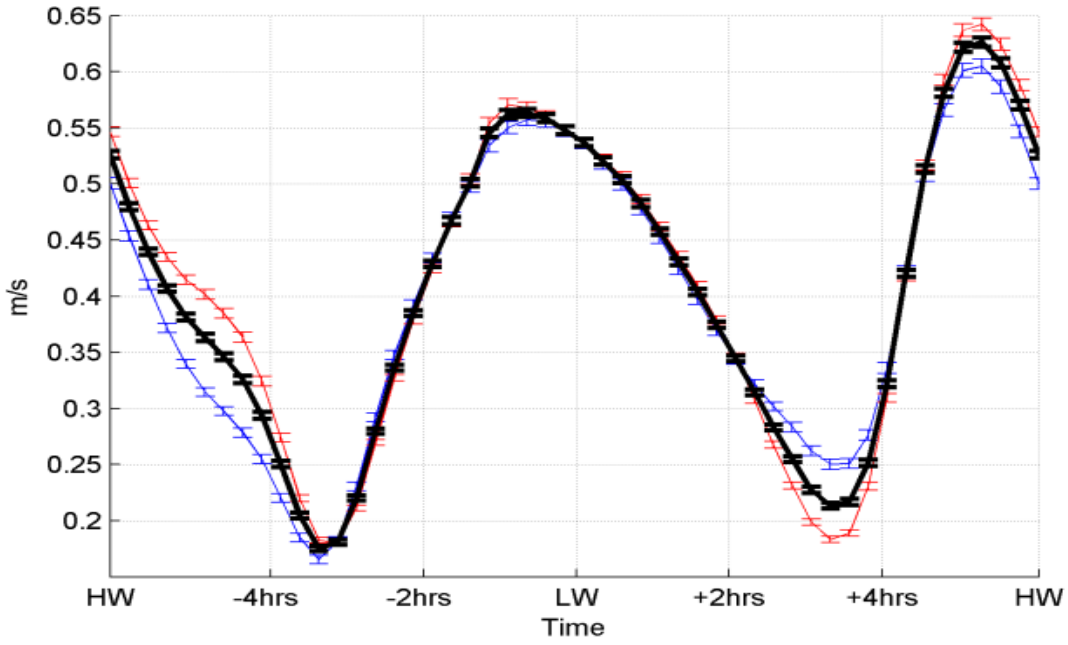

Figuur 4.3: Verticaal gemiddelde stroming tijdens de winter (blauw), de zomer (rood) en alle data (zwart). (uit Fettweis et al. 2014a).

4.2. SPM concentratie: Getijamplitude en seizoenen

De getijcycli werden gegroepeerd volgens getijamplitude en seizoenen, zie tabellen 4.2-4.4 en Figuren 4.4-4.6. Getijamplitude heeft een groot effect op het verloop van de gemiddelde SPM concentratie tijdens een getij. Naast een verschil in concentratie is zien we ook dat het tijdstip van de maximale SPM concentratie tijdens vloed ongeveer 1.3 uur later is tijdens een superspringtij dan een superdoodtij. De maximale SPM concentratie treed daarentegen ongeveer 1 uur vroeger op tijdens een superspringtij dan een superdoodtij Vloed-eb kentering treed ongeveer één uur later, en eb-vloed kentering ongeveer één uur vroeger op tijdens een superspringtij dan een superdoodtij.

De seizoenale effecten werden boven beschreven, samenvattend zien we ook hier dat SPM concentraties in de winter hoger zijn dan in de zomer (zie Tabel 4.5). Ook tijdens kentering zijn de SPM concentraties altijd hoger in de winter dan de zomer. In functie van de getijamplitude zijn er wel verschillen zichtbaar (zie Figuur 4.7).

Op 2 m boven de bodem is de SPM concentratie altijd hoger in de winter, behalve tijdens een super-springtij en springtij, waar de SPM concentraties omstreeks HW en LW (enkel super-springtij) hoger zijn in de zomer. De hogere waarden in de zomer komen overeen met een snellere stijging van de SPM concentratie tijdens vloed en een hoger piekwaarde tijdens eb, bij deze getijamplitudes. Op 0.2 m boven de bodem is de SPM concentraties hoger in de winter, behalve tijdens super-doodtij, doodtij, springtij en superspringtij waar de SPM concentraties tussen HW en ongeveer 2 uur na HW en tijdens het begin van de eb (enkel super-doodtij en super-springtij) hoger zijn in de zomer.

Tabel 4.2: Invloed van seizoenen en getijamplitude op SPM concentratie tijdens een getij: Maxima en minima.

	SPM 0.2 mab (mg/l)		SPM 2 mab (mg/l)	
	year, super spring tide (tidal range > 4.41 m, P90)			
max flood	2.5h after HW	689	1.5h after HW	246
slack	4.0h after HW	278	4.2h after HW	108
max ebb	0.7h before LW	921	0.7h before LW	369
slack	1.4h before HW	217	1.7 before HW	101
	year, spring tide (tidal range > 3.31, P66)			
max flood	1.7h after HW	558	1.5h after HW	220
slack	3.7h after HW	262	4.0h after HW	97
max ebb	0.7h before LW	763	0.7h before LW	369
slack	1.7h before HW	226	2.0h before HW	63
	year, mean tide (tidal range: 3.31-3.95m)			
max flood	1.7h after HW	415	1.2h after HW	173
slack	3.7h after HW	219	4.0h after HW	83
max ebb	0.7h before LW	537	0.5h before LW	238
slack	2.0h before HW	192	2.0h before HW	84
	year, neap tide (tidal range < 3.31, P33)			
max flood	1.5h after HW	288	1.0h after HW	122
slack	3.7h after HW	198	3.5h after HW	76
max ebb	0.2h before LW	358	0.2h before LW	151
slack	2.2h before HW	182	2.0h before HW	73
	year, super neap tide (tidal range: < 2.70m, P10)			
max flood	1.2h after HW	235	0.5h after HW	99
slack	3.2h after HW	180	3.5h after HW	67
max ebb	0.2h after LW	282	0.2h after LW	114
slack	2.2h before HW	166	2.2 before HW	63

Tabel 4.3: Invloed van seizoenen en getijamplitude op SPM concentratie (mg/l) tijdens een getij in de winter: Maxima en minima.

	SPM 0.2 mab (mg/l)		SPM 2 mab (mg/l)	
	winter, super spring tide (tidal range > 4.41 m, P90)			
max flood	2.2h after HW	729	2.0h after HW	271
slack	3.7h after HW	369	4.2h after HW	166
max ebb	0.7h before LW	966	0.7h before LW	428
slack	2.0h before HW	297	2.0 before HW	128
	winter, spring tide (tidal range > 3.31, P66)			
max flood	2.2h after HW	600	1.7h after HW	269
slack	3.7h after HW	314	4.2h after HW	147
max ebb	0.7h before LW	832	0.7h before LW	398
slack	1.7h before HW	296	2.0h before HW	139
	winter, mean tide (tidal range: 3.31-3.95m)			
max flood	2.0h after HW	482	1.7h after HW	226
slack	3.7h after HW	283	4.0h after HW	119
max ebb	0.8h before LW	607	0.7h before LW	277
slack	2.0h before HW	192	2.0h before HW	84
	winter, neap tide (tidal range < 3.31, P33)			
max flood	2.2h after HW	298	1.2h after HW	136
slack	3.7h after HW	228	3.5h after HW	102
max ebb	0.2h before LW	376	0.2h before LW	175
slack	2.2h before HW	212	2.2h before HW	98
	winter, super neap tide (tidal range: < 2.70m, P10)			
max flood	1.2h after HW	218	1.2h after HW	99
slack	3.2h after HW	186	3.5h after HW	84
max ebb	LW	280	0.2h after LW	125
slack	2.7h before HW	191	2.2 before HW	81

Tabel 4.4: Invloed van seizoenen en getijamplitude op SPM concentratie (mg/l) tijdens een getij in de zomer: Maxima en minima.

	SPM 0.2 mab (mg/l)		SPM 2 mab (mg/l)	
	summer, super spring tide (tidal range > 4.41 m, P90)			
max flood	2.5h after HW	640	0.7h after HW	263
slack	4.0h after HW	188	4.2h after HW	63
max ebb	0.7h before LW	883	0.7h before LW	505
slack	1.4h before HW	145	1.4 before HW	68
	summer, spring tide (tidal range > 3.31, P66)			
max flood	1.7h after HW	549	0.7h after HW	212
slack	3.7h after HW	213	4.0h after HW	62
max ebb	0.5h before LW	703	0.7h before LW	343
slack	1.7h before HW	168	2.0h before HW	63
	summer, mean tide (tidal range: 3.31-3.95m)			
max flood	1.5h after HW	361	0.5h after HW	149
slack	3.7h after HW	159	4.0h after HW	55
max ebb	0.7h before LW	447	0.5h before LW	201
slack	2.0h before HW	131	2.0h before HW	54
	summer, neap tide (tidal range < 3.31, P33)			
max flood	0.5h after HW	312	0.5h after HW	111
slack	3.7h after HW	163	3.7h after HW	51
max ebb	0.5h before LW	292	0.2h after LW	124
slack	1.7h before HW	140	2.0h before HW	49
	summer, super neap tide (tidal range: < 2.70m, P10)			
max flood	1.2h after HW	266	0.5h after HW	97
slack	3.5h after HW	170	3.7h after HW	47
max ebb	0.5 before LW	292	0.2h after LW	99
slack	2.2h before HW	127	1.7 before HW	43

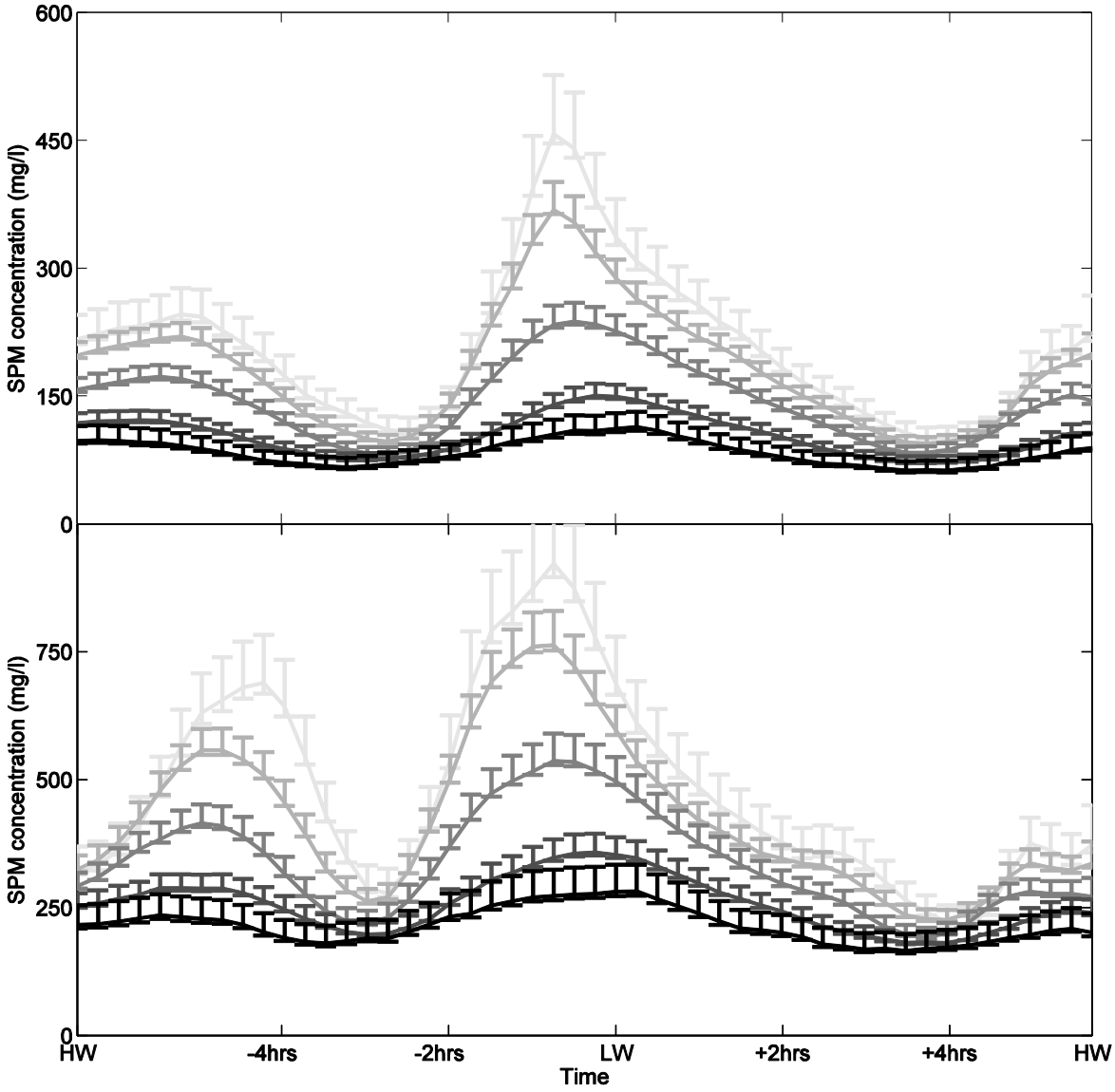

Figuur 4.4: Gemiddelde SPM concentratie(mg/l) tijdens een getij voor een superdoodtij (zwart), doodtij, gemiddeld tij, springtij en superspringtij (licht grijs) voor alle data op 2 mab (boven) en 0.2 mab (onder).

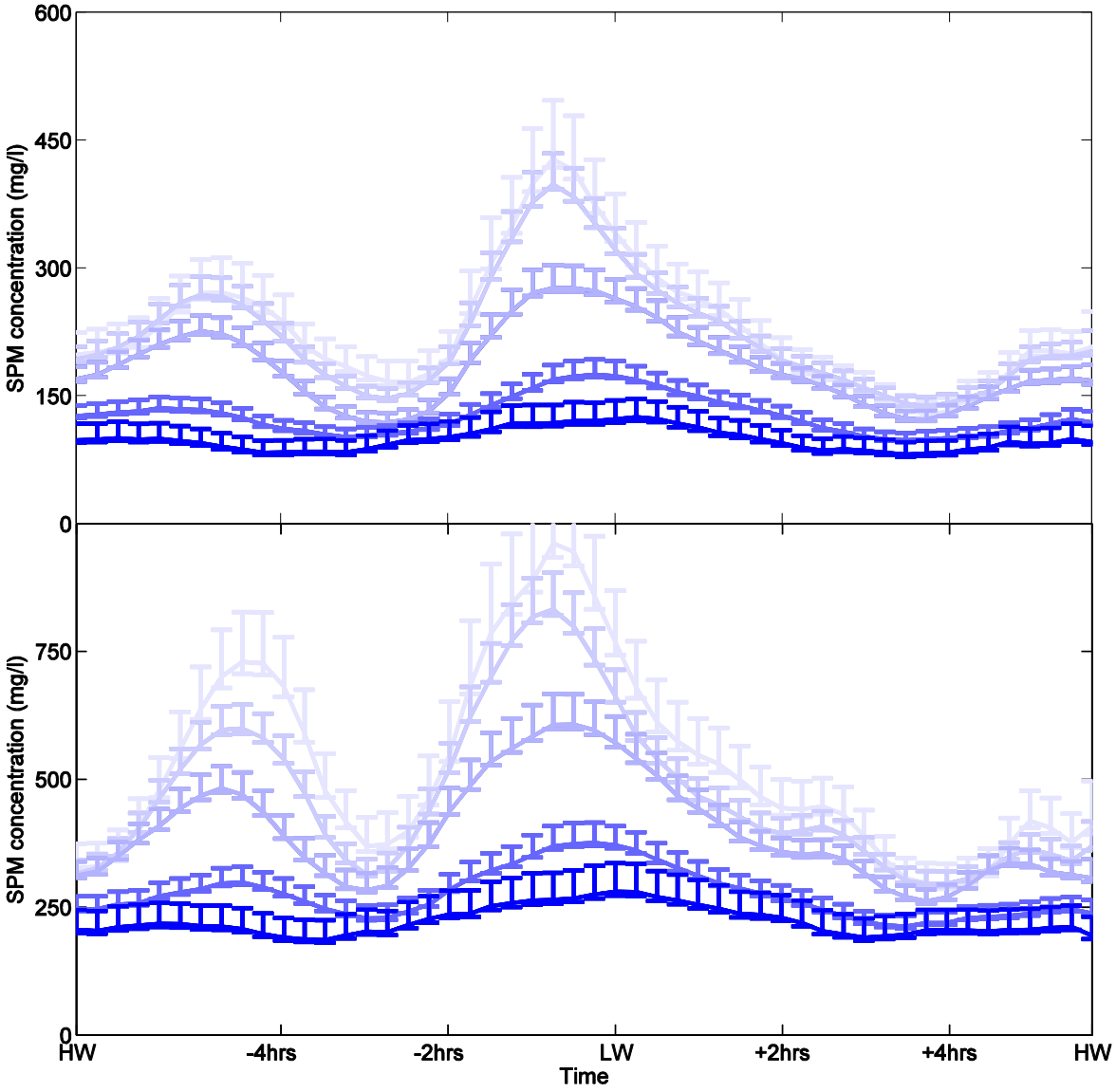

Figuur 4.5: Gemiddelde SPM concentratie(mg/l) tijdens een getij voor een superdoodtij (donker blauw), doodtij, gemiddeld tij, springtij en superspringtij (licht blauw) voor de winter op 2 mab (boven) en 0.2 mab (onder).

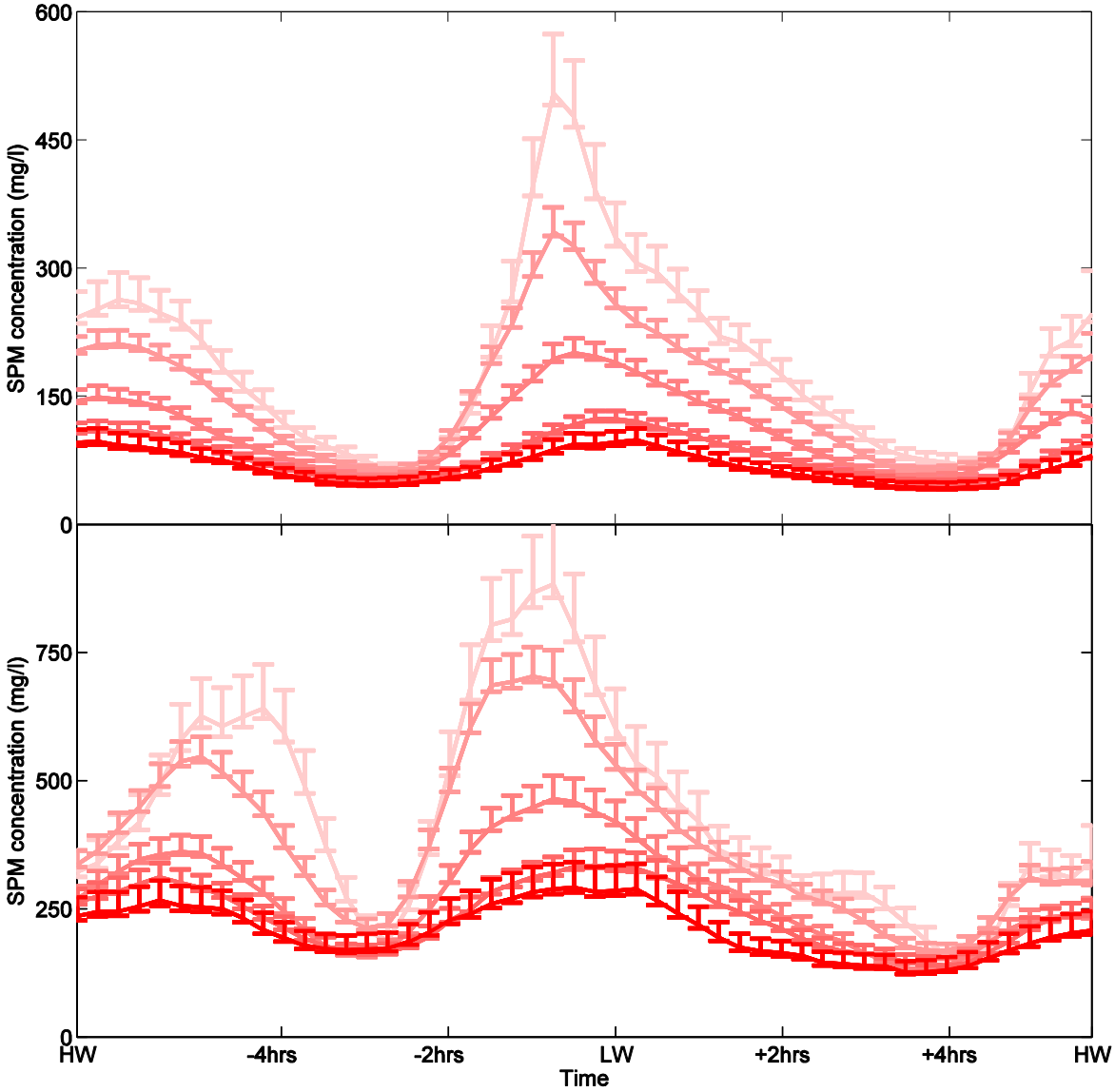

Figuur 4.6: Gemiddelde SPM concentratie(mg/l) tijdens een getij voor een superdoodtij (donker rood), doodtij, gemiddeld tij, springtij en superspringtij (licht rood) voor de zomer op 2 mab (boven) en 0.2 mab (onder).

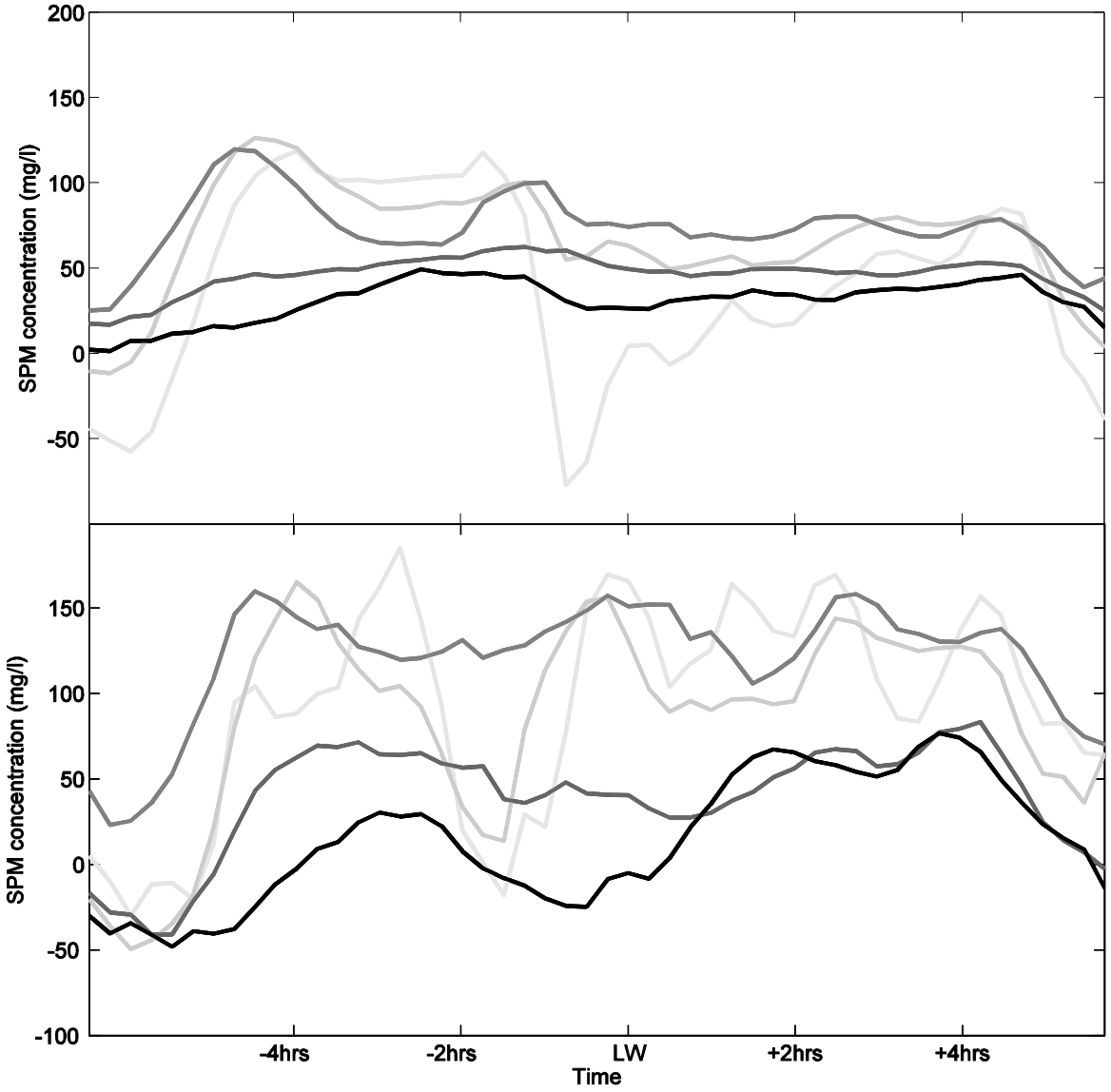

Figuur 4.7: Verschil in SPM concentratie (mg/l) tussen winter en zomer (positief: winter hogere waarden, negatief: zomer hogere waarden, zie Figuren 3.5 en 3.6) tijdens een getij voor een superdoodtij (zwart), doodtij, gemiddeld tij, springtij en superspringtij (licht grijs) voor de zomer op 2 mab (boven) en 0.2 mab (onder).

Tabel 4.5: Getijgemiddelde SPM concentratie per seizoen en getijamplitude.

	super spring	spring tide	mean tide	neap tide	super neap
SPM concentration 2 mab (mg/l)					
year	208±88	183±71	144±46	104±23	84±15
winter	230±74	221±67	185±47	127±22	98±13
summer	190±108	153±75	110±44	80±24	67±18
SPM concentration 0.2 mab (mg/l)					
year	478±191	423±151	336±99	257±52	215±34
winter	524±185	467±151	397±101	275±47	222±28
summer	431±199	382±154	277±96	236±61	208±51

4.3. SPM concentratie: Getijamplitude, seizoen en alongshore stroming

De effecten van de residuele alongshore stroming, seizoenen en getijamplitude zijn gebundeld in Figuren 4.8-4.10 en Tabel 4.6. Zonder rekeneing te houden met seizoenen zien we dat de SPM concentratie altijd groter is bij een NE dan bij een SW gerichte alongshore stroming en dit zowel op 2 als 0.2 m boven de bodem. Enkel tijdens het begin van de eb zijn deze verschillen minder uitgesproken.

In de winter (Figuur 4.9) is op 2 m boven de bodem de gemiddelde SPM concentratie tijdens springtij hoger bij een NE gerichte alongshore stroming, met uitzondering bij het begin van de eb (3 uur voor LW tot ongeveer LW) waar de SPM concentratie bij een SW gerichte alongshore stroming ongeveer even groot of groter is dan deze bij een NE gerichte. Gelijkaardige verlopen zijn er op 0.2 m boven de bodem, maar nu is de periode met hogere SPM concentratie tijdens SW gerichte stroming langer en dit vooral tijdens doodtij en springtij. Ook tijdens de zomer (Figuur 4.10) treden kwalitatieve verschillen op tussen de SPM concentratie op 0.2 en 2 m boven de bodem. Terwijl dicht tegen de bodem de SPM concentratie altijd hoger is bij een NE gerichte alongshore stroming, is er op 2 m boven de bodem de SPM concentratie gemiddeld hoger tijdens het begin van de eb voor een SW gerichte stroming.

De verschillen in SPM concentratie kunnen worden verklaard door golfwerking en advectie. In de ADP resultaten (zie Figuur 4.13 uit Fettweis et al. 2014a) is de (verticaal gemiddelde) SPM concentratie groter als de stroming in dezelfde richting wijst als de residuele alongshore stroming, dus bij eb is dit bij een SW gerichte en bij vloed bij een NE gerichte residuele stroming. Dit is ook aanwezig in het OBS signaal op 2 m boven de bodem, maar minder uitgesproken. Dicht tegen de bodem is het signaal meer verstoord (zie 0.2 mab en zomer) en volgt het niet meer het signaal hogerop in de waterkolom. Mogelijks is dit 'verstoord' signaal ook het gevolg van het relatief gering aantal getijcyclus in deze klasse (28). Maar er is ook een fysische oorzaak, met name een hogere SPM concentratie dicht tegen de bodem in de zomer tengevolge van een hogere bezinking van het SPM. De hogere SPM concentratie dicht tegen de bodem wordt mogelijks door advectie bij een NE gerichte alongshore versterkt.

De resultaten tonen aan dat te MOW1 het materiaal over het algemeen uit de richting van de Westerschelde komt tijdens eb, en in de richting van de Westerschelde getransporteerd wordt tijdens vloed, met uitzondering dicht tegen de bodem. Het feit dat de verschillen tussen NE en SW gerichte alongshore stroming meer uitgesproken zijn in de zomer dan de winter is deels het gevolg van de seizoensgebonden verschillen in SPM concentratie dicht tegen bodem.

Tabel 4.6: Getijgemiddelde SPM concentratie per seizoen, getijamplitude en alongshore stroming.

	NE-wards alongshore currents			SW-wards alongshore currents		
	spring tide	mean tide	neap tide	spring tide	mean tide	neap tide
SPM concentration 2 mab (mg/l)						
year	228±80	164±63	111±27	163±76	102±39	83±25
winter	284±98	215±70	124±30	188±78	154±55	132±40
summer	149±62	128±59	97±32	149±74	80±31	62±19
SPM concentration 0.2 mab (mg/l)						
year	544±138	440±149	308±61	388±155	234±73	235±52
winter	517±141	482±154	323±54	436±175	396±117	368±115
summer	628±165	409±154	291±85	353±144	176±60	177±38

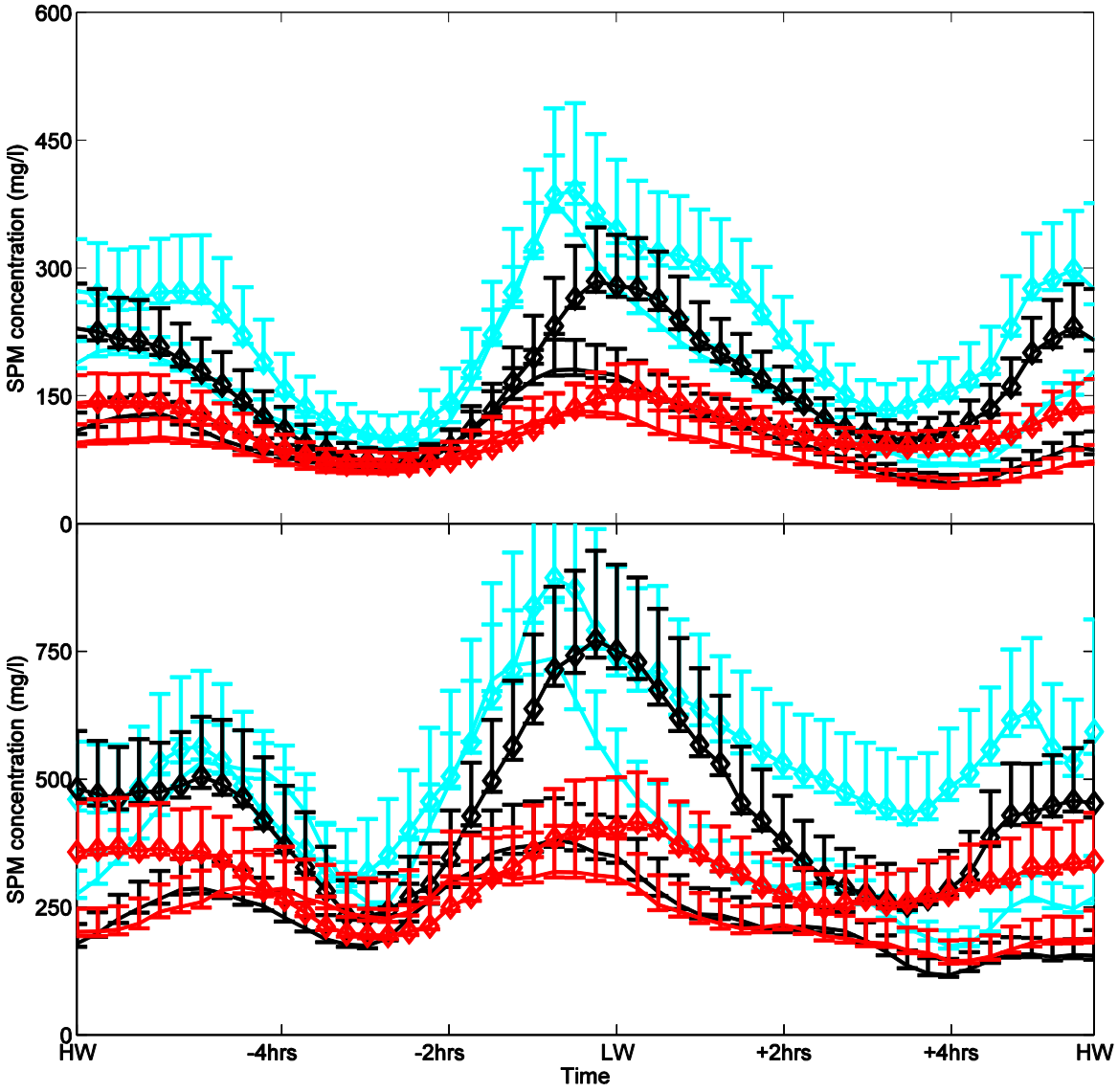

Figuur 4.8: Gemiddelde SPM concentratie(mg/l) tijdens een getij in functie van de alongshore stroming (all data). Springtij (cyaan) + NE (diamant) en SW gerichte stroming; gemiddeld tij (zwart) + NE (diamant) en SW gerichte stroming; doodtij (rood) + NE (diamant) en SW gerichte stroming op 2 mab (boven) en 0.2 mab (onder).

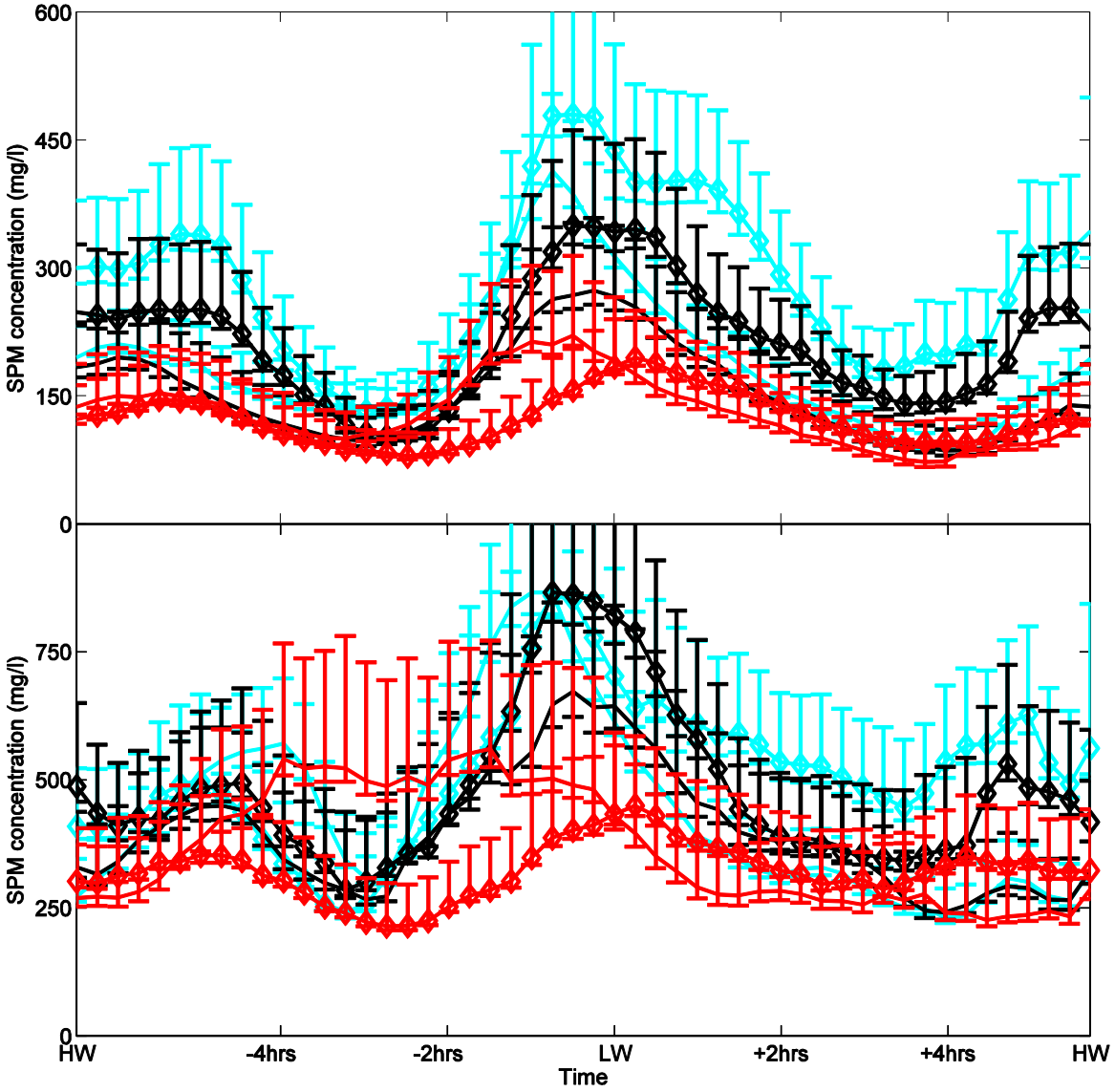

Figuur 4.9: Gemiddelde SPM concentratie(mg/l) tijdens een getij in functie van de alongshore stroming (winter). Springtij (cyaan) + NE (diamant) en SW gerichte stroming; gemiddeld tij (zwart) + NE (diamant) en SW gerichte stroming; doodtij (rood) + NE (diamant) en SW gerichte stroming op 2 mab (boven) en 0.2 mab (onder).

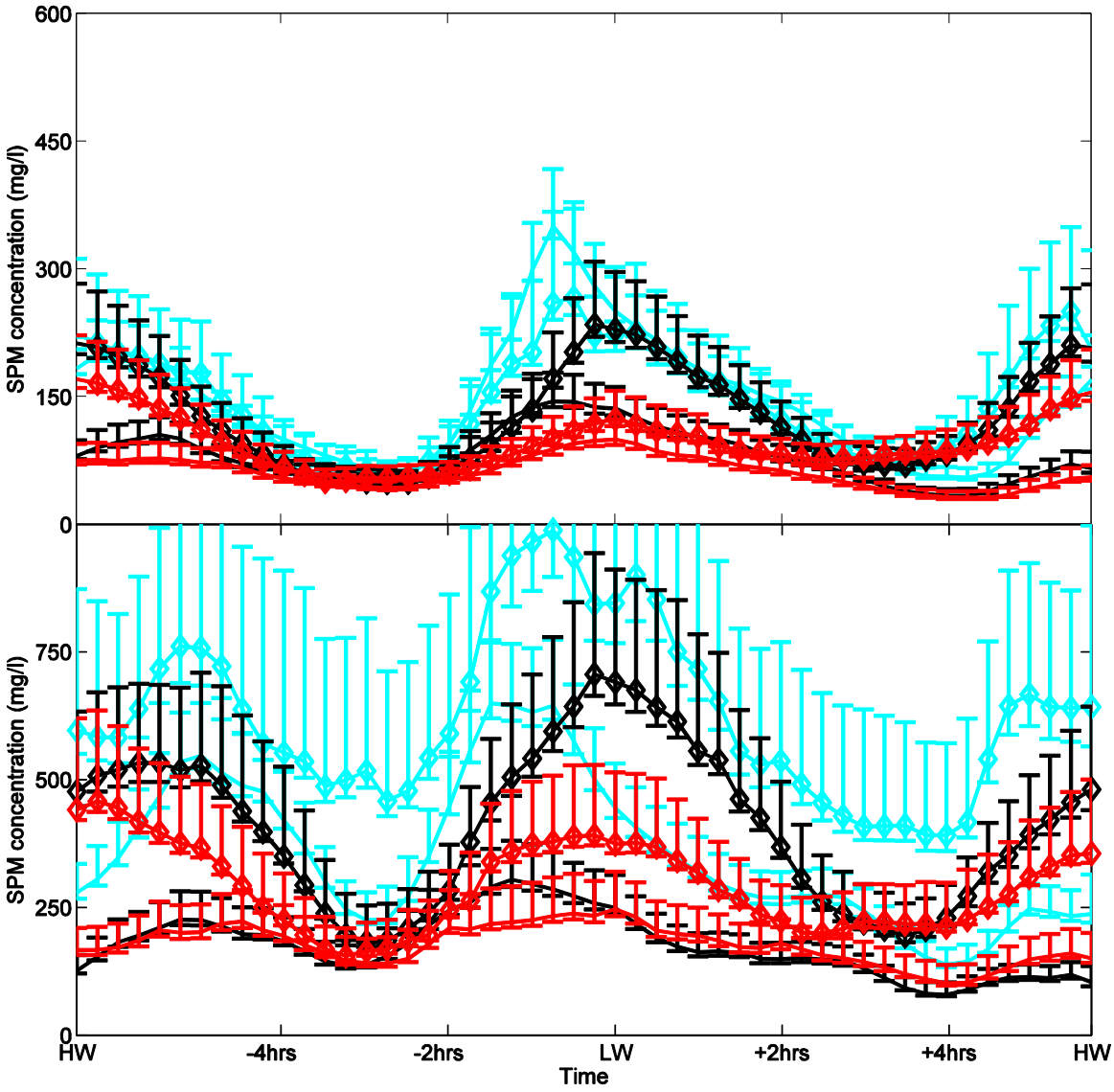

Figuur 4.10: Gemiddelde SPM concentratie(mg/l) tijdens een getij in functie van de alongshore stroming (zomer). Springtij (cyaan) + NE (diamant) en SW gerichte stroming; gemiddeld tij (zwart) + NE (diamant) en SW gerichte stroming; doodtij (rood) + NE (diamant) en SW gerichte stroming op 2 mab (boven) en 0.2 mab (onder).

4.4. Vergelijking SPM concentratie ADP-OBS

Een OBS en een ADP kan gebruikt worden om de SPM concentratie te meten, zie het vorige MOMO rapport voor de ADP resultaten (Fettweis et al. 2014a). De meetmethode van beide meettoestellen is verschillend zodat er zich de vraag opdringt over de nauwkeurigheid en vergelijkbaarheid van de meetresultaten. We zullen hier dit onderwerp enkel kort aanhalen, een uitgebreide vergelijking en inschatting van de onzekerheid van de beide meetmethodes is later gepland (zie taak 4.1 in hoofdstuk 1). Beide meettechnieken (akoestisch en optisch) zijn gebaseerd op het principe dat de partikels een deel van het door de externe bron uitgezonden signaal (bij de OBS is dit licht, bij de ADP geluid) reflecteren. De hoeveel aan teruggekaatst signaal is een functie van de concentratie en de eigenschappen (grootte, kleur, dichtheid, vorm, samenstelling) van de deeltjes. Calibratie van het signaal dient te gebeuren om SPM concentratie te bekomen. en is onderhevig aan een calibratieprocedure. Optische en akoestische signalen reageren verschillend, waardoor de gemeten SPM concentraties niet noodzakelijk gelijk zijn.

4.4.1. Calibratie van een OBS

Downing (2006) vermeld dat het OBS signaal verandert in functie van (in afnemende volgorde van belang) de SPM concentratie, partikelgrootte en partikelvorm. Voor de optische metingen met een OBS geldt dat bij (relatief) lage SPM concentraties (<5-g/l slib; <50-g/l zand) en voor deeltjes met een uniforme diameter, de belichte oppervlakte van het deeltje en aldus ook het weerkaatste licht, proportioneel is met de SPM massa concentratie. Door de filtratie van waterstalen kan een OBS worden gecalibreerd. De waterstalen werden zo dicht mogelijk bij de OBS genomen en er werd een numeriek verband (lineaire regressie) tussen het OBS signaal en de SPM concentratie berekend (Sternberg et al. 1991). De correlatiecoëfficiënt tussen de OBS waarden en de gefiltreerde waterstalen is hoog (R^2>0.9) te MOW1 (zie bv Backers et al. 2013), zodat we kunnen veronderstellen dat de SPM concentratie afgeleid uit de OBS een nauwkeurige weergave is van de concentratie bekomen door filtratie. De regressiecoëfficiënten zijn echter niet constant en kunnen (lichtjes) varieren tussen de meetcampagnes. Het is op dit moment niet helemaal duidelijk of deze variaties het gevolg zijn van meetfouten of getuigen van veranderingen in partikeleigenschappen.

4.4.2. Calibratie van een ADP

Na omvorming naar decibels, werd de signaalsterkte gecorrigeerd voor geometrische spreiding en afzwakking (attenuation) in het water. Nadien werd gebruik gemaakt van een iteratieve benadering (Kim et al. 2004) om het signaal te corrigeren. SPM concentratie afgeleid uit de bovenste OBS (OBS2) werd gebruikt om de eerste bin van de ADP te calibreren. De drie ADP's die gebruikt werden in de verankeringen werden telkens gecalibreerd voor 1 verankering. De bekomen regressiecoëfficiënten werden dan toegepast op alle verankeringen met deze ADP.

De correlatiecoëfficiënt tussen de ADP en de OBS SPM concentratie is minder goed (R^2~0.5), Figuur 4.11. De slechtere correlatie tussen ADP en OBS is waarschijnlijk het gevolg van verschillende reactie van de twee signalen op partikeleigenschappen. Zo werd in Fettweis et al. (2012) opgemerkt voor de tripode metingen te Blankenberge dat de OBS en de ADP bij bepaalde omstandigheden anders reageren waardoor de SPM concentraties significant kunnen verschillen. Zo was tijdens een SW storm de SPM concentratie van de OBS lager dan van de ADP. Het lagere OBS signaal tijdens de storm werd waarschijnlijk veroorzaakt door de gevoeligheid van de OBS voor veranderlijke korrelgrootte, omdat de OBS niet gecalibreerd werd voor zand maar voor slib (Baeye et al. 2011). Wegens deze korrelgrootteafhankelijkheid tijdens calibratie zou men een schijnbare stijging van de optische terugkaatsing moeten waarnemen wanneer vlokken uiteenbreken en dus een schijnbare verhoging van de concentratie (Agrawal & Traykowski 2001). Dit soort situaties, waar een veranderende partikelgrootte in suspensie een schijnbare verhoging van de SPM concentratie veroorzaakte, werden ook vermeld door Downing (2006) en treden op wanneer verschillende soorten sediment samenkomen.

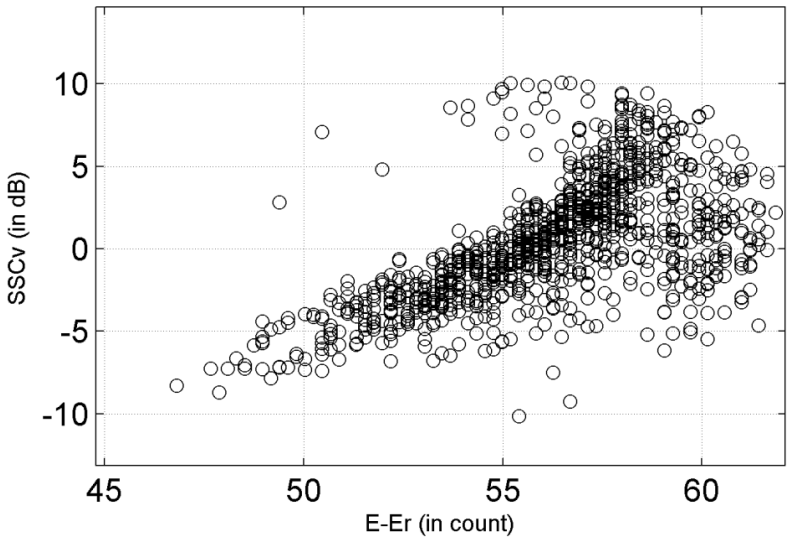

Figuur 4.11: Correlatie tussen ADP (1.8 mab) en OBS (2 mab) signaal (R^2=0.53) voor verankering 10 (zie tabel 2.2).

4.4.3. Vergelijking

In figuren 4.12-4.13 wordt de SPM concentratie van de OBS en deze van de ADP vergeleken. We zien dat alhoewel het verloop gelijkaardig is, dat de SPM concentratie sterk verschilt. Deze wordt onderschat door de ADP hoger in de waterkolom en overschat dichter tegen de bodem. Deze extremere SPM concentraties bij de ADP werd ook in vorige paragrafen aagehaald bij de vergelijking van de geklasseerde resultaten.

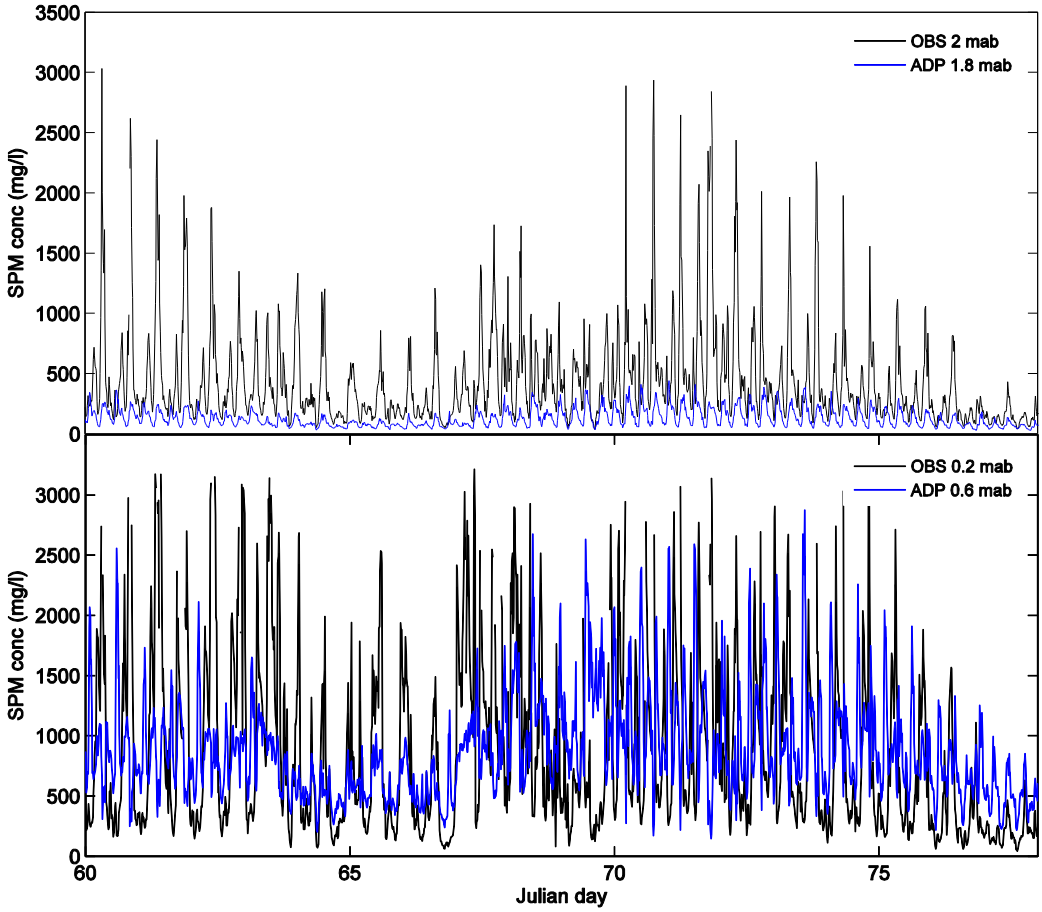

Figuur 4.12: Vergelijking tussen OBS en ADP signaal (maart 2009).

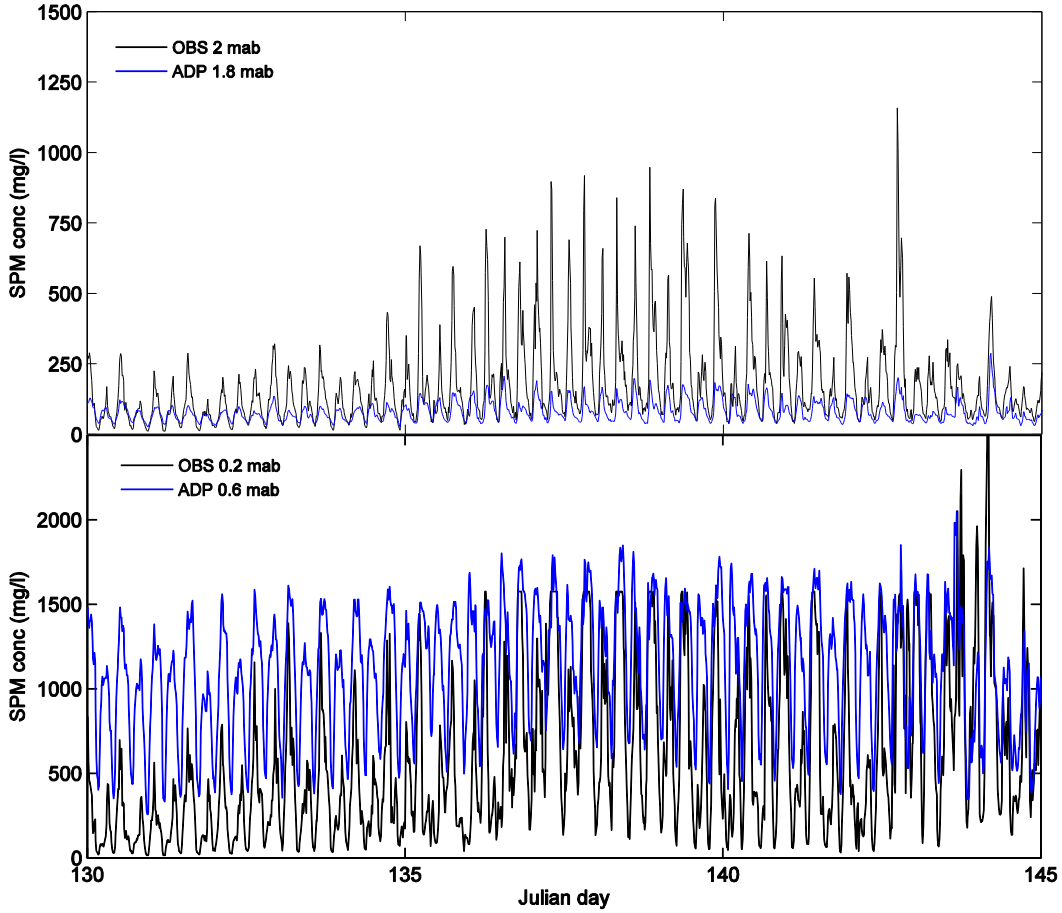

Figuur 4.13: Vergelijking tussen OBS en ADP signaal (mei 2011).

5. Conclusies

Bodemnabije SPM concentratie uit het turbiditeitsmaximum ter hoogte van de Belgische kust werd geanalyseerd over de periode 2005-2013. De belangrijkste bevindingen zijn:

1. Gemiddeld is de SPM concentratie lager in de zomer dan de winter en dit zowel op 0.2 mab als op 2 mab. Dit is niet volledig in overeenstemming met de bevindingen van de ADP-SPM concentraties (zie Fettweis et al. 2014b). De trend met de ADP is echter gelijkaardig, met toenemende afstand van de bodem wordt het verschil tussen zomer en winter groter.

1. Tijdens kentering is het verschil tussen de seizoenen meer uitgesproken dan in de rest van de getijcyclus. In de zomer daalt dan de SPM concentratie relatief meer dan in de winter. Deze bevinding is in overeenstemming met de hogere frequentie aan macrovlokken in de zomer.

2. Getijamplitude heeft een sterke invloed op de gemiddelde SPM concentratie. Naast een verschil in SPM concentratie treed er ook een verschil in het tijdstip van de piek concentratie op.

3. In de winter is op 2 mab de gemiddelde SPM concentratie tijdens springtij hoger bij een NE gerichte alongshore stroming, uitgezonderd bij het begin van de eb. Gelijkaardige verlopen zijn er op 0.2 mab, maar nu is de periode met hogere SPM concentratie tijdens SW gerichte stroming langer en vooral bij doodtij en springtij. Ook tijdens de zomer treden kwalitatieve verschillen op tussen de SPM concentratie op 0.2 en 2 m boven de bodem. Terwijl dicht tegen de bodem de SPM concentratie altijd hoger is bij een NE gerichte alongshore stroming, is er op 2 m boven de bodem de SPM concentratie gemiddeld hoger tijdens het begin van de eb voor een SW gerichte stroming.

4. SPM concentratie uit ADP en OBS heeft kwalitatief een gelijkaardig verloop. De verschillen tussen beiden zijn echter groot, zodat er een hercalibratie van de ADP nodig is.

6. Referenties

Backers J, Francken F, Hindryckx K, Vanaverbeke W. 2013. Rapport van de RV Belgica. Meetcampagnes en Verankering van Meetsystemen MOMO–2012. BMM-rapport, BMM-MDO/2013-24/MOMO/2012, 123pp.

Baeye M, Fettweis M, Voulgaris G, Van Lancker V. 2011. Sediment mobility in response to tidal and wind-driven flows along the Belgian inner shelf, southern North Sea. Ocean Dynamics 61, 611-622.

Belgische Staat. 2012a. Initiële beoordeling van het Belgisch marien ecosysteem voor de Kaderrichtlijn Mariene Strategie. – Art 8 lid 1a & 1b. BMM, Federale Overheidsdienst Volksgezondheid, Veiligheid van de Voedselketen en Leefmilieu, Brussel, België, 81pp.

Belgische Staat 2012b. Omschrijving van Goede Milieutoestand en vaststelling van Milieudoelen voor de Belgische mariene wateren. Kaderrichtlijn Mariene Strategie – Art 9 & 10. BMM, Federale Overheidsdienst Volksgezondheid, Veiligheid van de Voedselketen en Leefmilieu, Brussel, België, 34pp.

Downing, J. 2006. Twenty-five years with OBS sensors: The good, the bad, and the ugly. Continental Shelf Research, 26 (17-18), 2299-2318.

Fettweis M, Baeye M, Lee BJ, Chen P, Yu JCR. 2012. Hydro-meteorological influences and multimodal suspended particle size distributions in the Belgian nearshore area (southern North Sea). Geo-Marine Letters 32, 123-137.

Fettweis M, Baeye M, Francken F, Van den Eynde D, Van Lancker V. 2014a. MOMO activiteitsrapport (1 juli 2013 - 31 december 2013). BMM-rapport MOMO/6/MF/201401/NL/AR/4, 47pp + app.

Fettweis M, Baeye M, Van der Zande D, Van den Eynde D, Lee BJ. 2014b. Seasonality of floc strength in the southern North Sea. Journal of Geophysical Research 119, 1911–1926,

Flagg CN, Vermersch JA, Beardsley RC. 1976. 1974 MIT New England shelf dynamic experiment (March 1974) data report, part II: The moored array. Report 76-1, Massachussets Institute of Technology.

Kim HY, Gutierrez B, Nelson T, Dumars A, Maza M, Perales H, Voulgaris G (2004) Using the acoustic Doppler current profiler (ADCP) to estimate suspended sediment concentration. Technical Report CPSD #04-01.

Lauwaert B, Fettweis M, Cooreman K, Hillewaert H, Moulaert I, Raemaekers M, Mergaert K, De Brauwer D. 2004. Syntheserapport over de effecten op het mariene milieu van baggerspeciestortingen. BMM, DVZ & aMT rapport, BL/2004/01, 52pp.

Lauwaert B, De Brauwer D, Fettweis M, Hillewaert H, Hostens K, Mergaert K, Moulaert I, Parmentier K, Verstraeten J. 2006. Syntheserapport over de effecten op het mariene milieu van baggerspeciestortingen (vergunningsperiode 2004-2006). BMM, ILVO & aMT rapport, BL/2006/01, 87pp.

Lauwaert B, Bekaert K, Berteloot M, De Brauwer D, Fettweis M, Hillewaert H, Hoffman S, Hostens K, Mergaert K, Moulaert I, Parmentier K, Vanhoey G, Verstraeten J. 2008. Syntheserapport over de effecten op het mariene milieu van baggerspeciestortingen (vergunningsperiode 2006-2008). BMM, ILVO, aK & aMT rapport, BL/2008/01, 128pp.

Lauwaert B, Bekaert K, Berteloot M, De Backer A, Derweduwen J, Dujardin A, Fettweis M, Hillewaert H, Hoffman S, Hostens K, Ides S, Janssens J, Martens C, Michielsen T, Parmentier K, Van Hoey G, Verwaest T. 2009a. Synthesis report on the effects of dredged material disposal on the marine environment (licensing period 2008-2009) Report by MUMM, ILVO, CD, aMT & WL, BL/2009/01. 73pp.

Lauwaert B, Bekaert K, Berteloot M, De Backer A, Derweduwen J, Dujardin A, Fettweis M,

Hillewaert H, Hoffman S, Hostens K, Ides S, Janssens J, Martens C, Michielsen T, Parmentier K, Van Hoey G, Verwaest T. 2009b. Syntheserapport over de effecten op het mariene milieu van baggerspeciestortingen (vergunningsperiode 2008-2009). Rapport uitgevoerd door BMM, ILVO, CD, aMT & WL, BL/2009/01. 18pp.

Lauwaert B, Delgado R, Derweduwen J, Devriese L, Fettweis M, Hostens K, Janssens J, Robbens J, Timmermans S, Van Hoey G, Verwaest T. 2011a. Synthesis report on the effects of dredged material disposal on the marine environment (licensing period 2010-2011). Report by MUMM, ILVO, CD, aMT & WL, BL/2011/12, 85pp.

Lauwaert B, Delgado R, Derweduwen J, Devriese L, Fettweis M, Hostens K, Janssens J, Robbens J, Timmermans S, Van Hoey G, Verwaest T. 2011b. Synthese rapport over de effecten op het mariene milieu van baggerspeciestortingen (vergunningsperiode 2010-2011). Rapport uitgevoerd BMM, ILVO, CD, aMT & WL, BL/2011/12, 16pp.

Lauwaert B, Fettweis M, De Witte B, Van Hoey G, Timmermans S, Martens C. 2014. Vooruitgangsrapport (januari 2012 – juni 2014) over de effecten op het mariene milieu van baggerspeciestortingen. Rapport door KBIN-BMM, ILVO, CD & aMT, BL/2014/01, 21pp.

Sternberg, R.W., Kineke, G.C., Johnson, R.V. 1991. An instrument system for profiling suspended sediment, fluid, and flow conditions in shallow marine environments. Continental Shelf Research, 11, 109-122.

COLOPHON

Dit rapport werd voorbereid door de BMM in augustus 2014
Zijn referentiecode is .MOMO/7/MF/201408/NL/AR/1

De scheepstijd met de RV Belgica werd vorzien door BELSPO en KBIN-OD Natuur

Indien u vragen hebt of bijkomende copies van dit document wenst te verkrijgen, gelieve een e-mail te zenden naar m.fettweis@mumm.ac.be, met vermelding van de referentie, of te schrijven naar:

Koninklijk Belgisch Instituut voor Natuurwetenschappen
OD Natuur - BMM
100 Gulledelle
B–1200 Brussel
België
Tel: +32 2 773 2111
Fax: +32 2 770 6972
http://www.mumm.ac.be/

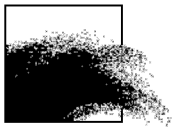

APPENDIX 1

Bijdragen VLIZ Young Scientist Day 7 March 2014, Brugge.

- Baeye M, Francken F, Fettweis M, Van den Eynde D. 2014. The first buoy for continuous measuring of surface Suspended Particulate Matter concentration on the Belgian inner shelf.
- Fettweis M, Baeye M, Van der Zande, Van den Eynde D, Lee BJ. 2014. Seasonality of nearshore marine snow in the southern North Sea.
- Thant S, Baeye M, Fettweis M, Monbaliu J, Van Rooij D. 2014. Extreme values of Suspended Particulate Matter concentration and their relation to wave systems along the Belgian inner shelf.

The first buoy for continuous measuring of surface Suspended Particulate Matter concentration on the Belgian inner shelf

Matthias Baeye[1], Frederic Francken[1], Michael Fettweis[1], Dries Van den Eynde[1]

[1] Royal Belgian Institute of Natural Sciences (RBINS), Operational Directorate Natural Environment (OD Nature), Gulledelle 100, B-1200 Brussels, Belgium
Email: Matthias.Baeye@mumm.ac.be

SPM concentration is a key parameter to describe the environmental status, and to evaluate and understand the impact of human activities in nearshore areas. Long-term measurements are needed in order to resolve all variations in SPM concentration. In fall 2013, continuous buoy measurements of SPM concentration were initiated and realized in close cooperation with DAB Vloot who is the responsible for maintaining the navigational buoys in the Belgian waters. Both parties agreed upon to select the AW cardinal buoy for holding the OBS-5+ (optical backscatter point sensor) at its side. The stand-alone OBS-5+ is equipped with an anti-biofouling wiper and installed in a stainless steel frame hanging at about 1.5 m under sea surface. Both in situ and in lab sensor calibrations were performed, together with burst sampling over long enough time guaranteeing qualitative SPM concentration data. The AW buoy (51°22.42'N 3°7.05'E) is located at about 6 km off Zeebrugge harbor, in a water depth of 10 m and in the direct proximity of the benthic tripod location MOW1 (51°22.04'N 3°6.95'E, measurements since 2005). The motivation for having both types of in situ measurements co-located is the RBINS-OD Natural Environment commitment within in the European framework JERICO (www.jerico-fp7.eu) WP 10.6, *viz.* inter-comparison study between SPM concentrations derived from different platforms (i.e. buoys, benthic frames, satellite). In a second phase, an upgrade of the system with a second water quality sensor (e.g. fluorimeter) and a module for real-time data transmission is foreseen (currently under market study investigation).
Processes affecting SPM concentration are turbulence, tides, neap-spring cycles, meteorological events, season, and other long-term fluctuations. In this poster a time-series of about 20 days (September 26 – October 16, 2013) reveals new insights in the short- (storms) and medium-term (spring–neap cycle) sediment dynamics at different depths, such as vertical mixing and sediment stratification. Once (much) more data have been gathered, correlation with satellite imagery (downloadable from the GRIMAS extraction tool website) will be investigated.

First buoy for continuous measuring of surface Suspended Particulate Matter concentration in the Belgian coastal ocean

Matthias Baeye, Frederic Francken, Michael Fettweis, Dries Van den Eynde and Lieven Naudts
RBINS ODNature, Gulledelle 100, 1200 Brussels, BELGIUM matthias.baeye@mumm.ac.be

Conclusion

Optical backscatter sensor instrumented on a surface buoy is a valuable tool towards better understanding SPM dynamics in the high-turbidity area in front of the Belgian coast. Continuous time-series of suspended particulate matter (SPM) concentration near the surface covers a wide range of hydro-meteo conditions. Data-analysis reveals that wind forcing is the dominant controlling factor for subtidal SPM dynamics, together with the lunar phases (*i.e.* spring-neap cycles). Wind direction and speed are responsible for (1) waves, (2) residual flows, and (3) coastal set-up or set-down. Continuous data give the full picture of SPM concentration variation in the study area, whereas other sensors or platforms (such as satellites, ships) undersample this variability.

Sensor

OBS-5+ (Campbell Sc., Inc.) is an optical backscatter point sensor measuring turbidity. It is stand-alone, equipped with an anti-biofouling wiper and installed in a stainless steel frame hanging at about 1.5 m under sea surface. Both *in situ* and in lab sensor calibrations were performed, together with burst sampling over long enough time guaranteeing qualitative SPM concentration data. The AW buoy (51°22.42'N 3°7.05'E) is located at about 6 km off Zeebrugge (ZB) harbor, in water depths of ~10 m and in the direct proximity of the benthic tripod frame location MOW1 (51°22.04'N 3°6.95'E, measurements since 2005).

Aim

Motivation for having both surface buoy and benthic tripod *in situ* measurements co-located is the commitment by RBINS-OD Natural Environment within the European framework programme JERICO (*www.jerico-fp7.eu/about*) WP 10.6, *viz.* inter-comparison study between SPM concentrations derived from different platforms and sensors (*i.e.* surface buoys, benthic frames, satellites).

Location

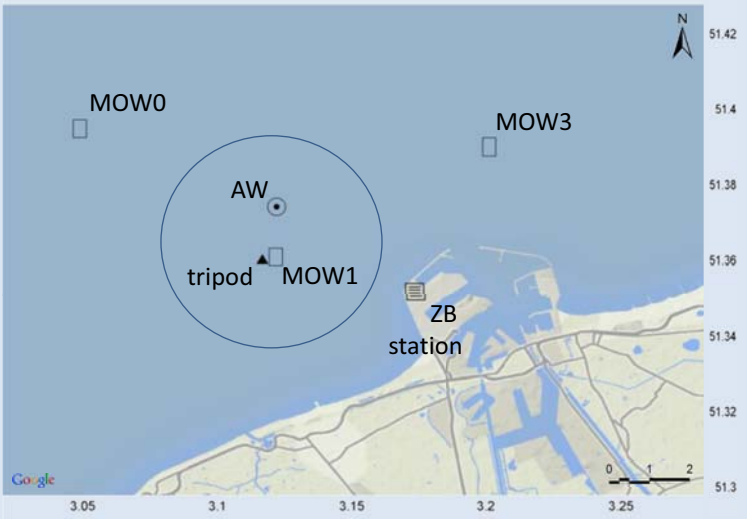

Results

Tidal forcing, without wind forcing, typically results in 2 SPM concentration peaks per tidal cycle - one peak around HW and one around LW. Concentrations vary between 0.5 and 50 NTU, with higher value ranges during spring tides (>3.6 m tidal amplitude) and the smaller ranges during neap tides (<3.6 m). As shown in A (spring tide conditions and no wind forcing), the peak around high water is much lower (4 x) than around LW, and is 1 hour behind. For all SPM peaks (A), one observes that there is an immediate increase followed by a gradual decrease. In B, a storm ("Sinterklaasstorm") is characterized with highest SPM concentrations recorded so far (up to 250 NTU). This storm was a SW storm (waves up to 3.5 m) followed by a N storm (swell waves up to 5 m). The first part deals with highest concentrations, whereas the NTU values decrease under swell wave conditions. Surprisingly, but likely to be associated with strong coastal set-up. However, for period E similar swell wave conditions were recorded and the set-up is 1 m less, but the concentrations remain relatively low. Time period C corresponds to a SSW wind forcing enhancing the flood current and as a result, a short-term increase (up to 70 NTU) is recorded. Note that this meteorological condition implies higher concentrations than those under swell event E, even though the waves are 2x higher during E. Possible explanation is the vertical mixing of the water column that is less during swell waves, and this in combination with a coastal set-up. Under W-SW-SSW wind forcing, increased flood currents (no associated set-up) tend to better mix the water column. Further, land breeze also increases surface SPM concentration, as shown from day 350 onwards . This wind direction typically induces a coastal set-down. Another explanation is the offshore-directed drift (residual transport) of SPM away from the high-turbidity zone.

Time-series

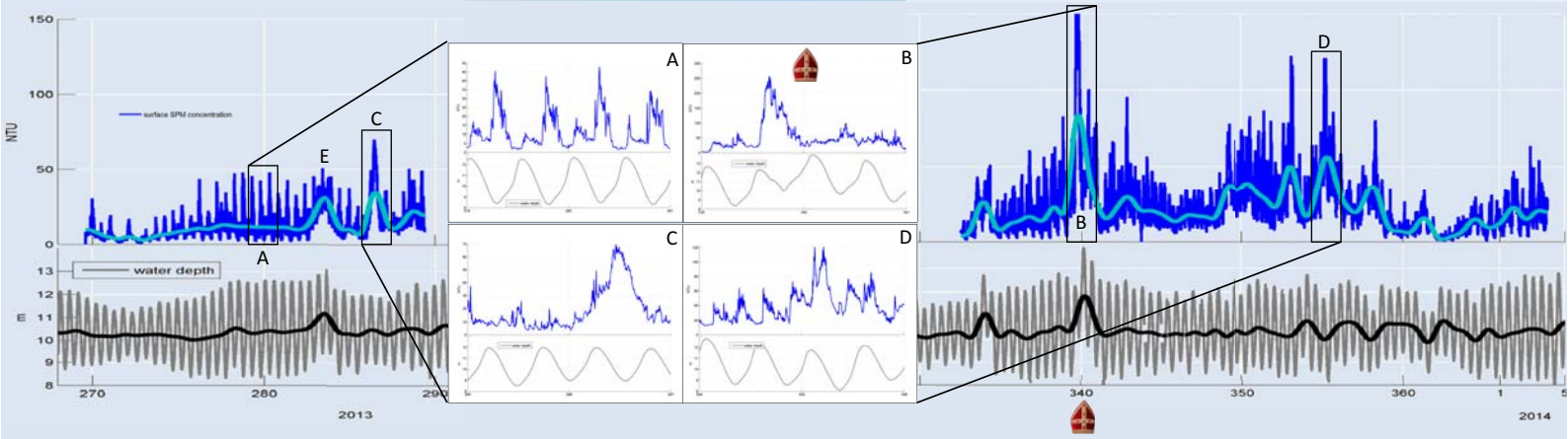

Operational Directorate Natural Environment
Royal Belgian Institute of Natural Sciences (RBINS)

Shiptime RV Belgica was provided by BELSPO and RBINS–OD Nature.
We acknowledge the Ministry of the Flemish Community (DAB Vloot) for using the AW buoy.

Poster presented at VLIZ Marine Scientists' Day, Bruges Belgium 7/03/2014

Seasonality of nearshore marine snow in the southern North Sea

Michael Fettweis[1], Matthias Baeye[1], Dimitry Van der Zande[1], Dries Van den Eynde[1], Byung Joon Lee[2]

[1] Royal Belgian Institute of Natural Sciences – Operational Directorate Natural Environment, Gulledelle 100, B-1200 Brussels, Belgium
E-mail: m.fettweis@mumm.ac.be

[2] School of Constructional and Environmental Engineering, Kyungpook National University, 2559 Gyeongsang-daero, Sangju, Gyeongbuk, 742-711, Republic of Korea

The suspended particulate matter (SPM) concentration in the high turbidity zones of the southern North Sea is inversely correlated with chlorophyll (Chl) concentration. During winter SPM concentration is high and Chl concentration low and vice versa during summer. This seasonality has often been associated with seasonal pattern in wind forcing. However, the decrease in SPM concentration corresponds well with the spring algae bloom. Does the decrease of SPM concentration caused by changing wind conditions, causes the start of algae bloom, or does the algae bloom decrease SPM concentration through enhanced flocculation and deposition? In order to answer the question, measurements from 2011 of particle size distribution (PSD), SPM and Chl concentration from the southern North Sea have been analyzed. The results indicate that the frequency of occurrence of macroflocs has a seasonal signal and not its size. The data from a highly turbid coastal zone suggest that the maximum size of the macroflocs is controlled by turbulence and the available flocculation time during a tidal cycle, but the strength of the macroflocs is by the availability of sticky organic substances associated with enhanced primary production during spring and summer. The results highlight the shift of mainly microflocs and flocculi in winter towards more muddy marine snow with larger amounts of macroflocs in spring and summer. The macroflocs will reduce the SPM concentrations in the turbidity maximum area as they settle faster. Consequently, the SPM concentration decreases and the light condition increases in the surface layer enhancing further algae growth.

Seasonality of nearshore marine snow in the southern North Sea

Michael Fettweis[1], Matthias Baeye[1], Dimitri Van der Zande[1], Dries Van den Eynde[1], Byung Joon Lee[2]

[1]Royal Belgian Institute of Natural Sciences – Operational Directorate Natural Environment, Gulledelle 100, B-1200 Brussels, Belgium

[2]Kyungpook National University, School of Constructional and Environmental Engineering, 2559 Gyeongsang-daero, Sangju, Gyeongbuk, 742-711, South Korea

Facts: Seasonal pattern in SPM and Chl concentration

The suspended particulate matter (SPM) concentration in the Belgian coastal area (southern North Sea) is inversely correlated with chlorophyll (Chl) concentration. During winter SPM concentration is high and Chl concentration low and vice versa during summer.

REMOTE SENSING DATA

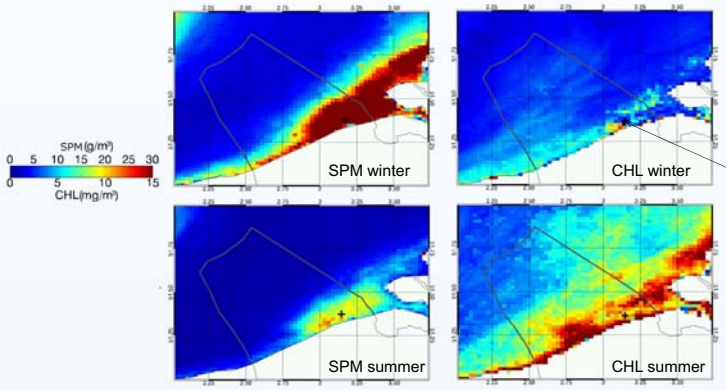

IN SITU DATA: MOW1 (Belgian coastal area)

Chicken or Egg ?

Hypothesis A: Physical Forcing

The water clears as a result of reducing wind stirring and sediment re-suspension after winter storms. This physical clearing of the water induces higher light levels and contributes to the subsequent onset of the spring bloom. According to this hypothesis, the turbidity decreases BEFORE the spring bloom.

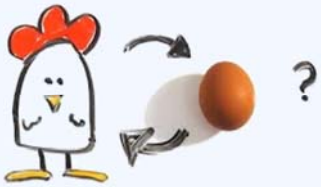

Hypothesis B: Biology

The turbidity decreases because of increased aggregation of particles brought about by biological activity (TEP concentration) during the bloom and biological activity in summer. According to this hypothesis, the bloom itself is the trigger for higher transparency and the water clears DURING and AFTER the spring bloom.

Hypothesis testing: data 2011

The hypothesis have been tested using in situ data of SPM concentration, floc size, turbulence; remote sensing data of chlorophyll concentration and meteorological and wave data at MOW1 site (Belgian nearshore area).

Physical forcing proxy: Kolmogorov microscale of turbulence (high values = low turbulence; low values = high turbulence)

Biology proxy: Chl concentration as indication of TEP concentration

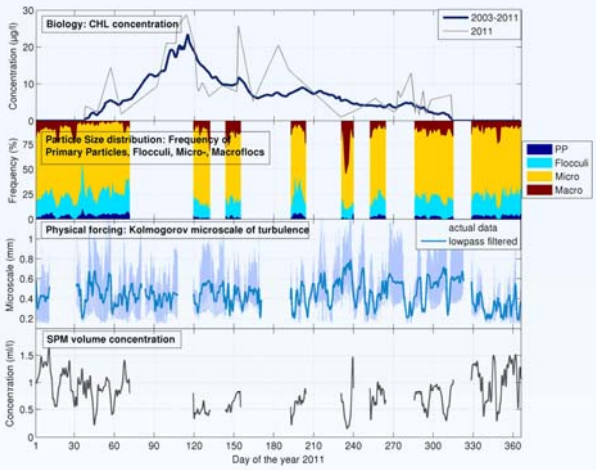

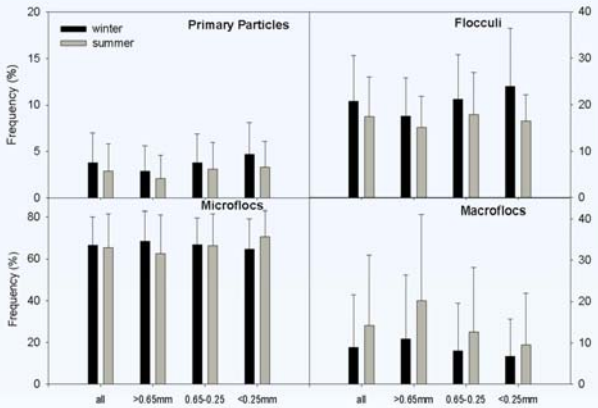

Winter
less macroflocs
more PP and flocculi

Summer
less PP & flocculi
more macroflocs

Frequency of primary particles, flocculi, microflocs and macroflocs for the summer and winter season and according to Kolmogorov microscale

Conclusions

Wind strengths and wave heights have a seasonal signal, but these are not sufficient to explain the large differences observed in SPM concentration.

Biomass effects increase the strength of macroflocs rather than their size. The results highlight the transformation of mainly microflocs and flocculi in winter towards more muddy marine snow with larger amounts of macroflocs in spring and summer. The larger fraction of macroflocs reduces the SPM concentrations as they settle faster, increases light condition in the surface layer and enhances algae growth.

It is mainly the biological activity in spring and summer that lead to a decrease in SPM concentration rather than the (weak) seasonal pattern in physical forcing.

Further reading: *Fettweis M, Baeye M, Van der Zande D, Van den Eynde D, Lee BJ. 2014. Seasonality of floc strength in the southern North Sea. Journal of Geophysical Research.*

Ship Time RV Belgica was provided by BELSPO and RBINS–Operational Directorate Natural Environment.

Extreme values of Suspended Particulate Matter concentration and their relation to wave systems along the Belgian inner shelf

Silvy Thant[1], Matthias Baeye[2], Frederic Francken[2], Michael Fettweis[2], Jaak Monbaliu[3], David Van Rooij[4]

[1] Ghent University - Oceans and Lakes
Email: S.Thant@ugent.be

[2] Royal Belgian Institute of Natural Sciences (RBINS), Operational Directorate Natural Environment (OD Nature), Gulledelle 100, B-1200 Brussels, Belgium
Email: Matthias.Baeye@mumm.ac.be

[3] Katholieke Universiteit Leuven (KUL), Department of Civil Engineering, Kasteelpark Arenberg 40, B-3001 Leuven

[4] Ghent University (UGENT), Department of Geology and Soil Science, Renard Centre of Marine Geology (RCMG), Krijgslaan 281 S8, B-9000 Gent

SPM concentration is a key parameter to describe the environmental status, and to evaluate and understand the impact of human activities in nearshore areas. Long-term measurements are needed in order to resolve all variations in SPM concentration. Processes affecting SPM concentration are turbulence, tides, neap-spring cycles, meteorological events, season, and other long-term fluctuations. SPM concentration has been measured since 2005 at the MOW1 site, situated at about 5 km northwest of Zeebrugge in the high-turbidity zone off the Belgian-Dutch coast. The measurements have been carried out using a benthic tripod that allowed measuring during all meteorological conditions, including storms.
Storm effects on sediment re-suspension and SPM concentration have been investigated using meteorological and wave data from IVA MDK (afdeling Kust - Meetnet Vlaamse Banken). SPM concentration data from MOW1 (51°22.04'N 3°6.95'E) were estimated using the backscatterance from a 3 MHz acoustic Doppler profiling current meter. Because of the large amount (~1220 days) of SPM concentration data, an automatic detection algorithm for identifying extreme events was developed. A low-pass filter was run on the SPM concentration time-series in order to remove the tidal signal. A polynomial de-trending of the low-pass filtered data was then accomplished to filter out the spring-neap signal. A peak detection function of these processed data allowed eventually cataloging the extreme SPM concentrations and relating them to storm events and wave system data. The method used allows identifying and understanding the controlling factors, i.e. influence of wave systems on the SPM concentration. It is a promising method that could also be used to analyze and classify the surface SPM concentration maps derived from polar orbiting or geo-stationary satellites.

APPENDIX 2

Fettweis M, Baeye M, Van der Zande D, Van den Eynde D, Lee BJ. 2014. Seasonality of floc strength in the southern North Sea. Journal of Geophysical Research 118.

AGU PUBLICATIONS

JGR

Journal of Geophysical Research: Oceans

RESEARCH ARTICLE

10.1002/2013JC009750

Key Points:
- SPM and Chl concentration have opposing seasonal signal
- The seasonality of SPM concentration is mainly caused by biological effects
- Macroflocs are more abundant and stronger in summer than winter season

Correspondence to:
M. Fettweis,
m.fettweis@mumm.ac.be

Citation:
Fettweis, M., M. Baeye, D. Van der Zande, D. Van den Eynde, and B. J. Lee (2014), Seasonality of floc strength in the southern North Sea, *J. Geophys. Res. Oceans*, *119*, 1911–1926, doi:10.1002/2013JC009750.

Received 19 DEC 2013
Accepted 28 FEB 2014
Accepted article online 4 MAR 2014
Published online 14 MAR 2014

Seasonality of floc strength in the southern North Sea

Michael Fettweis[1], Matthias Baeye[1], Dimitry Van der Zande[1], Dries Van den Eynde[1], and Byung Joon Lee[2]

[1]Operational Directorate Natural Environment, Royal Belgian Institute of Natural Sciences, Brussels, Belgium, [2]School of Constructional and Environmental Engineering, Kyungpook National University, Sangju, South Korea

Abstract The suspended particulate matter (SPM) concentration in the high turbidity zones of the southern North Sea is inversely correlated with chlorophyll (Chl) concentration. During winter, SPM concentration is high and Chl concentration is low and vice versa during summer. This seasonality has often been associated with the seasonal pattern in wind forcing. However, the decrease in SPM concentration corresponds well with the spring algal bloom. Does the decrease of SPM concentration caused by changing wind conditions cause the start of algae bloom, or does the algae bloom decrease SPM concentrations through enhanced flocculation and deposition? To answer the question, measurements from 2011 of particle size distribution (PSD), SPM, and Chl concentrations from the southern North Sea have been analyzed. The results indicate that the frequency of occurrence of macroflocs has a seasonal signal, while seasonality has little impact upon floc size. The data from a highly turbid coastal zone suggest that the maximum size of the macroflocs is controlled by turbulence and the available flocculation time during a tidal cycle, but the strength of the macroflocs is controlled by the availability of sticky organic substances associated with enhanced primary production during spring and summer. The results highlight the shift from mainly microflocs and flocculi in winter toward more muddy marine snow with larger amounts of macroflocs in spring and summer. The macroflocs will reduce the SPM concentrations in the turbidity maximum area as they settle faster. Consequently, the SPM concentration decreases and the light condition increases in the surface layer enhancing algae growth further.

1. Introduction

Seasonal variations are characteristic for biogeochemical processes on tide-dominated midlatitude continental shelves. They are primarily caused by the seasonality of solar forcing that drives physical (e.g., weather conditions, thermal stratification, light) and biological (e.g., primary production) processes. Suspended Particulate Matter (SPM) concentration in the North Sea has a typical seasonal variation with high values in winter and low values in summer [e.g., *Howarth et al*., 1993]. Very often the seasonal pattern in wind and waves, with more storms in winter than summer, is put forward to explain the seasonality [*Eleveld et al*., 2008; *Dobrynin et al*., 2010]. The spring and early summer phytoplankton blooms have been associated with the seasonality of SPM concentration through the formation of larger flocs, and increasing the settling of SPM toward the seafloor [*Jago et al*., 2007; *Borsje et al*., 2008; *Van Beusekom et al*., 2012] and reducing the erodibility of bed sediments [*Black et al*., 2002].

Flocculation is the combined process of particle size growth and decay through aggregation and breakage in a turbulent flow field, thereby determining the size and settling velocity of SPM. A low turbulent flow enhances particle aggregation and increases the size and settling velocity of particles, but a high turbulent flow enhances floc breakage and decreases the size and settling velocity [*Winterwerp*, 2002]. Flocculation also combines biomass and minerals particles together into larger aggregates with often multimodal floc size distributions and different floc strength [*Verney et al*., 2009; *Lee et al*., 2012]. Flocculation depends on the attractive forces acting between the suspended particles that are caused by the surface properties of the particles. These properties are controlled by cohesive forces of clay minerals and by the microbial products consisting of sticky gel-like particles, called TEP (Transparent Extracellular Polymer) that interact with mineral particles and alter the properties of the SPM [*Passow*, 2002]. In coastal zones, the SPM is composed mainly of mineral particles and these organic products are acting as an additional binding agent [*Hamm*, 2002; *Fettweis et al*., 2006; *Maggi*, 2009; *Bainbridge et al*., 2012].

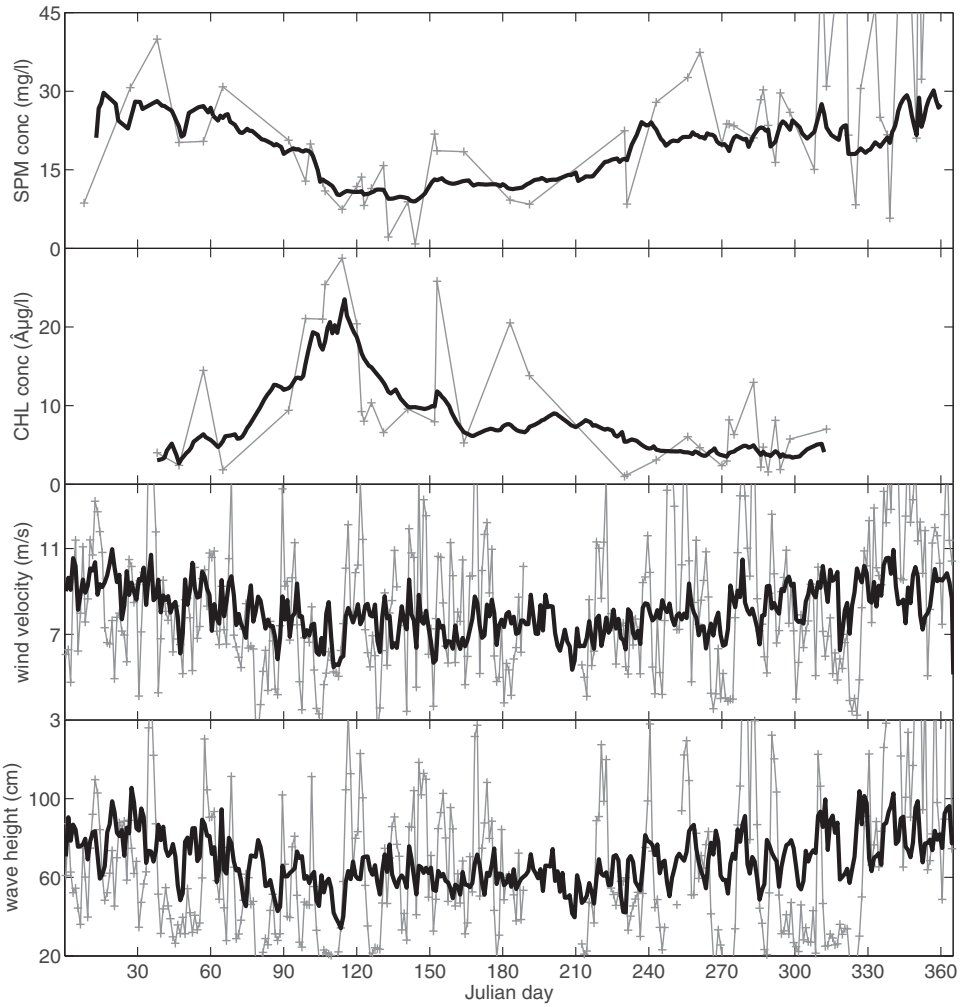

Figure 1. Surface SPM and Chl concentration from MERIS for the period 2003–2011 (thick black line) and for 2011 (gray line). Below are the daily averaged wind velocity and significant wave heights for the period 2001–2012 (thick black line) and for 2011. All data are for the station MOW1 (see Figure 2).

Despite the improved understanding of flocculation dynamics and their interaction with turbulence and biomineralogical composition, our knowledge is still insufficient to describe the impact of high primary production in spring and summer on floc sizes that induce changes in settling, formation of high-concentration mud suspensions, and resuspension of fine-grained sediments. Does a decrease of SPM concentration caused by changing wind and wave conditions trigger the start of the phytoplankton bloom in a high turbidity zone, or does the bloom decrease SPM concentration through enhanced flocculation and deposition? Both processes have a seasonal signal (Figure 1). Since the Belgian nearshore area, located in the southern North Sea, is very turbid and characterized by intense algae blooms, it is a relevant site to investigate links between biomass, SPM concentration and seasonal hydrometeorological.

1.1. Region of Interest

The Belgian nearshore area is situated in the southern North Sea and is characterized by high SPM concentrations (Figure 2). SPM concentration ranges between 20 and 100 mg/L at the surface and between 100 and more than 3000 mg/L near the bed; lower values (<100 mg/L) occur offshore [*Fettweis et al.*, 2010; *Baeye et al.*, 2011]. In situ measurements are available at MOW1 (51°21.63′N,

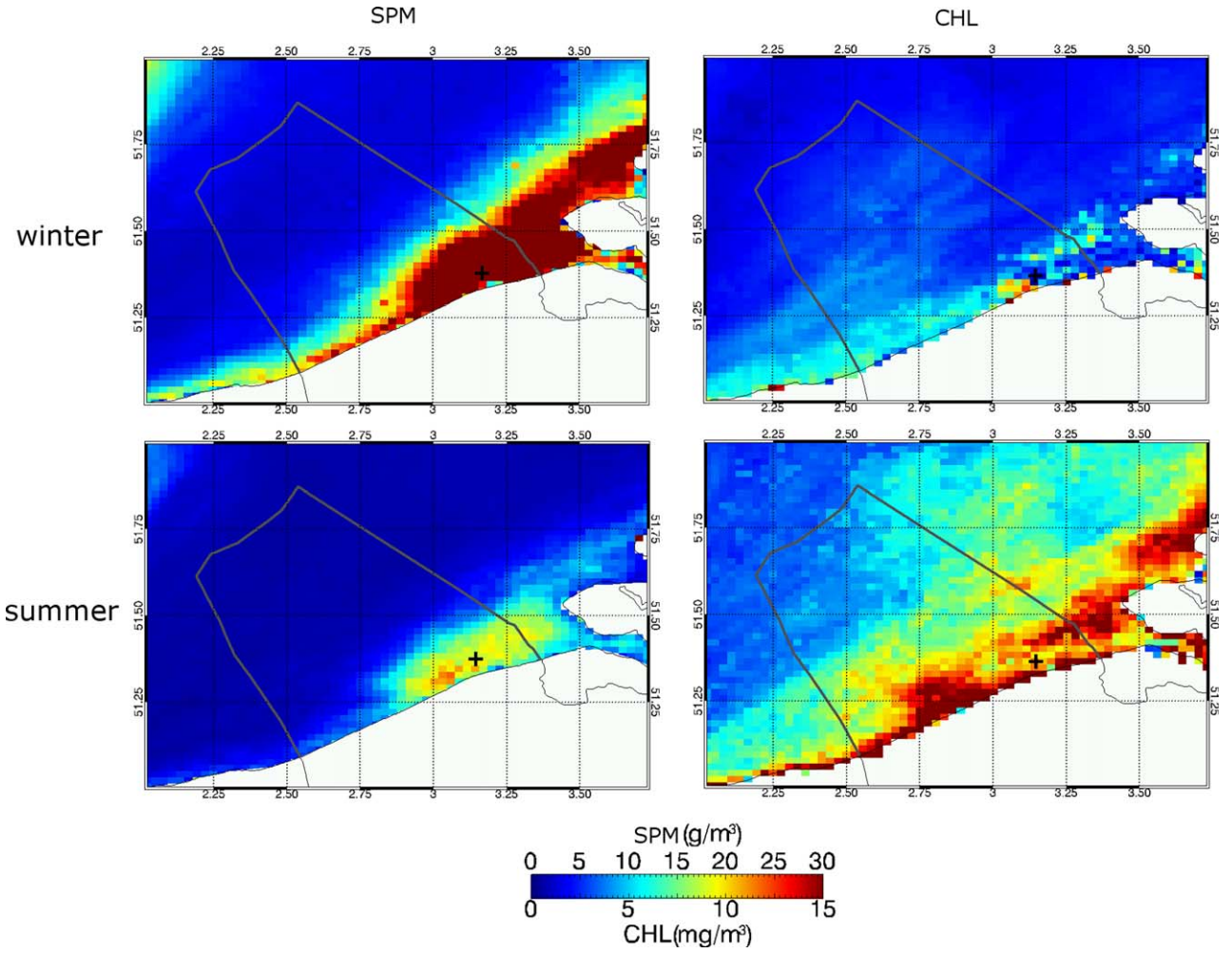

Figure 2. The 2011 (left) mean surface SPM and (right) Chl concentration during winter and summer in the Belgian coastal area (southern North Sea). Data are from MERIS satellite. The cross indicates the in situ measuring station MOW1.

3°7.41′E) located in the turbidity maximum zone (water depth about 10 m Mean Lower Low Water Spring (MLLWS)). Holocene medium-consolidated mud characterizes the seabed at the MOW1 site, albeit covered with an ephemeral fluffy mud layer (fluid mud) or muddy fine sand layer with a median grain size of about 170 μm [*Fettweis and Van den Eynde*, 2003; *Verfaillie et al*., 2006]. The suspended matter forms flocs that are built of clay and silt-sized particles, $CaCO_3$, and organic carbon with a median particle size of <2 μm [*Fettweis*, 2008]. The tidal regime is semidiurnal, and the mean tidal range near MOW1 is 4.3 and 2.8 m at spring and neap tide, respectively. The tidal current ellipses are elongated in the nearshore area and become gradually more semicircular toward the offshore. The current velocities at the measuring location MOW1 vary from 0.2 to 1.5 m/s during spring tide and 0.2 to 0.6 m/s during neap tide [*Fettweis and Van den Eynde*, 2003]. The strong tidal currents and the low freshwater discharge of the Scheldt (yearly average is 100 m^3/s) result in a well-mixed water column with almost no salinity and temperature stratification throughout the water column [*Lacroix et al*., 2004]. South-westerly winds dominate the overall wind climate, followed by winds from the NE sector (Figure 3). Maximum wind speeds coincide with the south-westerly winds; nevertheless, the highest waves are generated under north-westerly winds. The phytoplankton bloom starts in early spring with a diatom bloom and shifts toward a phaeocystis bloom in April and May [*Lancelot et al*., 1987]. Diatoms and phaeocystis concentrations decrease during June due to a shortage in nutrients and an increase in predation pressure by heterotrophic plankton species [*Rousseau et al*., 2002].

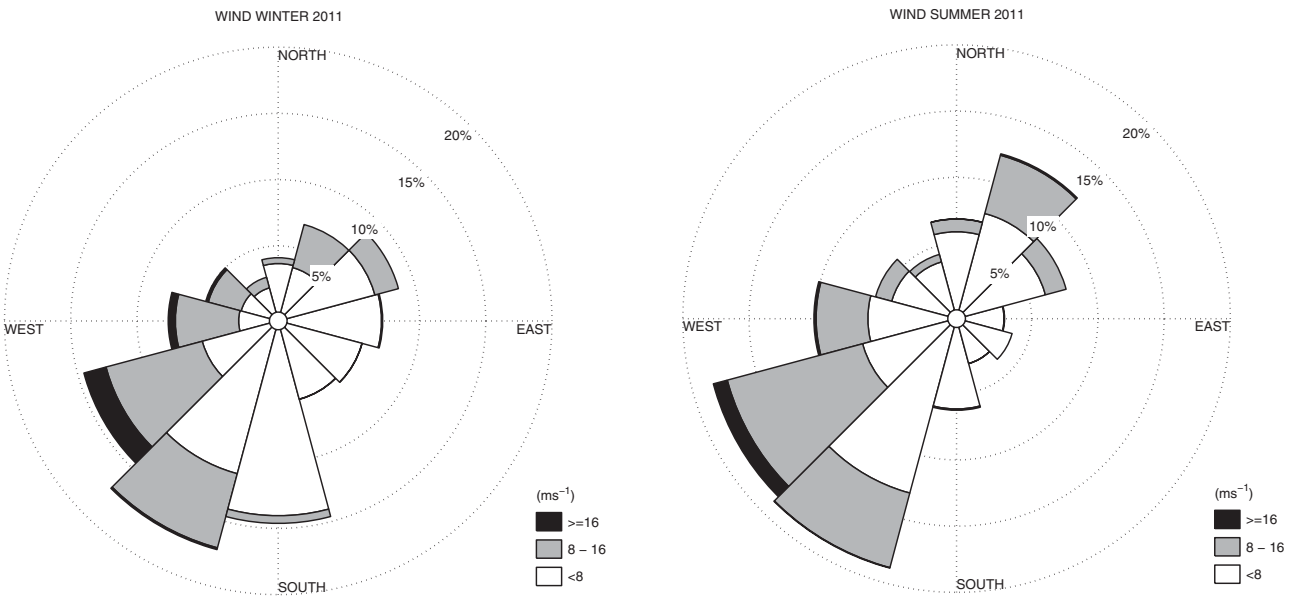

Figure 3. Wind rose diagrams showing (a) the 2011 winter wind data and (b) the 2011 summer data. Legend values are in m s^{-1}.

2. Material and Methods

2.1. In Situ Measurements

Data were collected with a tripod to measure currents, salinity, temperature, turbulence, SPM concentration, and Particle Size Distribution (PSD). The instrumentation suite consisted of three D&A optical backscatter sensors (OBSs), a SonTek 5 MHz Acoustic Doppler Velocimeter (ADV) Ocean, and a Sequoia Scientific LISST (laser in situ scattering and transmissometry) 100 X type C. The ADV was used to measure the three velocity components at 25 Hz at 18 cm above the bed and to estimate the turbulent kinetic energy from the turbulent fluctuations (see below). The LISST-100C measures PSDs in 32 logarithmically spaced size groups over the range of 2.5–500 μm [*Agrawal and Pottsmith*, 2000]. The volume concentration of each size group is estimated with an empirical volume calibration constant, which is obtained under a presumed sphericity of particles. Uncertainties of the LISST-100C detectors may arise from various causes [*Mikkelsen et al*., 2007; *Andrews et al*., 2010; *Davies et al*., 2012, *Graham et al*., 2012]. In the study area, these uncertainties are most probably caused by nonspherical particles, particles exceeding the instrument size range, or a too high SPM concentration.

All data (except LISST) were stored in two SonTek Hydra data logging systems. The LISST was mounted at 2 m above the bed (hereafter referred to as mab) and the OBSs at 0.2, 1, and 2 mab. The OBS signal was used to estimate SPM concentration. OBS voltage readings were converted into SPM concentration by calibration against filtered water samples collected during four tidal cycles every year, see *Fettweis* [2008] for a description of the method. Data gaps in the PSD time series occurred due to biofouling (mainly summer), too low transmission, too short battery life time, or instrument failure. The OBSs used were formatted to measure concentration of up to 3 g/L. During high energy conditions, SPM concentration was regularly higher than 3 g/L. Under these circumstances the OBS will saturate and underestimate the actual SPM concentration.

The tripod was moored at the location between 3 and 6 weeks and was then recovered and replaced with a similar tripod system. Ten deployments were carried out between 15 December 2010 and 18 January 2012. The long deployment ensured accurate assessments of conditions over neap and spring tides, and included a variety of meteorological events. From these, 208 days of good LISST data in 2011 remained after quality check, with about 2/3 recorded during winter (January-March and October-December) and 1/3 during summer (April-September). Good quality data have an optical transmission between 15% and 98%; show no gradual or sudden decrease (increase) in transmission (volume concentration) during the measurements and have a smooth PSD. A gradual decrease is often the result of biofouling and occurs mainly in

spring and summer. A sudden decrease in transmission is generally caused by a physical obstruction (e.g., cord entangled in optical path). A misaligned laser beam may cause high peaks in a few size classes making the PSD not smooth; these peaks remain during the whole measurements. The LISST 100 is a delicate instrument, misalignment of the laser beam may occur during deployment or other physical disturbances (collision with fishing gear).

2.2. Remote Sensing Measurements

The satellite-based imagery selected for this study was provided by the Medium Resolution Imaging Spectrometer (MERIS, https://earth.esa.int/web/guest/missions/esa-operational-eo-missions/envisat/instruments/meris). This multispectral sensor was on board of ENVISAT, a polar orbiting satellite which was launched in 2002 and provided data until April 2012. MERIS images were available with a daily temporal frequency and spatial resolution of 2×2 km^2 and provided water leaving reflectance information for 15 bands across 390–1040 nm. Oceanographic parameters related to ocean color, such as the chlorophyll-a (Chl) and SPM concentration were derived from the water leaving reflectance in specific spectral bands. Chl concentration was estimated using the MERIS case 2 algorithm (version MEGS 7.5) as described by *Doerffer and Schiller* [2006]. A quality control has been applied according to the standard MERIS product confidence flags. Remotely sensed SPM concentration is estimated from water leaving reflectance at 667 nm using the generic multisensor algorithm of *Nechad et al.* [2010]. In case of quality issues due to atmospheric correction error, stray light or sun-glint, the pixel was masked as unreliable and rejected. Surface Chl and SPM concentration time series were extracted from the imagery data using a 5×5 kernel for the location of the MOW1 station for 2011 (Figure 1). The Chl and SPM concentration climatology for the period 2003–2011 was generated by linearly interpolating the available data at a yearly basis after which a interannual mean was calculated per day. Additionally, for both Chl and SPM concentration, multitemporal composite maps were generated for the winter (January-March, October-December) and summer (April-September) season of 2011 (Figure 2).

Satellites cover large-scale scenes, but at a low time resolution, limited to surface data and with gaps in data often occurring during stormy weather conditions, though missing the high ranges of SPM concentrations. Satellites can be seen as random samplers biased toward good weather conditions as they represent only the cloud-free data, but also to nonsatellite-saturating data which occur at high SPM concentration levels. *Fettweis and Nechad* [2011] have shown that 60 satellite images per year are representative of the mean SPM concentration during good weather. In 2011, 67 good satellite images are available at MOW1 for SPM concentration (46% in winter, 54% in summer) and 37 for Chl concentration (38% in winter, 62% in summer).

2.3. Kolmogorov Scale of Turbulence From ADV

Turbulence in coastal areas controls the flocculation of fine-grained material and impacts the vertical and horizontal flux of SPM. The length scale of the smallest dissipating eddies (Kolmogorov scale of turbulence, λ_k) generally limits the size of the flocs [*van Leussen*, 1999; *Fettweis et al.*, 2006; *Cross et al.*, 2013]. Assuming that turbulent kinetic energy production is equal to dissipation, this scale can be calculated as $\lambda_k = (\nu^3/\varepsilon)^{1/4}$, where ν is the kinematic viscosity (10^{-6} m^2 s^{-1}) and ε is the turbulent energy dissipation (m^2 s^{-3}). The turbulence dissipation can be derived from $\tau = \rho\ (\varepsilon\ \kappa\ z)^{2/3}$, where τ is the shear stress, z the elevation above the bed, κ the von Karman constant, and ρ the water density. The turbulent kinetic energy (TKE) and the shear stress can be calculated using the variance of velocity fluctuation from the high-frequent ADV measurements [*Stapleton and Huntley*, 1995; *Thompson et al.*, 2003]. MOW1 is situated in shallow waters where wave effects are important; therefore, the shear stress was corrected for the advection by waves following the approach of *Trowbridge and Elgar* [2001], *Sherwood et al.* [2006], and *Fettweis et al.* [2010]. With the turbulence dissipation known, the Kolmogorov length scale can be calculated. The length scale was low-pass filtered using the PL64 filter described in *Flagg et al.* [1976] with a 33 h half-amplitude cutoff to remove tidal and higher-frequency signals.

2.4. Statistical Methods to Analyze PSD

A curve-fitting technique and a statistical method (entropy analysis) were used to analyze the large PSD data set in order to identify seasonality in an objective way. The curve-fitting software (DistFit^{TM}, Chimera Technologies Inc., USA) was used to decompose the multimodal PSD into four subordinate lognormal PSDs and to quantify the geometric mean diameter, standard deviation, and volume fraction of them. The

lognormality describes a more or less skewed distribution toward small size and the multimodality describes a distribution consisting of multiple modal peaks. The multimodal lognormal distribution function can be written as an integrated distribution function of four lognormal distribution functions [*Whitby*, 1978; *Jonasz and Fournier*, 1996]:

$$\frac{dW}{dD} = \sum_{i=1}^{4} \frac{\overline{W}_i}{\sqrt{2\pi}\ln(\sigma_i)} \exp\left[-\frac{1}{2}\left(\frac{\ln(D/\overline{D}_i)}{\ln(\sigma_i)}\right)^2\right]$$

where D is the particle diameter, W the volume concentration, $\bar{D}_i$ the geometric mean diameter, σ_i the multiplicative standard deviation, and $\bar{W}_i$ the volumetric fraction of an ith unimodal PSD. The choice of four lognormal functions is based on the fact that flocculation of fine-grained material in coastal areas develops a four-level structure consisting of primary particles, flocculi, microflocs, and macroflocs [*van Leussen*, 1999; *Lee et al*., 2012], see Figure 4. The 32 size classes measured by the LISST can thus be reduced to four groups that represent physical concepts rather than numbers. Primary particles consist of various organic and mineral particles (clay and other minerals, calcareous particles, picophytoplankton, bacteria). Flocculi are breakage-resistant aggregates of mainly clay minerals. Microflocs are the medium size aggregates and macroflocs are the very large aggregates that can reach hundreds to thousands of micrometers in organic-rich low-energy conditions, but only up to a few hundred micrometers in organic-limited high energy conditions [*Fettweis et al*., 2006]. The DistFit software (Chimera Technologies) was applied to the PSDs averaged over 10 min to generate the bestfits, defined as the minimum errors between fitted and measured PSDs [*Whitby*, 1978]. For two modal peaks, fixed sizes of 3 μm (lowest size class of the LISST) and 15 μm were chosen; the modal peaks of the bigger fractions were variable and chosen in order to represent the larger size classes of the LISST instrument (15–200 and 150–500 μm). The standard deviations varied between 1 and 2.5. The choice of parameters is based on assumptions and experiences [*Lee et al*., 2012].

A rising tail in the lowest size classes of the LISST is frequently observed in data and is caused by the presence of particles up to 10 times smaller than the smallest size bin of the instrument (i.e., 0.25–2.5 μm). *Andrews et al*. [2010] reported that fine out of range particles affect the entire PSD, with a significant increase in the volume concentration of the first two size classes of the LISST, a decrease in the next size classes and, surprisingly, an increase in the largest size classes. Similar remarks have been formulated by *Graham et al*. [2012], who observed an overestimation of 1 or 2 orders of magnitude in the number of fine particles measured by the LISST. They argue that due to flocculation small particles (such as individual grains, phytoplankton cells, bacteria, and viruses) probably do not exist as isolated individuals in large numbers in coastal waters. The 3 μm mode, therefore, most likely is an overestimation of fine particles due to inaccuracy of the LISST instrument when particles become too small for its range. The volume fraction calculated for this size distribution is interpreted as an indication of the presence of very fine particles rather than providing a correct number. This bias may further enhance the separation between the two peaks of primary particles and flocculi and develop a small peak of macroflocs during the peak flows. In case of low turbulent condition, it may also indicate the presence of very large particles [*Andrews et al*., 2010]. Particles exceeding the LISST size

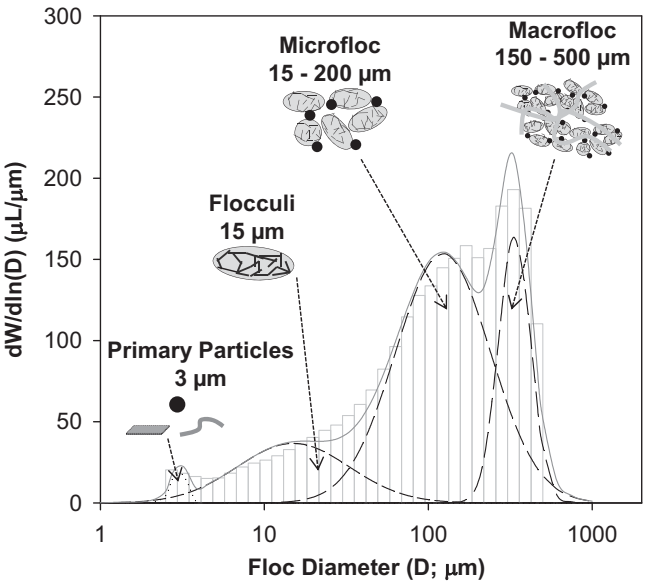

Figure 4. A multimodal PSD and its subordinate lognormal PSDs of primary particles, flocculi, microflocs, and macroflocs (adapted after *Lee et al*. [2012]).

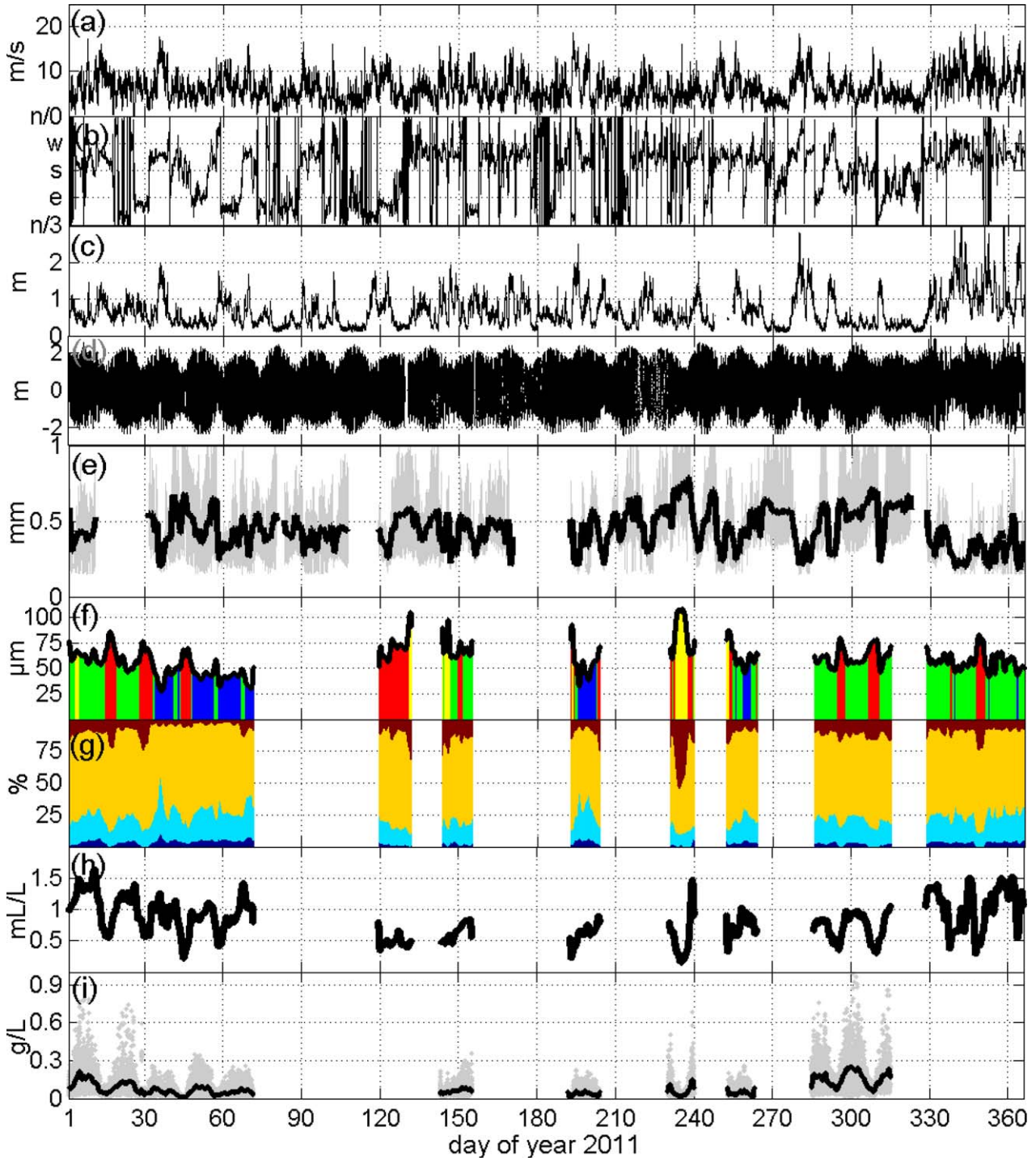

Figure 5. The 2011 time series (in days of the year) of (a) wind velocity; (b) wind direction; (c) significant wave height; (d) tidal elevation; (e) Kolmogorov scale (gray) and low-pass filtered signal (black); (f) low-pass filtered median floc size and entropy groups (group 1: blue, group 2: green, group 3: red, group 4: yellow, see Figure 6); (g) frequency of the four type of SPM constituents obtained by curve fitting: primary particles (dark blue), flocculi (light blue), microflocs (yellow), and macroflocs (brown); (h) SPM volume concentration at 2 mab; and (i) SPM mass concentration at 0.2 mab (gray) and low-pass filtered signal (black).

range of 500 μm also contaminate the PSD. *Davies et al*. [2012] reported that large out of range particles increase the volume concentration of particles in multiple size classes in the range between 250 and 400 μm and in the smaller size classes and recommended to interpret the PSD with care in case particles outside

Table 1. Geometric Mean and Standard Deviation of SPM Mass Concentration (mg/L) From the OBS at 0.2 and 1 m Above Bed (mab) and the SPM Volume Concentration (μL/L) From the LISST at 2 mab (mg/L and μL/L)[a]

	0.2 mab (mg/L)	1 mab (mg/L)	2 mab (μL/L)
Winter 2011			
all	431 */2.1	145 */2.6	674 */1.9
$\lambda_k > 0.6$ mm	420 */1.8	136 */1.8	545 */2.0
$0.3 < \lambda_k < 0.6$ mm	448 */2.0	146 */2.5	718 */1.9
$\lambda_k < 0.3$ mm	484 */2.0	205 */2.3	664 */1.9
Summer 2011			
all	357 */2.5	117 */2.2	449 */2.2
$\lambda_k > 0.6$ mm	304 */2.6	110 */2.2	338 */2.2
$0.3 < \lambda_k < 0.6$ mm	374 */2.4	118 */2.2	495 */2.2
$\lambda_k < 0.3$ mm	449 */2.2	119 */1.8	423 */2.0

[a]The data are calculated according to season and low-pass filtered Kolmogorov scale (λ_k); $\lambda_k < 0.3$ and $\lambda_k > 0.6$ mm are the 15th and 85th percentiles, corresponding to periods with significant high wave heights greater than about 1.50 m and lower than about 0.75 m.

the size range may potentially occur. The importance of these spurious results depends on the number of large particles in the distribution [*Davies et al*., 2012]. No particle size data obtained with other methods (video system, holography) are available at the MOW1 site. Macrofloc sizes recorded by a video system at an estuarine sites with similar tidal dynamics were generally smaller than 580 μm [*Winterwerp et al*., 2006], which indicates that most of the larger flocs are not exceeding the size limit of the LISST.

The structure of the PSD time series is further investigated using the concepts of entropy and complexity. Entropy analysis has been successfully applied to time series of LISST particle size distributions of suspended matter [*Mikkelsen et al*., 2007; *Fettweis et al*., 2012]. Entropy-based algorithms quantify the regularity of a time series. Entropy increases with the degree of disorder and is maximal for completely random systems. Applied to PSDs, entropy analysis allows grouping the size spectra without assumptions about the shape of the spectra. It is therefore suited to analyze unimodal and bimodal as well as multimodal distributions. The PSD time series has first been low-passed filtered using a filter of 33 h to remove the tidal signal, before the entropy classification with four PSD groups was carried out using the FORTRAN routine of *Johnston and Semple* [1983]. The entropy group PSD time series were then evaluated to assess the effects of the neap-spring tidal signal, meteorological effects, and seasons.

3. Results

The time-varying PSD, SPM concentration, Chl concentration, wind, wave, and hydrodynamics parameters constitutes a scientific record of flocculation and transport of the constituent particles and aggregates throughout 1 year that allows understanding of the possible causes of change in PSD and SPM concentration. The temporal distribution of the four constituents of the PSDs (primary particles, flocculi, microflocs, and macroflocs) are shown in Figure 5 with the entropy analysis of the low-passed filtered PSD data, the low-passed filtered SPM volume and mass concentration, the actual and the low-passed filtered Kolmogorov length scale, the significant wave height, tidal elevation, and the wind direction and strength. The curve-fitting analysis of the PSD has been low-pass filtered in the figure for clearness. The linear correlation between the low-pass filtered Kolmogorov scale and the logarithm of the significant wave height is significant ($R^2 = -0.77$, $N = 36499$). The low-pass filtered Kolmogorov length scale can thus be used as a proxy of the nontidal (waves and wind) turbulence intensity in shallow waters. The data are divided in three groups according to the turbulent intensity as follows: $\lambda_k < 0.28$ mm, 0.28 mm $< \lambda_k < 0.58$ mm, and $\lambda_k > 0.58$ mm. These groups correspond roughly with periods where the significant high wave heights are greater than 1.50 m, between 0.75 and 1.50 m, and lower than 0.75 m. The $\lambda_k = 0.58$ and 0.28 mm are the 15th and 85th percentiles of the low-pass filtered Kolmogorov-scale data, respectively.

The seasonality of SPM and Chl concentration is obvious from satellite images and in situ data at MOW1 (Figures 1 and 5 and Table 1). The geometric mean near-bed SPM concentrations are 28% higher during calm weather in winter than in summer. With increasing wave influence, these differences decrease to 17% (0.28 mm $< \lambda_k < 0.58$ mm) and 7% ($\lambda_k < 0.28$ mm) at 0.2 mab. Higher in the water column (1 mab) similar trends are observed, except that in summer the geometric mean SPM concentration during higher waves ($\lambda_k < 0.28$ mm, 119 mg/L) is almost the same as during lower wave conditions (0.28 mm $< \lambda_k < 0.58$ mm,

Table 2. Frequency (%) of Primary Particles (PP), Flocculi, Microflocs, and Macroflocs of the Four Entropy Groups (Figure 6)[a]

	PP	Flocculi	Microflocs	Macroflocs
Group 1	5.6	29.5	54.9 (52 μm)	10.1 (250 μm)
Group 2	10.7	13.9	54.1 (52 μm)	21.4 (250 μm)
Group 3	2.3	14.1	66.0 (66 μm)	17.4 (249 μm)
Group 4	1.7	11.7	47.7 (70 μm)	38.8 (249 μm)

[a]The geometric mean floc size is shown between brackets for the microfloc and macrofloc. Primary particles and flocculi have constant size of 3 and 15 μm, respectively.

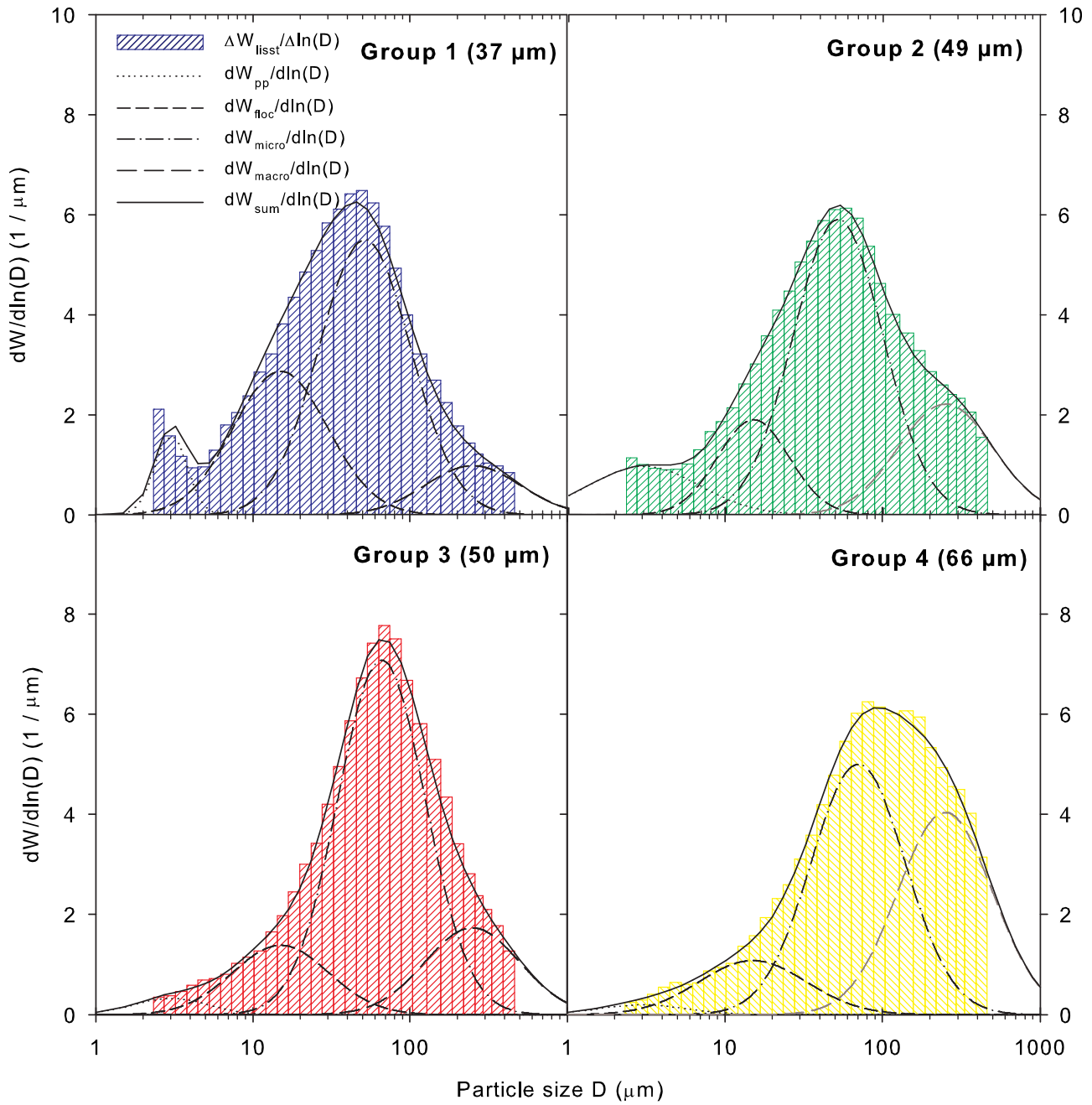

Figure 6. The PSD of the four entropy groups of the low-pass filtered data. Also shown are the subordinate lognormal PSDs of primary particles, flocculi, microflocs, and macroflocs obtained by curve fitting (see also Table 2).

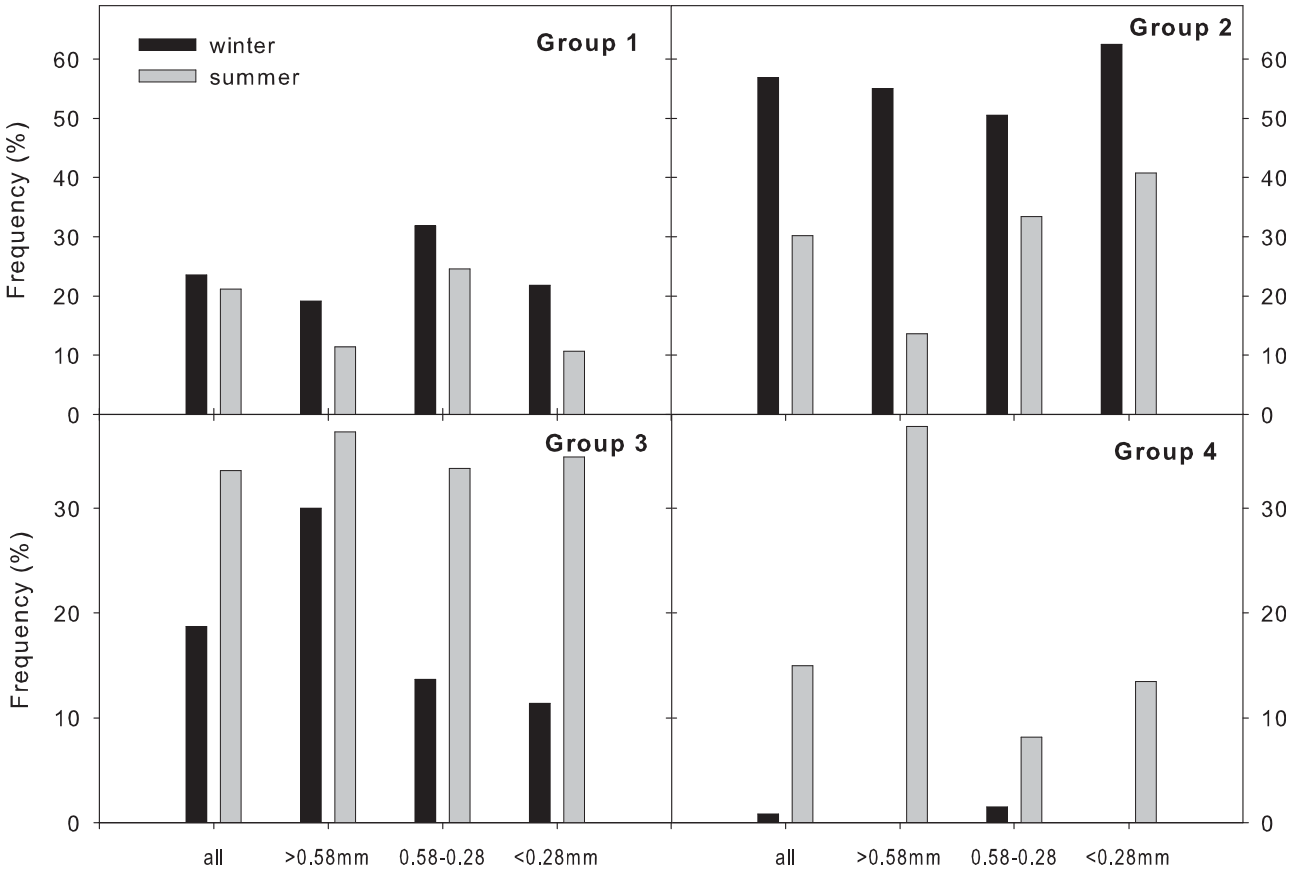

Figure 7. Frequency (%) of the four entropy groups for the summer and winter season and according to the low-pass filtered Kolmogorov scale (λ_k); $\lambda_k < 0.28$ and $\lambda_k > 0.58$ mm are the 15th and 85th percentiles, corresponding to periods with significant high wave heights greater than about 1.50 m and lower than about 0.75 m.

118 mg/L). The latter is probably caused by the limited amount of data fitting this criterion in summer. Surface SPM concentrations from satellite images are about 100% higher in winter than summer. The seasonal variation in Chl concentration is shown in Figure 1b, the mean Chl concentration during summer 2011 was 11 μg/L (maximum is 29 μg/L) and during winter 3 μg/L (maximum is 14 μg/L).

The PSD of the four entropy groups can be found in Figure 6 and Table 2. The groups are ordered in increasing size of the median particle size. The entropy analysis was based on the low-passed filtered data and the tidal variability of the PSDs was thus removed prior to analysis. The resulting classification into the four groups reflects the neap-spring and meteorological variations and not the tidal variations. In Figures 7 and 8 and Table 1, seasonality is investigated by grouping the data into a summer (April to September) and winter (October to March) period. These months have been chosen based on Figure 1 and correspond with a biological (Chl concentration) and physical (Wind, waves) influenced season. In winter, groups 1 and 2 occur during spring tides and storm periods. The differences between groups 1 and 2 are not very large, but are significant. A shift from group 2 in January toward group 1 in February and March is visible in Figure 5. This difference is correlated with changes in wind direction from S-SW toward an eastern direction (SE-E-NE). Group 3 is typically associated with neap tides and low waves. Nevertheless in May, it was dominant during spring tide conditions, indicating that the turbulence was not strong enough to break the flocs into smaller constituents and as a result microfloc and macrofloc were more abundant. Group 4 occurs mainly during summer and is characterized by a shift of the PSD toward larger size classes. Macroflocs are most abundant in this group, and represent about 40% of the total volume concentration. The frequency of the four groups is shown in Figure 7 as a function of season and turbulence intensity (low-pass filtered Kolmogorov scale). During storm periods ($\lambda_k < 0.28$ mm, $H_s > 1.50$ m), groups 1 and 2 are occurring more frequently, whereas the frequency of occurrence of group 3 is lower and of group 4 absent. Seasonal

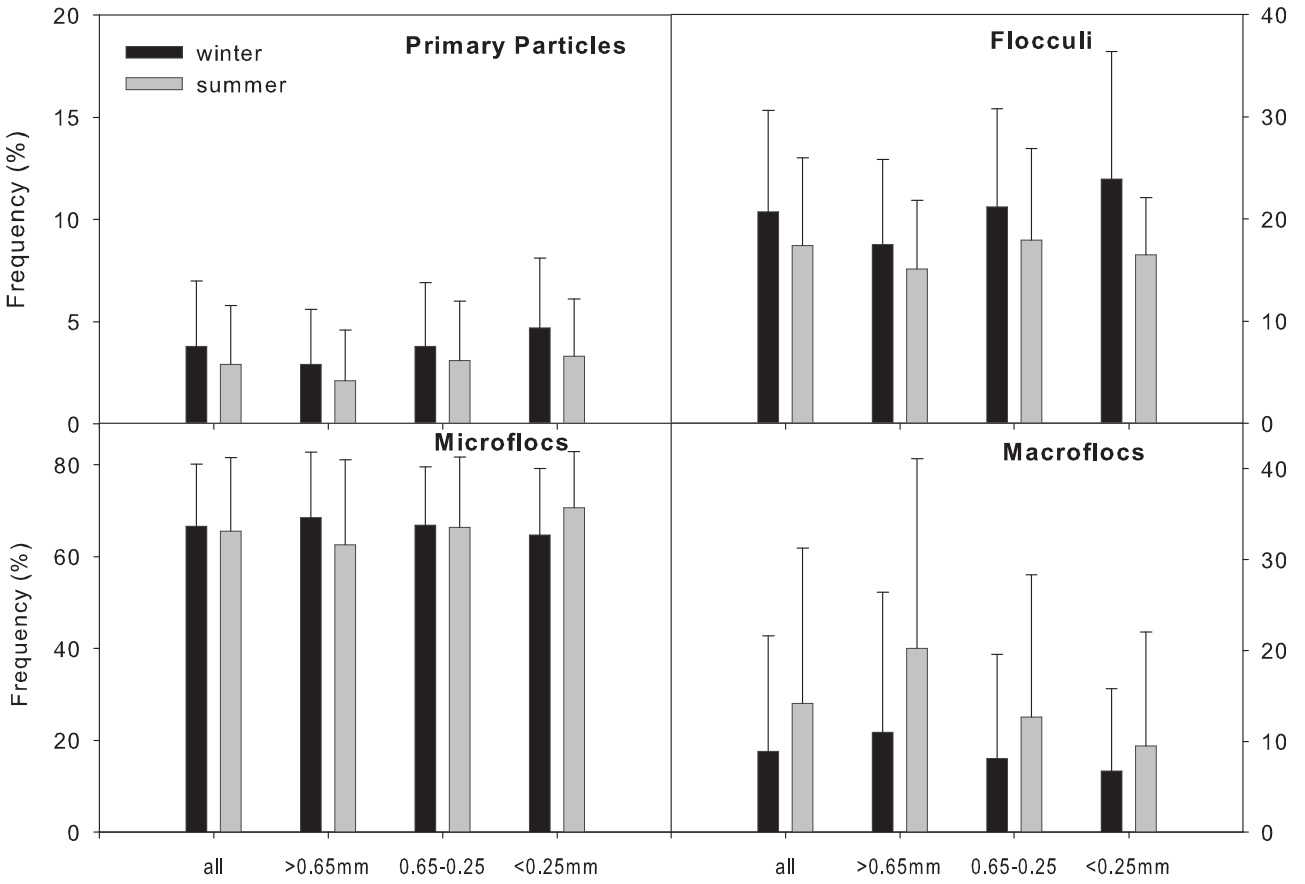

Figure 8. Frequency of primary particles, flocculi, microflocs, and macroflocs for the summer and winter season and according to Kolmogorov scale (λ_k); $\lambda_k < 0.25$ and $\lambda_k > 0.65$ mm are the 15th and 85th percentiles. The geometric mean size of the microflocs is 66 ± 24 μm (winter) and 73 ± 21 μm (summer), and for the macroflocs 222 ± 44 μm (winter) and 220 ± 44 μm (summer). Primary particles and flocculi have constant size of 3 and 15 μm, respectively.

variations in the distribution of the groups can be distinguished. Group 2 is most frequent during winter (57%) followed by groups 1 (24%), 3 (19%), and 4 (1%). Group 3 is associated with neap and group 2 with spring tidal conditions during calm weather. During summer, group 3 emerges as most frequent (34%) followed by groups 2 (30%), 1 (21%), and 4 (15%). During this season, group 4 is typically associated with neap and group 3 with spring tidal conditions during calm weather.

In contrast with the entropy grouping (Figures 5f and 7), the curve-fitting grouping (Figures 5g and 8) is based on physical and not mathematical characteristics of the PSD time series. The results indicate that microflocs are most abundant in terms of volume concentration, followed by flocculi, macroflocs, and primary particles. Yearly average percentages of these four constituents are 3% (primary particles), 20% flocculi, 66% microflocs, and 11% macroflocs (Figure 8). The data are divided in three groups in a similar way as the entropy groups, but now using the (not low-pass filtered) Kolmogorov-scale data. The 15th and the 85th percentile are $\lambda_k = 0.65$ mm and $\lambda_k = 0.25$ mm, respectively. Primary particles and flocculi are abundant during breakup periods as well as microflocs. During periods with lower turbulence, i.e., large Kolmogorov-scale numbers, macroflocs are more abundant. The geometric mean size of the microflocs is 69 ± 23 μm (all year) with slightly lower values during winter (66 ± 24 μm) and slightly higher ones during summer (73 ± 21 μm). The geometric mean size of the macroflocs is 221 ± 44 μm (all year) with almost no variation between seasons (winter: 222 ± 44 μm, summer: 220 ± 44 μm). In contrast with microflocs that do not show a strong seasonal signal, macroflocs are found to be more frequent in summer than in winter (14.2% versus 8.9%, see Figure 8). The frequency of macroflocs in the SPM during periods with high turbulence ($\lambda_k < 0.25$ mm), is on average 9.5% during summer and 6.7% during winter. During calm periods, macroflocs are almost 2 times more abundant in summer than during similar periods in winter (20.2% versus

11.0%). The higher/lower frequency of macroflocs in summer/winter is compensated by lower/higher frequencies of primary particles and flocculi.

4. Discussion

SPM dynamics are controlled by flocculation, which influences the size and deposition rate of the SPM [*Winterwerp*, 2002]. Flocculation depends on the turbulent intensity (tides, wind, waves) and on the surface properties of the suspended particles, which are of electrochemical or microbial origin [*Mietta et al*., 2009]. Microbial products, such as TEPs, are released by algae and bacteria and influence aggregation [*Logan et al*., 1995; *Engel*, 2000]. Chl concentration, wind velocity, and wave height all have a seasonal signal. The seasonality of the Chl concentration signal is, however, more pronounced (Figure 1). Below, we will discuss to what extent the seasonality of floc size is controlled by these physical and biological effects.

4.1. Physical Controls

The hydrodynamics (i.e., flow velocity and turbulent intensity) vary with meteorological conditions, neap-spring and tidal periods. As tidal forcing is approximately equal during both seasons, we will focus on meteorological conditions. The wind climate in the study area is characterized by mainly SW and NE winds (Figure 3), which affect the direction and strength of alongshore water mass transport. During summer, the main wind sectors are WSW and NNE and during winter S to SW and NE. These small shifts in the main wind sectors do not affect the direction of the residual alongshore transport [*Baeye et al*., 2011]. A modification of the residual transport influences the position of the coastal turbidity maximum and thus the SPM concentration at the measuring site [*Baeye et al*., 2011]. The influence of this alongshore advection is reflected in the shift from entropy groups 2 and 3 toward groups 1 and 2 during the first 3 months of the year (Figure 5). This shift is caused by changes in wind direction from S-SW toward more easterly directions (SE toward NE) and also reflects a change in source of the SPM. During SW winds the suspended matter is transported toward the NE and the PSD correspond with group 2 (spring tide) and group 3 (neap tide), whereas during E wind direction the SPM is advected out of the Scheldt estuary and transported toward the SW. During these conditions, spring tides and storms have PSD according to group 1 and neap tides according to group 2 or 3. The frequency of both dominant wind directions does not vary significantly between seasons and therefore, they cannot explain seasonal variations in SPM concentration (Figure 3).

The data indicate that the differences in wind direction and strength between the seasons are small. The wind speeds smaller than 8 m/s are more frequent in summer (55% versus 46%), whereas wind speeds between 8 and 16 m/s are more frequent during winter (49% versus 42%). Storms ($>$16 m/s) are more frequent (5%) in winter than summer (3%). Similar results have been obtained for the waves. The mean significant wave height (Hs) during winter 2011 was 0.55 m and during summer 0.50 m. The mean Hs during the LISST measurements at MOW1 were 0.56 m during summer and 063 m during winter. The mean during the measurements was thus slightly higher than the mean over the whole year. Significant wave heights greater than 1.5 m during the LISST measurements were less frequently in summer (2% versus 7%), whereas periods with low wave heights ($<$0.75 m) were less frequently in winter (60% versus 65%). A seasonal signal exists for wave heights greater than 1.5 m for 2011. The 75% of the higher wave heights occurred during winter and the mean of these waves was higher during winter (1.89 m) than during summer (1.60 m). The summer of 2011 was, compared with the mean occurrence of significant wave heights greater 1.5 m during the period 2001–2012, less stormy. Periods with significant wave heights greater than 1.5 m occurred during 4.1 days versus 7.8 days in the summers of 2001–2012. The frequency of significant wave heights greater than 1.5 m during the winter of 2011 was nearly equal to the mean value (12.5 versus 12.3 days).

Floc size and SPM concentration have been evaluated as a function of sea state characterized by the low-pass filtered Kolmogorov length scale. The geometric mean SPM concentration at MOW1 increased from 357 mg/L (117 mg/L) during summer toward 431 mg/L (145 mg/L) during winter at 0.2 mab (1 mab). The influence of waves is significant (Table 1): the geometric mean SPM concentration was 64 mg/L (145 mg/L) lower during calm conditions than during stormy periods in winter (summer). The volume concentration of the SPM had a slightly different response than the mass SPM concentration. The highest volume concentrations were occurring during intermediate wave conditions. During high wave conditions ($\lambda_k < 0.3$ mm) we observed a decrease of the volume concentration (Table 1). This reflects the fact that the volume concentration depends on effective density and floc size. In case of high waves, large portions of the macroflocs with

lower density were broken up into smaller particles with higher densities, resulting thus in a decrease of the volume concentration.

The effects of the storm extend a certain period after the storm. The duration of storm influence depends on wind direction, wind strength and wave height and can last up to a few days after the storm. The influence period is longer when waves are higher as more sediments have been resuspended or fluidized. Influence of storms is mainly detected in the near-bed layer and decreases toward the surface. Storms with wave heights of more than 2 m affect the SPM concentration for a period of about 5 days after the storm [*Fettweis et al*., 2010]. Storms with significant wave heights above 2 m occurred once during summer and nine times during winter. The total duration of these high wave events was 0.1 days (summer) and 4.3 days (winter). A 2.8 days of winter storms occurred during LISST measurements. Higher SPM concentration due to these meteorological conditions influenced the signal over a period of about 14 days. This represents 10% of the measurements in winter. It does not, however, explain the 20% higher SPM mass concentration and the 50% higher SPM volume concentration near the bed or the 100% higher SPM mass concentration in the surface during winter.

OBSs have primarily been designed to be most sensitive to SPM mass concentration; size effects are an order of magnitude lower than those of concentration, and flocculation effects are even smaller [*Downing*, 2006]. OBSs are most sensitive to fine-grained sediments. When SPM composition changes from very fine material (clay and silt particles or flocs) to silt-sized or sand-sized grains without changes in concentration, the optical backscatter signal will decrease, resulting in an apparent decrease in SPM mass concentration, without affecting SPM volume concentration. This apparent decrease has been observed at a nearby site during NE storm conditions when sand grains were resuspended [*Fettweis et al*., 2012]. However, as NE storms are not frequent these inaccurate SPM concentrations will only have a slight effect on the mean values.

4.2. Biological Controls

Flocculation in coastal waters depends on the attractive forces acting between the suspended particles. These forces depend on the surface properties of the particles, which are of physochemical and microbial origin. TEP was first described by *Alldredge et al*. [1993] and consists of mostly polysaccharides that are negatively charged, very sticky, and frequently colonized by bacteria. They interact with mineral particles and alter the properties of the SPM [*Passow et al*., 2001]. In general, TEPs are found to be in the same size and abundance range as phytoplankton [*Mari and Burd*, 1998]. The production of TEPs in the ocean has been connected with algae blooms and bacteria in that the formation of large aggregates following blooms was primarily controlled by TEP concentrations [*Logan et al*., 1995; *Mari and Burd*, 1998; *Passow et al*., 2001]. In shallow turbid systems, the phytoplankton balance is strongly affected by SPM dynamics. Phytoplankton growth in such environments depends on the light adsorption coefficient of the water, which varies according to the tidal and neap-spring variation of SPM concentration [*Desmit et al*., 2005]. Our data show that SPM concentration is highest during peak velocity during spring tide and lowest during slack water. *Desmit et al*. [2005] have shown that these short-term, tidally driven SPM concentration variations allow the incident sunlight energy to sustain phytoplankton production in these environments during spring and summer. The increase of Chl concentration during spring (Figure 1) indicates the start of the algae bloom and thus the start of the "biologically active" season. The surface Chl concentration drops after the spring bloom, and is followed by a summer bloom between day 150 and 190. Although the summer bloom was less pronounced as shown by the Chl concentration climatology (Figure 1b), it resulted in sufficiently Chl concentration levels that when combined with the TEP production by heterotrophic bacteria and macrobenthos was able to maintain the higher frequency of macroflocs found in the measurements.

Based on the decomposition of the measured PSD into four subordinate lognormal functions it was found, despite the seasonal signal in median floc size (D50-summer: 64 μm, D50-winter: 51 μm), that the sizes of macroflocs only show small variations during seasons (summer: 220 μm, winter: 222 μm). The frequency of macroflocs, however, has a seasonal signal. Macroflocs are more abundant in the SPM in summer than winter regardless of the turbulence intensity (Figure 8). Similar results are found in low-passed filtered entropy data. During neap tides and low wave activity entropy group 4 is dominant in summer and group 3 in winter. Group 4 is characterized by 39% of macroflocs and 48% of microflocs, whereas group 3 consists of 17% macroflocs and 66% microflocs. This observation is somewhat in contrast to other studies, arguing that for

a given turbulence level flocs become larger with abundant organic matters during summer [*Lunau et al*., 2006; *Cross et al*., 2013]. The rate of break up of large flocs and the equilibrium size of flocs in turbulent flow depend on their strength [*Kranenburg*, 1999; *Winterwerp*, 2002]. Our observations of PSDs from a highly turbid coastal zone suggest that the maximum size is mainly controlled by the intensity of turbulence (tidal signal and waves) and the flocculation time. The tidal current ellipses are elongated at the measuring site and time available for floc formation is limited to the short periods of slack water (current velocity below 0.2 m/s at 1.8 m above the bed last on average 45 min at the measuring location), which are not sufficient for the flocs to attain their equilibrium size. Mineralogical composition of the SPM shows only minor changes throughout the year [*Zeelmaekers*, 2011]. The data suggest that the TEP formed during spring and summer increases the strength of the macroflocs rather than their size. If the abundance of macroflocs as a function of turbulence intensity is a proxy of floc strength then Figures 8 shows that flocs in summer are stronger than in winter. In our data, we can see that group 3, which is typically correlated with neap tides during winter, was dominant in May 2011 during a spring tide (around day 120 in Figure 5). Turbulence was then apparently not strong enough to break up the flocs and to shift the PSD toward group 2. Similar results were observed by *Lee et al*. [2012] who found that aggregates were armored against breakage during the algae bloom in April 2008. The stronger flocs resist shear-induced breakup and—if we assume that the macroflocs behave similar as in other coastal and estuarine environments [*Winterwerp et al*., 2006]—the higher proportion of large flocs results in a higher settling rate during summer and thus a lower SPM concentration. Only during storms (wave height $>$ 2 m) in summer did a significant break up of the larger flocs into smaller particles (see around day 150 and 200 in Figure 5) occur.

The higher frequency of macroflocs in summer is compensated by lower frequencies of primary particles and flocculi. The size and frequency of the microfloc population in the PSDs, which is the major part of the SPM, has almost no seasonal signal (Figure 8). The predominance of these intermediate floc sizes can possibly be explained by a low TEP concentration relative to the mineral concentration. The sticky organic matter will decay and be quickly saturated by the mineral particles and will only help a limited part of the SPM to develop into breakage-resistant macroflocs.

Our results suggest that floc size controls settling and deposition and thus sediment dynamics. TEPs and other biostabilizators reduce erosion and resuspension of mud deposits [*Droppo et al*., 2001; *Black et al*., 2002; *Gerbersdorf et al*., 2008; *Maerz and Wirtz*, 2009]. Therefore, we presume that during summer a larger part of the cohesive sediments is kept in a high-concentration mud suspension (HCMS), fluid mud, or consolidated bed layer. The presence of HCMS or fluid mud results in a reduction of the bottom shear stress and thus a decrease of erosion [*Geyer et al*., 1996]. In winter, the strength of the deposits decreases, due to lower TEP concentrations flocs getting less strong and therefore are more easily resuspended, resulting in higher SPM concentrations. Evidence of HCMS formation during an algae bloom period was observed at a nearby site in April 2008 in contrast with a winter period [*Fettweis et al*., 2012]. The much greater decrease in surface SPM concentration compared with near-bed SPM concentration during summer suggests faster settling in the summer.

5. Conclusions

The annual cycle of SPM concentration in the high turbidity area off the Belgian coast is mainly caused by the seasonal biological cycle, rather than wind and waves. Wind strengths and wave heights have a seasonal signal, but these are not sufficient to explain the large differences observed in SPM concentration. The data are in line with the literature that emphasizes the stabilizing effect of biomass on bed erosion and floc strength. In the tidal-dominated southern North Sea, biomass effects increase the strength of macroflocs rather than their size, as was reported from other sites. The results highlight the transformation of mainly microflocs and flocculi in winter toward more muddy marine snow with larger amounts of macroflocs in spring and summer. The larger fraction of macroflocs reduces the SPM concentrations in the turbidity maximum area as they settle faster. The fact that macroflocs are more abundant and that SPM concentration decreases will increase light condition in the surface layer and enhance algae growth. Whence, it is mainly the biological activity in spring and summer that lead to a decrease in SPM concentration in the study area rather than the seasonal pattern in wind conditions. The data are, however, not able to explain the initiation of this transition as PSD and in situ Chl and TEP concentration are not available for

the 2011 spring algal bloom period. Nevertheless, our data clearly show the importance of microbial activity on the cohesive sediment dynamics. The proposed mechanisms may differ in other marine habits. To date, very little comparative data exist with which to contrast our results from a eutrophied high turbidity area, with areas that are less affected by excess supply of nutrients.

Acknowledgment

The study was supported by the Maritime Access Division of the Ministry of the Flemish Community (MOMO project). Ship Time RV Belgica was provided by BELSPO and RBINS–Operational Directorate Natural Environment. The wave and wind data are from the Ministry of the Flemish Community (IVA MDK—afdeling Kust—Meetnet Vlaamse Banken). We thank L. Naudts, J. Backers, W. Vanhaverbeke, and K. Hindryckx for all technical aspects of instrumentation and moorings; F. Francken for data processing and archiving; and K. Ruddick, X. Desmit, G. Lacroix, and Q. Vanhellemont for useful discussions. We would also like to acknowledge the two reviewers for useful comments on the first version of the manuscript.

References

Agrawal, Y., and H. Pottsmith (2000), Instruments for particle size and settling velocity observations in sediment transport, *Mar. Geol.*, *168*, 89–114.

Alldredge, A. L., U. Passow, and B. E. Logan (1993), The abundance and significance of a class of large, transparent organic particles in the ocean, *Deep-Sea Res., Part I*, *40*, 1131–1140.

Andrews, S., D. Nover, and S. Schladow (2010), Using laser diffraction data to obtain accurate particle size distributions: The role of particle composition, *Limnol. Oceanogr. Methods*, *8*, 507–526, doi:10.4319/lom.2010.8.507.

Baeye, M., M. Fettweis, G. Voulgaris, and V. Van Lancker (2011), Sediment mobility in response to tidal and wind-driven flows along the Belgian inner shelf, southern North Sea, *Ocean Dyn.*, *61*, 611–622, doi:10.1007/s10236-010-0370-7.

Bainbridge, Z. T., E. Wolanski, J. G. Álvarez-Romero, S. E. Lewis, and J. E. Brodie (2012), Fine sediment and nutrient dynamics related to particle size and floc formation in a Burdekin River flood plume, Australia, *Mar. Poll. Bull.*, *65*, 236–248, doi:10.1016/j.marpolbul.2012.01.043.

Black, K. S., T. J. Tolhurst, D. M. Paterson, and S. E. Hagerthey (2002), Working with natural cohesive sediments, *ASCE J. Hydraul. Eng.*, *128*, 2–8, doi:10.1061/(ASCE)0733–9429(2002)128:1(2)).

Borsje, B. W., M. B. de Vries, S. J. M. H. Hulscher, and G. J. de Boer (2008), Modeling large-scale cohesive sediment transport affected by small-scale biological activity, *Estuarine Coastal Shelf Sci.*, *78*, 468–480, doi:10.1016/j.ecss.2008.01.009.

Cross, J., W. A. M. Nimmo-Smith, R. Torres, and P. J. Hosegood (2013), Biological controls on resuspension and the relationship between particle size and the Kolmogorov length scale in a shallow coastal sea, *Mar. Geol.*, *343*, 29–38, doi:10.1016/j.margeo.2013.06.014.

Davies, E. J., W. A. M. Nimmo-Smith, Y. C. Agrawal, and A. J. Souza (2012), LISST-100 response to large particles, *Mar. Geol.*, *307-310*, 117–122, doi:10.1016/j.margeo.2012.03.006.

Desmit, X., J. P. Vanderborght, P. Regnier, and R. Wollast (2005), Control of phytoplankton production by physical forcing in a strongly tidal, well-mixed estuary, *Biogeosciences*, *2*, 205–218, doi:10.5194/bg-2–205-2005.

Dobrynin, M., G. Gayer, A. Pleskachevsky, and H. Günther (2010), Effect of waves and currents on the dynamics and seasonal variations of suspended particulate matter in the North Sea, *J. Mar. Syst.*, *82*, 1–20, doi:10.1016/j.jmarsys.2010.02.012.

Doerffer, R., and H. Schiller (2007), The MERIS case 2 water algorithm, *Int. J. Remote Sens.*, *28*, 517–535, doi:10.1080/01431160600821127.

Downing, J. (2006), Twenty-five years with OBS sensors: The good, the bad, and the ugly, *Cont. Shelf Res.*, *26*, 2299–2318, doi:10.1016/j.csr.2006.07.018.

Droppo, I. G., Y. L. Lau, and C. Mitchell (2001), The effect of depositional history on contaminated bed sediment stability, *Sci. Total Environ.*, *266*, 7–13.

Eleveld, M. A., R. Pasterkamp, H. J. van der Woerd, and J. D. Pietrzak (2008), Remotely sensed seasonality in the spatial distribution of sea-surface suspended particulate matter in the southern North Sea, *Estuarine Coastal Shelf Sci.*, *80*, 103–113, doi:10.1016/j.ecss.2008.07.015.

Engel, A. (2000), The role of transparent exopolymer particles (TEP) in the increase in apparent particle stickiness during the decline of a diatom bloom, *J. Plankton Res.*, *22*, 485–497.

Fettweis, M. (2008), Uncertainty of excess density and settling velocity of mud flocs derived from in situ measurements, *Estuarine Coastal Shelf Sci.*, *78*, 428–436, doi:10.1016/j.ecss.2008.01.007.

Fettweis, M., and B. Nechad (2011), Evaluation of in situ and remote sensing sampling methods for SPM concentrations on the Belgian continental shelf (southern North Sea), *Ocean Dyn.*, *61*, 157–171, doi:10.1007/s10236-010-0310-6.

Fettweis, M., and D. Van den Eynde (2003), The mud deposits and the high turbidity in the Belgian-Dutch coastal zone, Southern bight of the North Sea, *Cont Shelf Res.*, *23*, 669–691, doi:10.1016/S0278–4343(03)00027-X.

Fettweis, M., F. Francken, V. Pison, and D. Van den Eynde (2006), Suspended particulate matter dynamics and aggregate sizes in a high turbidity area, *Mar. Geol.*, *235*, 63–74, doi:10.1016/j.margeo.2006.10.005.

Fettweis, M., F. Francken, D. Van den Eynde, T. Verwaest, J. Janssens, and V. Van Lancker (2010), Storm influence on SPM concentrations in a coastal turbidity maximum area with high anthropogenic impact (southern North Sea), *Cont. Shelf Res.*, *30*, 1417–1427, doi:10.1016/j.csr.2010.05.001.

Fettweis, M., M. Baeye, B. J. Lee, P. Chen, and J. C. S. Yu (2012), Hydro-meteorological influences and multimodal suspended particle size distributions in the Belgian nearshore area (southern North Sea), *Geo Mar. Lett.*, *32*, 123–137, doi:10.1007/s00367-011-0266-7.

Flagg, C. N., J. A. Vermersch, and R. C. Beardsley (1976), 1974 MIT New England shelf dynamic experiment (March 1974) data report, part II: The moored array, *Rep. 76-1*, Mass. Inst. of Technol, Cambridge.

Gerbersdorf, S. U., T. Jancke, P. Westrich, and D. M. Paterson (2008), Microbial stabilization of riverine sediments by extracellular polymeric substances, *Geobiology*, *6*, 57–69, doi:10.1111/j.1472–4669.2007.00120.x.

Geyer, W. R., R. C. Beardsley, S. J. Lentz, J. Candela, R. Limeburner, W. E. Johns, B. M. Castro, and I. D. Soares (1996), Physical oceanography of the Amazon shelf, *Cont. Shelf Res.*, *16*, 575–616.

Graham, G. W., E. J. Davies, W. A. M. Nimmo-Smith, D. G. Bowers, and K. M. Braithwaite (2012), Interpreting LISST-100X measurements of particles with complex shape using digital in-line holography, *J. Geophys. Res.*, *117*, C05034, doi:10.1029/2011JC007613.

Hamm, C. E. (2002), Interactive aggregation and sedimentation of diatoms and clay-sized lithogenic material, *Limnol. Oceanogr.*, *47*, 1790–1795.

Howarth, M. J., et al. (1993), Seasonal cycles and their spatial variability, *Philos. Trans. R. Soc. London A*, *343*(1669), 383–403.

Jago, C. F., G. M. Kennaway, G. Novarino, and S. E. Jones (2007), Size and settling velocity of suspended flocs during a phaeocystis bloom in the tidally stirred Irish Sea, NW European Shelf, *Mar. Ecol. Prog. Ser.*, *345*, 51–62, doi:10.3354/meps07006.

Johnston, R. J., and R. K. Semple (1983), Classification using information statistics, in *Concepts and Techniques in Modern Geography*, vol. 37, 43 pp., GeoBooks, Norwich, U. K.

Jonasz, M., and G. Fournier (1996), Approximation of the size distribution of marine particles by a sum of log-normal functions, *Limnol. Oceanogr.*, *41*,744–754.

Kranenburg, C. (1999), Effects of floc strength on viscosity and deposition of cohesive sediment suspensions, *Cont. Shelf Res.*, *19*, 1665–1680.

Lacroix, G., K. Ruddick, J. Ozer, and C. Lancelot (2004), Modelling the impact of the Scheldt and Rhine/Meuse plumes on the salinity distribution in Belgian waters (southern North Sea), *J. Sea Res.*, *52*, 149–163, doi:10.1016/j.seares.2004.01.003.
Lancelot, C., G. Billen, A. Sournia, T. Weisse, F. Colijin, M. J. W. Veldhuis, A. Davies, and P. Wassman (1987), Phaeocystis blooms and nutrient enrichment in the continental coastal zones of the North Sea, *Ambio*, *16*, 38–46.
Lee, B. J., M. Fettweis, E. Toorman, and F. Molz (2012), Multimodality of a particle size distribution of cohesive suspended particulate matters in a coastal zone, *J. Geophys. Res.*, *117*, C03014, doi:10.1029/2011JC007552.
Logan, B. E., U. Passow, A. L. Alldredge, H.-P. Grossartt, and M. Simon (1995), Rapid formation and sedimentation of large aggregates is predictable from coagulation rates (half-lives) of Transparent Exopolymer Particles (TEP), *Deep Sea Res., Part II*, *42*, 203–214.
Lunau, M., A. Lemke, O. Dellwig, and M. Simon (2006), Physical and biogeochemical controls of microaggregate dynamics in a tidally affected coastal ecosystem, *Limnol. Oceanogr. Methods*, *51*, 847–859.
Maerz, J., and K. Wirtz (2009), Resolving physically and biologically driven suspended particulate matter dynamics in a tidal basin with a distribution-based model, *Estuarine Coastal Shelf Sci.*, *84*, 128–138, doi:10.1016/j.ecss.2009.05.015.
Maggi, F. (2009), Biological flocculation of suspended particles in nutrient-rich aqueous ecosystems, *J. Hydrol.*, *376*, 116–125, doi:10.1016/j.jhydrol.2009.07.040.
Mari, X., and A. Burd (1998), Seasonal size spectra of transparent exopolymeric particles (TEP) in a coastal sea and comparison with those predicted using coagulation theory, *Mar. Ecol. Prog. Ser.*, *163*, 53–76.
Mietta, F., C. Chassagne, A. J. Manning, and J. C. Winterwerp (2009), Influence of shear rate, organic matter content, pH and salinity on mud flocculation, *Ocean Dyn.*, *59*, 751–763, doi:10.1007/s10236-009-0231-4.
Mikkelsen, O., K. Curran, P. Hill, and T. Milligan (2007), Entropy analysis of in situ particle size spectra, *Estuarine Coastal Shelf Sci.*, *72*, 615–625, doi:10.1016/j.csr.2006.11.004.
Nechad, B., K. Ruddick, and Y. Park (2010), Calibration and validation of a generic multisensor algorithm for mapping of total suspended matter in turbid waters, *Remote Sens. Environ.*, *114*, 854–866, doi:10.1016/j.rse.2009.11.022.
Passow, U. (2002), Transparent exopolymer particles (TEP) in aquatic environments, *Prog. Oceanogr.*, *55*, 287–333.
Passow, U., R. F. Shipe, A. Murray, D. K. Pak, M. A. Brzezinski, and A. L. Alldredge (2001), The origin of Transparent Exopolymer Particles (TEP) and their role in the sedimentation of particulate matter, *Cont. Shelf Res.*, *21*, 327–346.
Rousseau, V., A. Leynaert, N. Daoud, and C. Lancelot (2002), Diatom succession, silicification and silicic acid availability in Belgian coastal waters (southern North Sea), *Mar. Ecol. Prog. Ser.*, *236*, 61–73.
Sherwood, C., J. Lacy, and G. Voulgaris (2006), Shear velocity estimates on the inner shelf off Grays Harbor, Washington, USA, *Cont. Shelf Res.*, *26*, 1995–2018, doi:10.1016/j.csr.2006.07.025.
Stapleton, R. L., and D. A. Huntley (1995), Seabed stress determination using the inertia dissipation method and the turbulent kinetic energy method, *Earth Surf. Processes Landforms*, *20*, 807–815.
Thompson, C. E. L., C. L. Amos, T. E. R. Jones, and J. Chaplin (2003), The manifestation of fluid-transmitted bed shear stress in a smooth annular flume—A comparison of methods, *J. Coastal Res.*, *19*, 1094–1103.
Trowbridge, J., and S. Elgar (2001), Turbulence measurements in the surf zone, *J. Phys. Oceanogr.*, *31*, 2403–2417.
Van Beusekom, J. E. E., C. Buschbaum, and K. Reise (2012), Wadden Sea tidal basins and the mediating role of the North Sea in ecological processes: Scaling up of management? *Ocean Coastal Manage.*, *68*, 69–78, doi:10.1016/j.ocecoaman.2012.05.002.
van Leussen, W. (1999), The variability of settling velocities of suspended fine-grained sediment in the Ems estuary, *J. Sea Res.*, *41*, 109–118, doi:10.1016/S1385-1101(98)00046-X.
Verfaillie, E., V. Van Lancker, and M. Van Meirvenne (2006), Multivariate geostatistics for the predictive modelling of the surficial sand distribution in shelf seas, *Cont. Shelf Res.*, *26*, 2454–2468, doi:10.1016/j.csr.2006.07.028.
Verney, R., R. Lafite, and J.-C. Brun-Cottan (2009), Flocculation potential of estuarine particles: The importance of environmental factors and of the spatial and seasonal variability of suspended particulate matter, *Estuaries Coasts*, *32*, 678–693, doi:10.1007/s12237-009-9160-1.
Whitby, K. (1978), The physical characteristics of sulfur aerosols, *Atmos. Environ.*, *41*, 25–49.
Winterwerp, J., A. J. Manning, C. Martens, T. De Mulder, and J. Vanlede (2006), A heuristic formula for turbulence-induced flocculation of cohesive sediment, *Estuarine Coastal Shelf Sci.*, *68*, 195–207, doi:10.1016/j.ecss.2006.02.003.
Winterwerp, J. C. (2002), On the flocculation and settling velocity of estuarine mud, *Cont. Shelf Res.*, *22*, 1339–1360.
Zeelmaekers, E. (2011), Computerized qualitative and quantitative clay minerology: Introduction and application to known geological cases, PhD thesis, Catholic Univ. Leuven, Belgium.

APPENDIX 3

Van den Eynde D, Fettweis M. 2014. Towards the application of an operational sediment transport model fort the optimisation of dredging works in the Belgian coastal zone (southern North Sea). In: Dahlin H., Flemming N.C., Petersson S.E. (Eds.). Sustainable Operational Oceanography, 250-257.

Towards the application of an operational sediment transport model for the optimisation of dredging works in the Belgian coastal zone (southern North Sea)

Dries Van den Eynde* and Michael Fettweis

Management Unit of the North Sea Mathematical Models, Royal Belgian Institute of Natural Sciences, Brussels, Belgium

Abstract

The Belgian Continental Shelf (BCS) is characterised by shallow waters, with an irregular bathymetry and systems of sand banks. The bottom sediments generally consist of fine to medium sand. In the coastal zone, high concentrations of fine-grained suspended particulate matter occur which are responsible for a significant siltation of the ports and navigation channels. Every year, about 11 million tons of dry material is dredged and dumped back into sea. The dumped matter is quickly resuspended and transported away from the dumping sites. A non-negligible part of it recirculates back towards the dredging places, raising the question of the efficiency of the dredging strategy.

To study this recirculation process, numerical models are developed, validated and used in an attempt to help the authorities in the choice of an optimum dredging methodology. A semi-Lagrangian two-dimensional sediment transport model is coupled to MUMM's three-dimensional baroclinic hydrodynamic models. Model results have been validated against observed dispersion of radio-active material dumped in the area as well as long term in-situ measurements. Other model applications dealt with the study of the mud balance in the BCS and the influence on it of dumping activities.

The selection of the optimal location for the dumping sites is an important concern. Optimal means: i) minimising recirculating to the dredging places, ii) confining the physical, chemical and biological effects and iii) keeping the distance between the dumping site and dredging places as short as possible. Different model simulations are carried out to investigate the influence of the position of the dumping sites and of the meteorological conditions on the recirculation process. A first step is made in the operational implementation of a tool that can help the authorities to make the best choice for the dumping site, taking into account the actual meteorological and hydrodynamic conditions.

Keywords: Dumping and dredging activities, dredging efficiency, operational forecasting, sediment transport modelling, southern North Sea, Belgium.

* Corresponding author, email: Dries.VandenEynde@mumm.ac.be

1. Introduction

The Belgian–Dutch coastal area is shallow, with water depths between 5 and 40 m and is characterised by strong vertical mixing and high tidal velocities. The sediment transport in the area is complex. High turbidity values (about a few hundred mgl^{-1}) are regularly observed between Oostende and Zeebrugge making the Belgian coastal waters one of the most turbid in the North Sea. Main Belgian sea ports (Oostende and Zeebrugge) and the main navigation channels towards the Westerschelde estuary must therefore be continuously dredged to maintain accessibility. Comparison between the natural input of the suspended particulate matter (SPM) in the coastal zone through (mainly) the Strait of Dover and the quantities dredged and dumped at sea show that an important part of the SPM is involved in the dredging/dumping cycle (Fettweis and Van den Eynde, 2003).

Dredging and dumping amounts to about 11 million tons of dry matter yearly, from which more than 70% is silt and clay. 10% of the total dredged quantity is dredged in the navigation channel connecting the port of Zeebrugge with the open sea and 62% in the port of Zeebrugge. The rest is extracted from the navigation channel towards the Westerschelde (22%) and the harbour of Oostende (5%).

Most of the dredged material is dumped back into the sea at selected dumping sites, from which the material is transported again, mainly in suspension. The dumping of this fine-grained material can disturb the nutrient dynamics in the water. A higher sediment concentration in the water column mainly influences the biota and filter-feeding organisms. At the dumping sites themselves, the benthos is disturbed due to burial.

Dredging works may be limited by reducing the sedimentation in harbours (transformation of the harbour entrance or current deflecting wall) or by applying a more efficient dumping scheme. The efficiency of a dumping place is determined by physical (sediment transport, hydrodynamics), economic and ecological aspects. An efficient dumping place has a minimal recirculation of dumped matter back to the dredging places, a minimal distance between the dumping place and the dredging area and a minimal influence on the environment.

Operational numerical hydrodynamic and sediment transport models can forecast the recirculation of dumped material during the next few days. The best dumping site can then be selected taking into account the present conditions.

This paper first briefly presents the numerical models. Then the results of model applications dealing with the evaluation of the efficiency of three different dumping schemes around Zeebrugge (east, west or as a function of tide) are presented and discussed. A fourth section is dedicated to a short presentation of a first implementation of an operational forecasting system. Finally, some conclusions and recommendations for further work are formulated.

2. Hydrodynamic and fine sediment transport forecasting tools

2.1 Main characteristics of the hydrodynamics and fine-grained sediment transport on the Belgian Continental Shelf

A detail of the bathymetry of the part of the BCS is shown in Figure 1. The water depth varies between three and about thirty metres. The navigation channels are dredged to

about fifteen metres below LAT (Lowest Astronomical Tide). The hydrodynamics of the Belgian coastal waters are determined mainly by tides, wind and wave activity. The tides are semi-diurnal and slightly asymmetrical. The mean tidal range at Zeebrugge is 4.3 m at spring tide and 2.8 m at neap tide. The tidal current ellipses are elongated in the coastal zone and become more broadly elliptical further offshore. The current velocities can reach more than 1 m s^{-1} at spring tide. The water column in the area is well mixed during the entire year. The freshwater outflow from the Westerschelde is low and has a long-term (1949–1997) annual mean of 107 m^3s^{-1}. The winds and consequently also the waves are mainly from the southwest or from the northeast. The winds are most of the time (90%) below 5 Bft (10.8 m s^{-1}). Significant wave height at Westhinder, 20 km from the coast, is 87% of the time below 2.0 m. The long term transport of the water is mainly to the northeast.

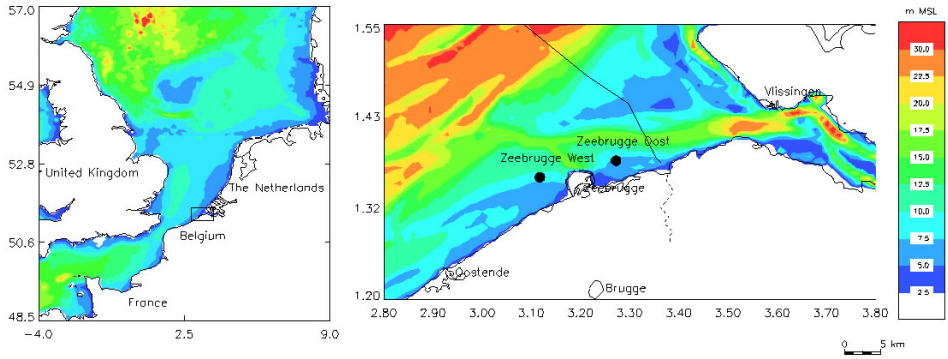

Figure 1 Left: Position of the study area. Right: Detail of the bathymetry of the 820 m × 772 m model grid of the Belgian Continental Shelf. Two possible dumping sites are indicated.

The surface sediments on the BCS consist mainly of medium to fine sand. Further from the coast, at water depths greater than 12 m, medium sand is found with a median grain size up to more than 400 µm. Nearer to the coast and east of Oostende, fine sands are found with a median grain size lower than 200 µm. In the eastern part large mud fields are found. These mud fields are partly correlated with the high turbidity zone between Oostende and the mouth of the Westerschelde.

2.2 Description of the numerical models

The core of the hydrodynamic models is the COHERENS code (Luyten *et al.*, 1999). Governing equations express conservation of mass, momentum, temperature and salinity. A transport equation for turbulent kinetic energy combined with an algebraic formulation for the length scale is used. These equations are solved using the mode splitting technique on an Arakawa-C model grid.

For operational purposes, three different implementation of the COHERENS code are used. Only the barotropic mode is turned on for the two-dimensional implementation, referred to as OPTOS-CSM, that covers the entire Northwest European Continental Shelf. Model forcing comes from the tide and the Numerical Weather Predictions (NPW) provided by the United Kingdom Meteorological Office. For the North Sea area as well as on the BCS, the full three-dimensional version of COHERENS is used. The North Sea

model, OPTOS-NOS, is forced along its open boundaries by OPTOS-CSM. Surface forcing is coming from the same NWP. Freshwater discharges (climatological values) from main European rivers are taken into account.

On the BCS, the model (referred to as OPTOS-BCS) is implemented on a grid with a resolution of about 1/84° in longitude (817–833 m) and 1/144° in latitude (772 m). Along the vertical, 20 σ-layers are used. Open boundary conditions are provided by OPTOS-NOS.

The OPTOS-BCS model was validated extensively, using 400 hours of current profiles on the BCS, measured with a bottom mounted Acoustic Doppler Current Profiler (ADCP), type Sentinel 1200 kHz Workhorse of RDInstruments (Dujardin *et al*., 2010).

The two-dimensional sediment transport model is a semi-Lagrangian model, based on the Second Moment Method (de Kok, 1994). In this method, all the material in a grid cell is represented by one rectangular mass, with the sides parallel to the direction of the model grid, and characterised by its zero order moment (total mass), its first order moments (position of mass centre) and its second order moments (the extension of the mass). Advection is represented by the advection of each of the sides of the rectangle. Diffusion is simulated by enlarging its extension. After each time step all material in a grid cell is recombined and represented by one new rectangle with the same zero, first and second order moments. The model can account for different sediment classes. In the applications reported in this paper, only mud, defined as the fraction smaller than 63 μm, is introduced. Erosion and sedimentation processes are governed by bottom friction, which is parametrised using an adaptation of the Bijker formula (Bijker, 1966). Erosion is modelled following Ariathurai (1974), while sedimentation is calculated using the formula from Krone (1966). The amount of material that is eroded depends on the erosion constant M ($\mathrm{kg\,m^{-2}\,s^{-1}}$) and of a critical bottom stress for erosion τ_s (Pa), while sedimentation uses parameters for the fall velocity of the sediment particles w_s ($\mathrm{m\,s^{-1}}$) and for the critical bottom stress for deposition τ_d (Pa). In this model, the critical bottom stress for erosion depends on the consolidation of the deposited material. The complete description of the consolidation model falls out of the scope of the present paper, but more information can be found in Fettweis and Van den Eynde (2003).

The critical bottom stress for erosion varies between 0.5 Pa for loosely deposited mud and 0.79 Pa for consolidated mud after 48 hours, the erosion constant M is set to $0.00012\ \mathrm{kg\,m^{-2}\,s^{-1}}$. The fall velocity is set constant and equal to $2\ \mathrm{mm\,s^{-1}}$. This rather high value implicitly accounts for flocculation processes and agrees with recent measured values. The critical bottom stress for deposition has a value of 0.5 Pa. This high value promotes the deposition of the sediments. The model was validated by comparing the model with in-situ measurements and by simulating radio-active tracer experiments (Van den Eynde, 2004).

3. Model simulations and results

3.1 Different scenarios

To demonstrate the possible useful application of the numerical models to select the most efficient dumping scheme, three different dumping strategies are evaluated. In the strategy “business as usual”, the material is dumped on the Zeebrugge-Oost dumping site

(ZBO), a site which is used at the present time, at a distance of about 4.5 km east of the harbour entrance. In a second dumping strategy, this site is moved to the west of Zeebrugge harbour (ZBW), at an equivalent distance with respect to the entrance. Both locations are indicated in Figure 1. In a third scenario (TDD), the dumping is tide dependent: during ebb (water transport to the west), the ZBW site is used, while during flood (currents to the east) material is dumped on ZBO site.

The efficiency of the dumping strategies is evaluated by calculating the recirculation from the dumping sites towards two dredging areas, i.e., the zone around the port (see Figure 2a) taken as a proxy for the recirculation to the harbour itself, and the zone around the navigation channels (see Figure 2b).

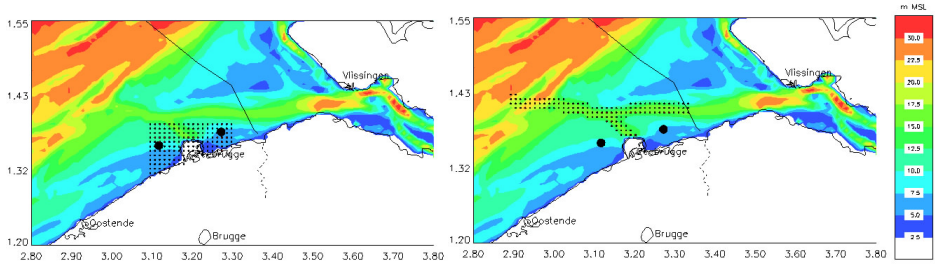

Figure 2 Two zones where the recirculation of the dumped material is being calculated. a: (left) Zone around Zeebrugge harbour; b: (right) Zone around the navigation channels.

A one month period, from 1 January – 1 February 2006, has been chosen. The period comprises two spring-neap tidal cycles with spring tides around 2, 16 and 31 January and neap tides around 9th and 24th January. The wind speed during the period stayed limited to less then 8 ms^{-1} most of the time, with wind peaks of more then 10 ms^{-1} on 10, 11, and 26 January. The wind direction was highly variable, with the winds coming most of the time from the south or the east. Simulations start at different dates during this period. Each simulation has a duration of 5 days and 5 hours (equivalent to the length of the actual model forecast).

Various surface forcing are considered: no wind forcing, realistic wind forcing, uniform in space and constant in time wind forcing (9 ms^{-1} from northwest, northeast or southwest). During each model run, 337.5 tons of mud is dumped according to one of the dumping schemes previously described. The efficiency of the dumping strategy is evaluated from the averaged amount of material found at the bottom in each dredging zone during the last day of the simulation.

Results from the simulations without wind forcing are presented in Figure 3. The last day averaged amount of material found at the bottom, in the two zones of interest and as a function of the starting date, is displayed. For the zone around the harbour of Zeebrugge (Figure 3, left), dumping on ZBO induces the largest recirculation of material. Concerning the two others dumping schemes (ZBW and TDD), results clearly indicate that the choice should be made according to the time start of the simulations. Sometimes it is better to dump continuously on Zeebrugge-West. Other times, it is better to use a tide dependent dumping strategy. For the zone around the navigation channels, the results vary more. The results indicate that dumping on ZBO at some times seems to be

the best choice. However, this is probably mainly due to the fact that the simulation is only executed over a short period of 5 days and 5 hours.

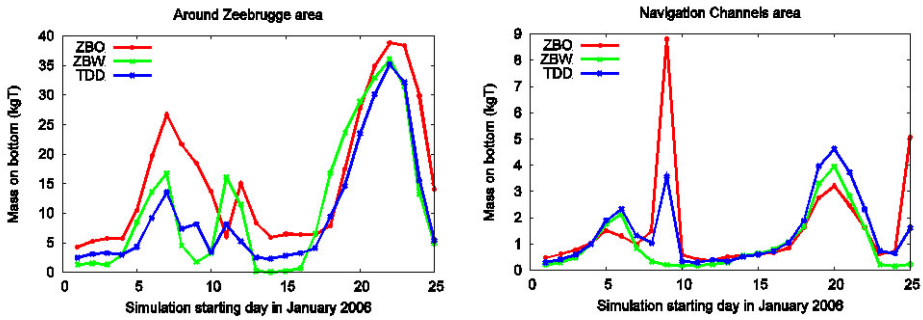

Figure 3 Amount of material on the bottom, averaged over the last day of the simulation, for the dumping at Zeebrugge-Oost (ZBO), at Zeebrugge-West (ZBW) or for tide dependent dumping (TDD) for the zone around Zeebrugge (left) and the zone around the navigation channels (right) and as a function of the starting date of the simulation. No meteorological conditions have been taken into account.

Results from the simulations made with different wind forcing are presented in Figure 4. Results are presented for one zone (around Zeebrugge) and two dumping schemes: ZBO (left) and ZBW (right). Also the influence of the meteorological conditions on the recirculation from the dumping sites is clear. The actual meteorological conditions can therefore influence the optimal dumping strategy to be applied.

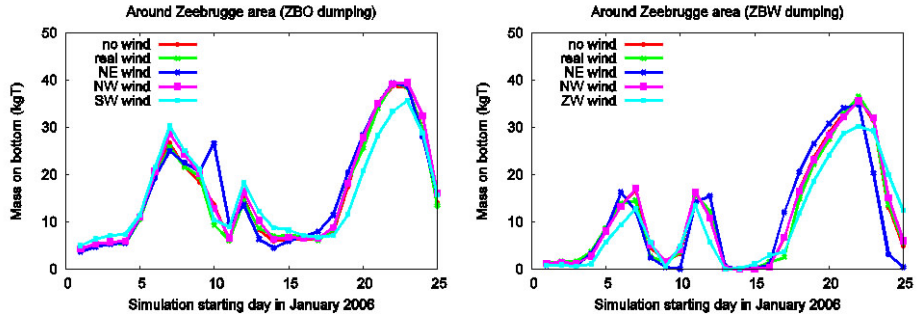

Figure 4 Amount of material on the bottom, averaged over the last day of the simulation, for the dumping at Zeebrugge-Oost (ZBO) (left) and at Zeebrugge-West (ZBW) (right) for the zone around Zeebrugge as a function of the starting date of the simulation for the different meteorological conditions.

4. Operational forecasts

To help the government to apply the most efficient dumping strategy, an operational tool is being set up, which can be used to decide where best to dump the dredged material, taking into account the actual situation. The model uses the operational forecasts of the currents and water elevations, which were executed twice a day, using the three-dimen-

sional hydrodynamic model, described above. The results of these operational currents and tidal elevations forecasts are presented on the MUMM website and are used for example for the operational forecasts of oil spills (Legrand and Dulière, 2012).

In addition to the hydrodynamic forecasts, every day two additional simulations are being executed now, using the sediment transport model. For the next five days, limited by the meteorological forecasts, the dispersion of the material is followed using the three dumping strategies. Automatically, an animation is prepared, presenting the evolution of the material in suspension and the material at the bottom during the simulated period, which can be consulted on a web site. An example of this movie for the dumping at Zeebrugge-Oost and Zeebrugge-West is presented in Figure 5. Furthermore, a table is automatically calculated and presented with the calculated recirculation averaged over the last day of the simulations, to the two zones, defined above. This table could be used to help the decision makers to decide which dumping strategy to follow during the next days, taking into account the actual situation and the actual hydrodynamic forecasts, to minimise the recirculation of the dredged material.

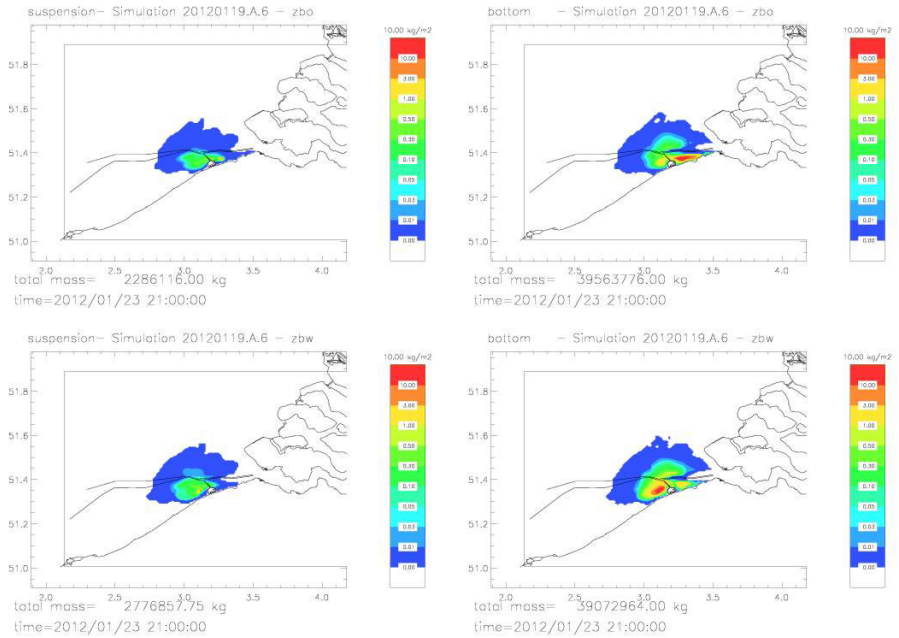

Figure 5 Operational forecasts of the dispersion of dredged material from two different dumping sites.

5. Conclusions and future work

This paper presents some work on the development of a tool that can be used to make the dumping of dredged material more efficient. For this purpose a semi-Lagrangian sediment transport model was set up, which follows the dumped material through the model grid, and which calculates the recirculation of the dumped material to predefined zones of interest, in this case the harbour of Zeebrugge and the navigation channels. Using operational hydrodynamic forecasts, also operational forecasts of the dispersion of

the dumped material are being produced. The results of these forecasts are easily accessible through a web site. This information then can be used by the responsible authorities, when deciding where to dump the dredged material.

It is clear that further research has to be carried out before the operational tool will be ready. First of all, the operational sediment transport model should be extended to include the influence of waves on the sediment transport. Furthermore, a good calibration of different model parameters and a proper validation of the model results has to be made. To this extent, a large scale measuring campaign is being set up, to measure the influence of the dumping site on the recirculation of the dumped material to the Zeebrugge harbour. These measurements will be of great importance to validate the operational sediment dispersion model.

Acknowledgements

This research was executed in the framework of the MOMO project, financed by the Coastal Waterways Division of the Ministry of the Flemish Community, Belgium. José Ozer and Frederic Francken from MUMM are acknowledged for the constructive remarks.

References

Ariathurai, C.R. (1974). A finite element model for sediment transport in estuaries. Ph.D. Thesis, University of California, Davis.

Bijker, E.W. (1966). The increase of bed shear in a current due to wave motion. In: Proceedings of the 10th Conference on Coastal Engineering, Tokyo, 746–765.

de Kok, J.M. (1994). Numerical modelling of transport processes in coastal waters. Ph.D. Thesis, Universiteit Utrecht, 158 pp.

Dujardin, A., D. Van den Eynde, J. Vanlede, J. Ozer, R. Delgado and F. Mostaert (2010). BOREAS – Belgian Ocean Energy Assessment, A comparison of numerical tidal models of the Belgian part of the North Sea. Version 2_0. WL Rapporten, 814_03. Flanders Hydraulics Research, Soresma & MUMM. Antwerp, Belgium, Belspo Contract SD/NS/13A, 62 pp.

Fettweis, M. and D. Van den Eynde (2003). The mud deposits and the high turbidity in the Belgian–Dutch coastal zone, southern Bight of the North Sea. Continental Shelf Research, 23, 669–691.

Krone, R.B. (1966). Flume studies of the transport of sediment in estuarial shoaling processes. Final Report, Hydr. Eng. Lab. And Sanitary Eng. Research Lab., Univ. California, Berkeley.

Legrand, S. and V. Dulière, 2012. OSERIT: a downstream service dedicated to the Belgian Coast Guard Agencies. This volume, page 181.

Luyten, P.J., J.E. Jones, R. Proctor, A. Tabor, P. Tett and K. Wild-Allen (1999). COHERENS: A Coupled Hydrodynamical-Ecological Model for Regional and Shelf Seas: User Documentation. Management Unit of the North Sea Mathematical Models, Brussels, 914 pp.

Van den Eynde, D. (2004). Interpretation of tracer experiments with fine-grained dredging material at the Belgian Continental Shelf by the use of numerical models, Journal of Marine Systems, 48, 171–189.